

**Establishing a Human Immune System Mouse Model
for Pulmonary and Disseminated Tuberculosis**

A Dissertation

Submitted in Partial Fulfillment of Requirements for degree of

Doctor rerum naturalium (Dr. rer. Nat)

To the Department of Biology, Chemistry, Pharmacy of Freie Universität Berlin

By

Frida Takubetang Arrey

from Cameroon

Berlin 2017

Commencement of doctoral studies: **November 2010**

Completion of doctoral studies: **April 2017**

Doctoral supervisor: **Prof Dr. Dr. h. c. Stefan H.E. Kaufmann**

Institute where doctorate was carried out: **Department of Immunology, Max Planck Institute for Infection Biology, Berlin**

1st Reviewer: **Prof Dr. Dr. h. c. Stefan H.E. Kaufmann**

2nd Reviewer: **Prof Dr. Constance Scharff**

Date of oral defence: **July 11th 2017**

Declaration of own work

I, Frida T. Arrey, confirm that the work for the following doctoral thesis with the title: " Establishing a Human Immune System Mouse Model for Pulmonary and Disseminated Tuberculosis" was solely undertaken by myself and that no help was provided from other sources as those allowed. All sections of the paper that use quotes or describe an argument or concept developed by another author have been referenced, including all secondary literature used, to show that this material has been adopted to support my thesis.

Summary

Animal models have long existed as part of the canonical approach to study a wide array of human infectious pathogens such as *Mycobacterium tuberculosis* (Mtb), the causative agent of tuberculosis (TB) disease. These models have served reasonably well in understanding the heterogeneity of pulmonary granulomas which are the main pathological hallmark of TB in humans. Nevertheless, there are several differences between the human immune system and the immune system of these species that play a role in TB pathogenesis. Ergo, in this thesis: a small animal model capable of delineating the human immune response in regards to TB granuloma heterogeneity is introduced which can serve as a pre-clinical drug platform. The NOD/SCID/IL-2 receptor gamma null (NSG) mouse is an immunodeficient strain capable of supporting human cell engraftment and was thus supplemented with human fetal liver derived stem cells. Upon human immune system (HIS) reconstitution, HIS NSG mice were infected with ultra-low dose aerosolized Mtb. HIS NSG mice developed a range of lung lesions; in particular caseous necrotic granulomas, with a cellular phenotypic spatial-organization similar to that observed in certain TB patients. The core consisted of neutrophilic and monocytic cellular debris, with an inner rim that consisted of elongated macrophages, and an outer lymphocyte cuff that consisted of T and B cells. In addition, disseminated TB was observed in other organs including spleen, liver, kidney and bone marrow. Furthermore, parameters such as cell phenotype, immune and inflammatory biomolecules and spatial-cellular organization were assessed as the disease progressed, leading to the observation that a primarily proinflammatory immune response was generated. This thesis shows that the HIS NSG mouse can provide *in vivo* validation of prior TB studies with focus on the human immune response. Finally, the HIS NSG mouse lays the groundwork as a novel animal model for investigating TB pathogenesis, TB drug development and eventually HIV-TB coinfection.

Zusammenfassung

Tiermodelle existieren seit langem als Teil des kanonischen Ansatzes, um eine breite Palette von humanen infektiösen Pathogenen wie *Mycobacterium tuberculosis* (Mtb), dem Erreger der Tuberkulose (TB) -Krankheit, zu untersuchen. Diese Modelle haben einigermaßen gut im Verständnis der pulmonalen Granulom Heterogenität, die die wichtigsten physiologischen Kennzeichen der TB bei Menschen. Dennoch gibt es einige Unterschiede zwischen dem menschlichen Immunsystem und dem Immunsystem dieser Arten, die eine Rolle bei der TB-Pathogenese spielen könnten. Ergo, in dieser These; Ein kleines Tiermodell, das in der Lage ist, die menschliche Immunantwort in Bezug auf TB-Granulom-Heterogenität abzugrenzen und als präklinische Arzneimittelplattform zu dienen, eingeführt wird. Die NOD/SCID/IL-2-Rezeptor-Gamma-NULL (NSG) -Maus ist ein immundefizienter Stamm, der in der Lage ist, die menschliche Zelltransplantation zu unterstützen, und wurde somit mit menschlichen fetalen Leber-abgeleiteten Stammzellen injiziert. Nach dem humanen Immunsystem (HIS) Rekonstitution wurde HIS NSG mit Ultra-Low Dose Aerosol-TB infiziert. HIS NSG-Mäuse entwickelten eine Reihe von Lungenläsionen; Insbesondere fallende nekrotische Granulome, mit einer zellulären phänotypischen Raumorganisation ähnlich denen, die bei einigen TB-Patienten beobachtet wurden. Der Kern bestand aus neutrophilen und Makrophagen-Zelltrümmern; Mit einem inneren Rand, der aus langgestreckten Makrophagen bestand, und eine äußere Lymphozytenmanschette, die aus T- und B-Zellen bestand. Darüber hinaus wurde disseminiertes TB in anderen Organen wie Milz, Leber, Niere und Knochenmark beobachtet. Darüber hinaus wurden Parameter wie Zellphänotyp, Immun- und Entzündungsbiochemikale und räumlich-zelluläre Organisation als fortschreitende Krankheit beurteilt, was zur Beobachtung führte, dass eine meist proinflammatorische Immunantwort erzeugt wurde. Diese These zeigt, dass die HIS-NSG-Maus in vivo-Bestätigung mit einem menschlichen Immunfokus von früheren TB-Studien liefern kann. Darüber hinaus legt die HIS NSG-Maus die Grundlage für ein neuartiges Tiermodell zur Untersuchung der TB-Pathogenese, der TB-Arzneimittelentwicklung und schließlich der HIV-TB-Coinfektion.

ACKNOWLEDGEMENTS

Victory is won through the guidance of many counselors, Proverbs 11:14

It is truly rare to be mentored on the professional and personal aspects of life from the same individual. Professor Dr. Dr. h.c. Stefan H.E. Kaufmann is that rare individual. This thesis has reached its completion due to your continuous constructive input and support. Thank you.

Thanks to Prof Dr. Constance Scharff for agreeing to be my Doktormutter at the Freie Universität Berlin and for providing advice in terms of planning a scientific career.

Many thanks to my Post Doctoral Supervisor, Dr Geraldine Nouailles for the biosafetly level 3 training, assistance in navigating German animal ethics and valuable scientific input. More importantly thank you for showing me what it truly means to be a Woman in Science.

Special thanks to Professor Christian Münz and Dr. Till Strowig for introducing me to the beauty of the humanized mouse model while at Rockefeller University, NY and their continuous mentorship.

Thanks to the many past and present postdoctoral scientists in the Kaufmann Laboratory that have taught me protocols, tutored me in various aspects of their field of expertise and challenged me to design and perform crisp experiments. In particular, Kellen Fae, Erica Houthys, Steve Reece, Martin Gengenbacher, Laura Lozza, Maurra Farinacci, Jeroen Maertzdorf, Macarena Beigier-Bompadre, Pedro Alves, January Weiner 3rd, Gopinath Krishnamoorthy, Maria Esterhuyse, Tatsiana Skrahina, Marco Iannaccone, Gang Pei, Hai Peng Liu, Hiroki Saigi, Anca Dorhoi, Alexis Vogelzang, Andreas Kupz and Natalie Nieuwenhuizen

No science can be performed without technical support. Thanks to Dr Gesa Rausch, Dr Uwe Klemm, Ines Neumann and Jens Otto for coordinating the mouse shipments and breeding. Thanks to Delia Loewe, Stefanie Kuhlmann, Silke Bandermann, Marion Klemm, Peggy Kaiser and all the other technical assistants for help in the biosafety level 3. Thanks to core facilities at the Max Planck Institute of Infection Biology and other Berlin, EU and US core facilities.

Thanks to my compatriots in the trenches; my fellow Kaufmann PhD students both past and present: Martin Rao, Maria Duque, Christian Ganoza, Julia Knaul, Carolina Perdoma, Natalie Zimmermann, Marina Bechtle, Fadhil Ahsan, Hellen Buijze, Andreas Puyskens, Lisa Scheuermann, Anne Stein and Teresa Domaszewska.

Thanks to the medical and hospital staff at Charité – Universitätsmedizin Berlin, their prompt care saved my life and their continuous aid in managing my Lupus has been immense.

Last but definitely not the least; I have infinite appreciation towards my parents, my brothers, my family, friends and church community for all the love and care throughout this PhD journey. Again, thank you.

Frida T. Arrey

April 2017

Table of contents

Introduction.....	12
1 Tuberculosis overview.....	12
1.1 Tuberculosis basic facts.....	12
1.2 Animal models of tuberculosis.....	18
1.3 Immune response to tuberculosis.....	27
2 Humanized mice.....	38
2.1 History of humanized mouse.....	38
2.2 Humanized mice and infectious disease.....	44
2.3 Rationale for thesis project	44
3 Aim of this PhD project.....	48
3.1 Establish a humanized mouse model for tuberculosis.....	48
3.2 Decipher human immune response during tuberculosis disease progression.....	48
Materials and Methods.....	49
1 Ethics.....	49
2 Statistical analysis.....	49
3 Human fetal liver stem cell isolation.....	49
4 Humanized mouse generation.....	50
5 Human immune reconstitution determination.....	50
5.1 Flow cytometry analysis.....	50
6 Bacteria strain and infection.....	52
7 Organ harvesting.....	52
8 Cell isolation for phenotypic analysis.....	53
8.1 Flow cytometric analysis.....	54
9 Cell isolation for bacterial burden enumeration.....	52

9.1 Bacterial burden enumeration.....	52
10 Cell isolation for biomolecules characterization.....	56
10.1 Biomolecules characterization.....	57
11 Pathological analysis.....	57
11.1 Hematoxylin and eosin histological stain.....	58
11.2 Ziehl-Neelsen mycobacteria identification stain.....	58
11.3 Immunohistochemistry stain.....	58
Results.....	61
1 Establishment of a humanized mouse model for tuberculosis.....	61
1.1 Generation of humanized mice.....	61
1.2 Characterization of tuberculosis infection in humanized mice.....	63
2 Decipher dynamics of a human immune response to tuberculosis.....	70
2.1 Aspects of the human immune response-lung.....	70
2.2 Aspects of the human immune response non-lung organs.....	75
2.3 Further Visual confirmation of these aspects.....	78
Discussion.....	82
Humanized mouse as a model for pulmonary tuberculosis.....	82
Dynamics deciphered confirms previous observations and sets groundwork for new directions.....	88
Conclusion and future perspectives.....	94
References.....	96
Abbreviations.....	123
Curriculum vitae.....	128

List of figures and tables by chapter

Introduction

Figures

Figure1. Epidemiology of all forms of new TB cases reported in 2015.....	13
Figure2. Prevalence of HIV in new TB cases reported in 2015.....	13
Figure3. Estimated TB deaths excluding HIV-TB reported in 2015.....	14
Figure4. Schematic depiction of the different granuloma phenotypes observed in humans.....	19
Figure5. Tissue sections displaying human granuloma heterogeneity.....	20
Figure6. Schematic depiction of the different granuloma phenotypes observed in humans and in the common laboratory mouse.....	23
Figure7. Haematoxylin and eosin Tuberculosis granuloma tissue sections from various animal models in comparison to human samples.....	24
Figure8. Haematoxylin and eosin Tuberculosis granuloma tissue sections from C3HeB/FeJ mice.....	25
Figure9. Haematoxylin and eosin Tuberculosis granuloma tissue sections from TNF- α and IFN- γ blocked Nos2 ^{-/-} mouse.....	26
Figure10. Schematic depiction of the first three stages of the immune process in Mtb infection and granuloma formation.....	27
Figure11. Timeline describing some of the significant advances in humanized mouse models.....	38
Figure12. Schematic depiction for the receptors of gamma chain cytokines and thymic stromal lymphopoietin.....	39
Figure13. Overview of the major humanized mouse models used in hematopoietic and infectious disease research.....	41
Figure 14. Schematic of the current model of lineage determination in the Human hematopoietic hierarchy.....	43

Tables

Table1. Factors to consider in Mtb lung granuloma development studies.....	21
Table2. Factors to consider in HIS mouse model generation.....	40
Table3. HIS NSG mouse Infectious disease studies	44

Materials and Methods**Tables**

Table4. Peripheral blood flow cytometry panel.....	52
Table5. Organ innate flow cytometry panel.....	55
Table6. Organ adaptive flow cytometry panel.....	56
Table7. Organ immunohistochemistry antibodies.....	59
Table8. Cohort for model establishment.....	60
Table9. Cohort for disease kinetics.....	60

Results**Figures**

Figure15. Generation of Human Immune System mice.....	61
Figure16. Human immune system reconstitution.....	62
Figure17. Human immune cell frequencies in peripheral blood.....	62
Figure18. Human immune cells reconstitution in naïve lung.....	63
Figure19. Aerosol tuberculosis infection of HIS NSG mice.....	64
Figure20. HIS NSG mice are susceptible to aerosolized tuberculosis.....	65
Figure21. HIS NSG mice develop lung lesions upon Mtb infection.....	66
Figure22. HIS NSG mice develop human like caseous necrotic granulomas.....	67
Figure23. HIS NSG mice caseous necrotic granulomas have Mtb in the center.....	68
Figure24. HIS NSG mice develop splenic lesions upon Mtb infection.....	69

Figure25. HIS NSG mice show signs of disseminated TB in other organs.....70

Figure26. Aerosol tuberculosis infection of HIS NSG mice.....71

Figure27. Tuberculosis disseminates from HIS NSG lungs as the disease progresses.....72

Figure28. Human immune cells in HIS NSG lung.....73

Figure29. Human immune cells are recruited to the HIS NSG lung upon infection.....74

Figure30. HIS NSG mice have a systemic immune response upon infection.....76

Figure31. Human biomolecules are secreted in the HIS NSG lung upon infection.....77

Figure32. HIS NSG lung architecture changes as the disease progresses.....79

Figure33. Recruited human immune cells develop a human like organization.....80

Figure 34. Enhanced view of human immune cell recruitment.....81

Tables

Table10. Biomolecules characterized in HIS NSG lung.....78

Discussion

Figures

Figure35. Possibility to study cellular and molecular mechanisms
of TB in HIS NSG mice.....95

1. Introduction

1.1 Fundamentals of Tuberculosis

In Berlin, on March 24 1882, Robert Koch presented his findings on an etiologic agent called *Mycobacterium tuberculosis* (Mtb) as the primary cause of the tuberculosis (TB) disease in humans in a presentation titled "Ueber Tuberculose" (1). Paul Ehrlich is quoted as stating that this presentation was "my single greatest scientific experience" (2) expressing the fascination scientists of that time period had with this deadly disease (3).

More than 133 years later, this fascination still persists as 1.7 billion individuals are estimated to be latently Mtb infected. This means that the human immune system is quite capable of containing the pathogen but inefficient at eradicating it (4, Figure 4). Infected individuals have a 10% lifetime risk of developing disease but a vast number of the infected individuals are at risk for reactivated TB once the immune system weakens. In 2015, there were 10.4 million new TB cases (Figure 1) and of this number 1.2 million were human immunodeficiency virus/tuberculosis (HIV-TB) coinfecting (Figure 2). Coinfection with both pathogens dramatically increases the risk of developing TB and 400,000 out of 1.8 million TB deaths in 2015 were due to HIV coinfection (Figure 3). In 2015, there were an estimated 2.9 million cases and 510,000 TB deaths among women as well as an estimated 530,000 cases and 80,000 deaths among children (4).

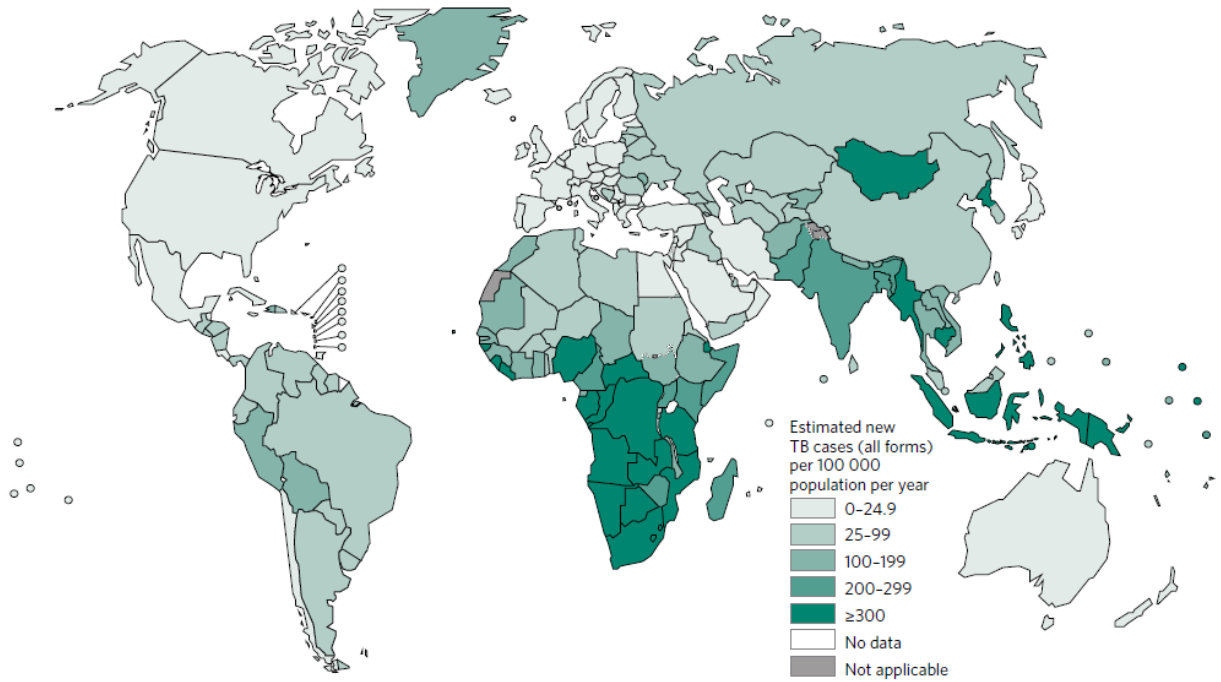


Figure1. Epidemiology of all forms of new TB cases reported in 2015. (Source: WHO Global TB report, 2016)

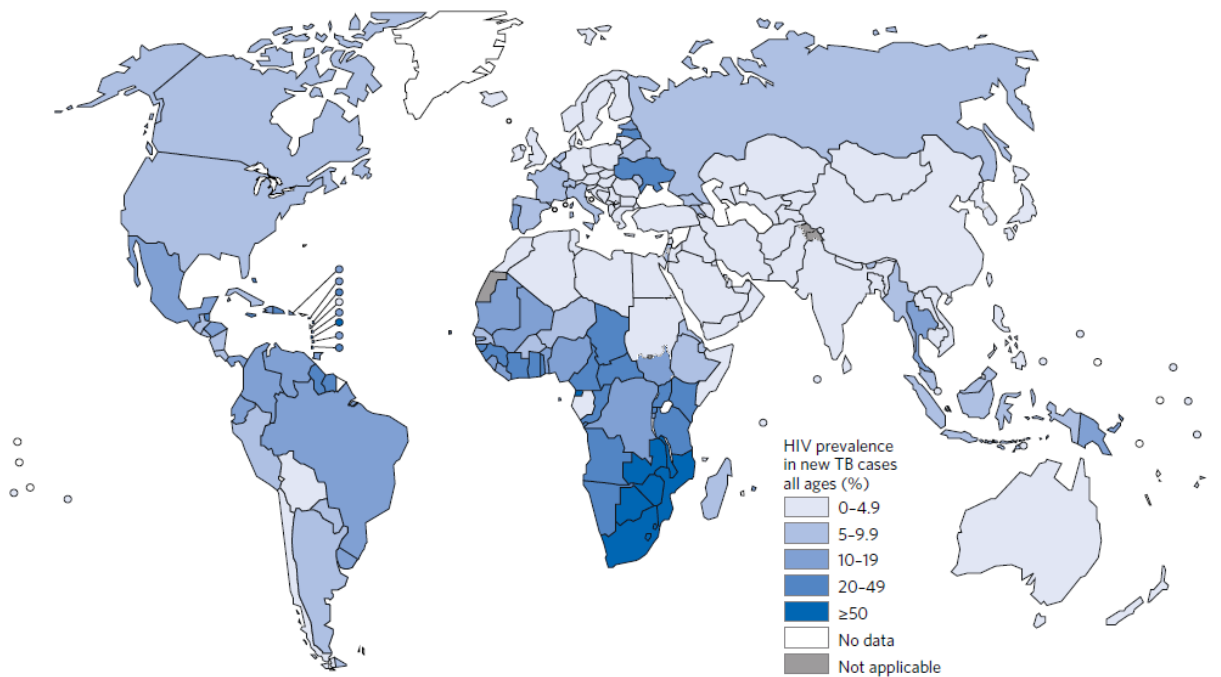


Figure2. Prevalence of HIV in new TB cases reported in 2015. (Source: WHO Global TB report, 2016)

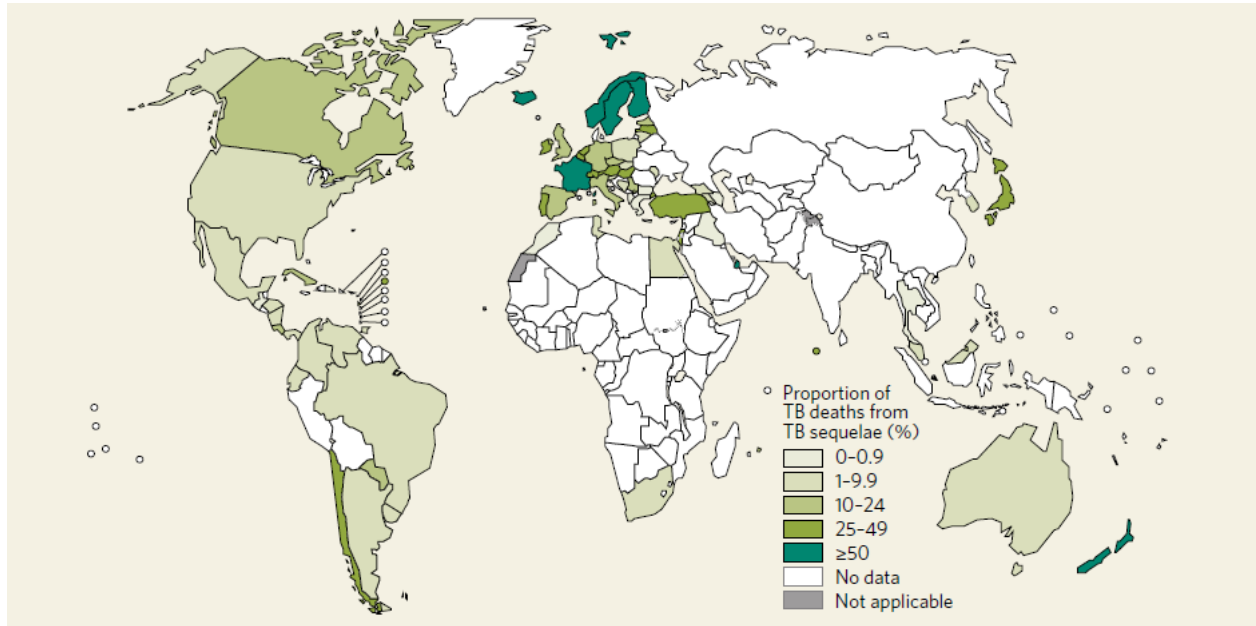


Figure3. Estimated TB deaths excluding HIV-TB reported in 2015. (Source: WHO Global TB report, 2016)

The number of TB cases and associated deaths remains abysmally large due to a suboptimal vaccine, difficulty in diagnosing the disease and intermittent compliance to anti tuberculosis drug therapy. The currently administered Bacille Calmette- Guérin (BCG) vaccine, which is an attenuated strain of the virulent *Mycobacterium bovis* (cattle TB) partially, protects infants but not adults against severe tuberculosis. Moreover, BCG faces safety issues in infants with HIV infection (4) as HIV infection abrogates the BCG- specific T cell responses in these infants and causes BCG-osis, a form of disseminated BCG (5).

Presently, there are various efforts to improve BCG vaccine efficacy (6). One of these efforts entails modifying BCG by the expression of a listeriolysin gene (*hly*) from *Listeria monocytogenes* and removing from the chromosome urease *c* gene (*rBCG Δ ureC:Hly⁺*) (7). This recombinant BCG vaccine also known as VPM1002 was generated by the Kaufmann laboratory and has been shown to provide better protection than parental BCG against TB by inducing type 1 and type 17 T cell cytokines in mice (8). In mice it has also been observed that apoptotic vesicles from VPM1002 infected macrophages induced greater multifunctional CD4⁺ and CD8⁺ T cell responses than parental BCG (9). In addition, VPM1002 is safer than BCG in immunocompromised mice (7) and is in Phase II trials for safety and immunogenicity in newborns (10). VPM1002 is currently undergoing Phase IIb trials for safety and immunogenicity

in HIV exposed and un-exposed infants (11). VPM1002 will soon be in phase III trials for protection against recurrence of TB after drug treatments in adults (Personal communication from Professor Kaufmann).

A new vaccine should also aim for low interference with TB diagnostics. One of the means by which TB is diagnosed is by purified protein derivative (PPD) skin test. PPD tuberculin is a precipitate of Mtb (12). It is administered intra-dermally and the subsequent skin swelling diameter is measured to gauge if there is a cellular immune response to Mtb. Basically, a greater than 10mm swelling is an indicator for TB. However, the non-specificity for Mtb of PPD permits it to cross react in BCG vaccinated individuals complicating diagnosis. The false positivity generated requires further testing by chest X-rays and Ziehl-Neelsen sputum testing (13). Ziehl-Neelsen acid fast is a stain that binds to the mycolic acids in the bacteria cell envelope aiding in Mtb visualization in sputum samples by light microscopy. The Ziehl-Neelsen test is limited by the difficulty in getting sputum from patients and the need for a high bacterial load in these samples for the test to be efficient. Subsequently, some active TB patients appear smear negative, and are thus the origin of 15 to 20% of transmission cases (83).

Therefore, another diagnostic method that is employed is the Interferon-Gamma Release Assays (IGRAs). Two popular IGRAs are the QuantiFERON TB gold test (15) and the TB-Elispot test (14). This assay determines the amount of interferon-gamma (IFN γ) released by T lymphocytes in a suspected TB patient's blood when mixed with certain Mtb antigens. These antigens are 6 kDa early secretory antigenic target (ESAT-6) and 10 kDa culture filtrate antigen (CFP-10). The genes encoding for these antigens are situated in region of difference 1 (RD1) of Mtb which is not present in BCG. Hence IGRAs are not affected by the BCG vaccine, but are affected by cross reactivity with *M. africanum* or *M. marinum* which also contain ESAT-6 and CFP-10. Lately, biomarkers have been proposed as the next line in the diagnostic arsenal. A biomarker is defined as a biological characteristic that is objectively measured and evaluated as an indicator of physiological or pathological processes (16). Biomarkers or bio signatures are in the form of transcriptomic, proteomic, metabolic profiling (17, 18) or epigenetic marks (19). Recently, a blood transcriptomic study showed that active TB patients have a neutrophil-driven interferon gene profile in comparison to systemic lupus erythematosus (SLE) patients that had a plasma

cell driven interferon profile (20). However, Maertzdorf J. and colleagues from the Kaufmann laboratory examined sarcoidosis patients (which have similar lung pathology to TB) to active TB patients, and observed that these two diseases have a similar interferon signature (21). To further discriminate between TB, healthy volunteers and other lung diseases, Maertzdorf J. and colleagues from the Kaufmann laboratory further examined gene sets in conjunction with certain algorithms. They observed that 4 particular genes could discriminate between these two groups. These genes were GBP1, ID3, P2RY14 and IFITM3 (248). Biomarkers are thus a promising diagnostic measure that will eventually provide a framework that will aid in determining which form of TB a patient has, thus giving further confidence in implementing the right therapy.

The therapy administered when drug susceptible TB is suspected consists of rifampicin, isoniazid, pyrazinamide and ethambutol given daily or intermittently for two months, followed by rifampin and isoniazid for four months. This regimen has been consistently given with few changes for the past 15 years (22). These drugs act by having an inhibitory effect on certain enzymes involved in cell wall biosynthesis, nucleic acid metabolism and protein synthesis or by disrupting the membrane structure. For example, rifampicin inhibits bacteria DNA-dependent RNA polymerase which further prevents bacteria DNA-dependent RNA synthesis (249). Unfortunately, poor regimen compliance occurs in low-income settings where therapeutic drug options are expensive and patients experience harsh side effects. In addition there is a challenge in treating HIV-TB patients as certain drugs such as rifampin interact with protease inhibitors thus reducing their effect on HIV (250). This contributes to the rise of multi-drug resistant strains (MDR-TB) and extensively drug resistant strains of Mtb (XDR-TB) via *de novo* mutations (4, 251). This is reflected by the 2015 numbers of an estimated 170,000 MDR-TB deaths and 450,000 MDR-TB incidence cases. In addition, XDR-TB has been detected in 105 countries (4). This requires the use of the diagnostic assay GeneExpert Mtb/Rif, which is a nucleic based assay that detects the presence of Mtb in sputum but also the *rpoB* gene that is responsible for rifampicin resistance (23). Hence, injectable agents such as kanamycin or amikacin or fluoroquinolones such as moxifloxacin are administered if susceptibility to these antibiotics is suspected (22). Lung surgical resection is another intervention to alleviate MDR-TB and XDR-TB (24). Currently, there have been reported cases of totally drug resistant TB (TDR-TB) (25).

This distressing scenario and the recent failed phase three drug trials of using fluoroquinolones in combination with other anti-TB drugs to shorten the time course from 6 months to 4 months by three independent groups, underscores the urgent need for new antibiotics or alternative treatment options for TB (26, 27 and 28). New antibiotics such as linezolid which has been used for skin infections and pneumonia due to methicillin-resistant *Staphylococcus aureus* have been integrated in new TB clinical trials. These clinical trials focused on MDR-TB and XDR-TB patients. Most patients (34 out of 39), had a negative sputum conversion within 6 months after linezolid was added to their drug regimen (29). In addition, positron emission tomography (PET) and computerized tomography (CT) imaging revealed reductions in pulmonary pathology in macaques with active TB and patients with XDR-TB that followed a linezolid added drug regimen (30). Another antibiotic regimen that has shown promise and is presently in phase 3 trials (252) is a three drug regimen comprised of pretomanid (Pa), moxifloxacin (M) and pyrazinamide (Z). The PaMZ combination in a phase 2b trial was found to be effective not only against drug-susceptible TB, but also MDR-TB and had TB-negative sputum after eight weeks (253). PaMZ regimen is also of great interest due to its potential use in HIV-TB patients as this regimen does not contain rifampicin.

The eventual likelihood of any new antibiotic to lose susceptibility in the short term is low, but indiscriminate administration of the drug will increase the probability of drug resistance to develop in the greater population in the long term. Therefore, host directed therapies (HDTs) have been proposed as an adjunct or alternative to traditional antibiotics (31). In the pre-antibiotic era, TB patients were sent to sanatoriums to get rest, fresh air, good nutrition and sunlight (32). This was essentially a means by which the body attempted to cure itself by resolving inflammatory pathways, inhibiting inflammation, reduce lung damage, induce autophagy and induce antimicrobial peptides. A basic example of HDTs is Vitamin D which is acquired from sunlight and supplementation. Others are repurposed drugs which can be brought through clinical trials quickly (382). Vitamin D induces production of cathelicidin and mediates initiation of autophagy via interferon gamma (IFN- γ), interleukin-15 (IL-15) and IL-32 in human macrophages (33, 34). New antibiotic regimens and various HDTs are currently undergoing *in vivo* validation in animal models and are in early stage human clinical trials (31).

1.2 Animal models of Tuberculosis

The 1800s till the 1960s is considered as the main pre-antibiotic era whence human lung TB samples were primarily gathered from autopsies (254). Whereas, in the post-antibiotic era, most human lung TB samples are gathered from resected MDR/XDR TB surgeries (232). Consequently, knowledge of various biological processes that occur in humans has been acquired by carrying out experimental studies in animal models, particularly in rodents (36). In the field of TB research, Robert Koch described naturally occurring TB in a variety of animal species and he successfully infected mice, rats, guinea pigs, rabbits, hedgehogs, hamsters, cats and dogs with the tubercle bacillus (1, 35). Hence, animal experiments were instrumental for the discovery and scientific proof of the etiologic agent of TB. Mtb infection in experimental animals can produce a diversity of outcomes therefore, a prominent method to compare the state of infection across the different animal models in relation to human disease is by examining the pathological hallmark of Mtb infection - the granuloma (Figure 4 and Figure 7).

Mtb infections starts with the inhalation of bacilli, either in an aerosol droplet generated by the cough or sneezes of an active TB patient and is followed by the arrival of the bacteria at the lung alveolar space. Mtb is then phagocytosed by the alveolar macrophages. A pro-inflammatory response is generated, which triggers the infected cells to migrate into the underlying epithelium. Concurrently, monocytes, neutrophils and dendritic cells are recruited from the circulation to the infection site, while new microvascular networks are formed. Granuloma associated macrophages (GAMs) undergo a differentiation program to form epitheloid cells, multi-nucleated giant cells and foamy cells containing lipids (37, 168). Subsequently, lymphocytes are recruited to the GAMs periphery. Further granuloma stratification occurs by the deposition of extracellular matrix material by fibroblasts outside the macrophage layer. A good number of the granulomas remain in this state, but a triggering event such as immunosuppression due to malnutrition (38) initiates vascularization loss which renders the granuloma hypoxic. This leads to increased necrosis and caseation in the granuloma and in some cases cavitation (255). Other forms of lung inflammation that occur are tuberculous pneumonia while in other situations, spontaneous lung healing leads to calcification and fibrosis of the granuloma which may be sterile or contain few bacteria (Figure 4 and Figure 5).

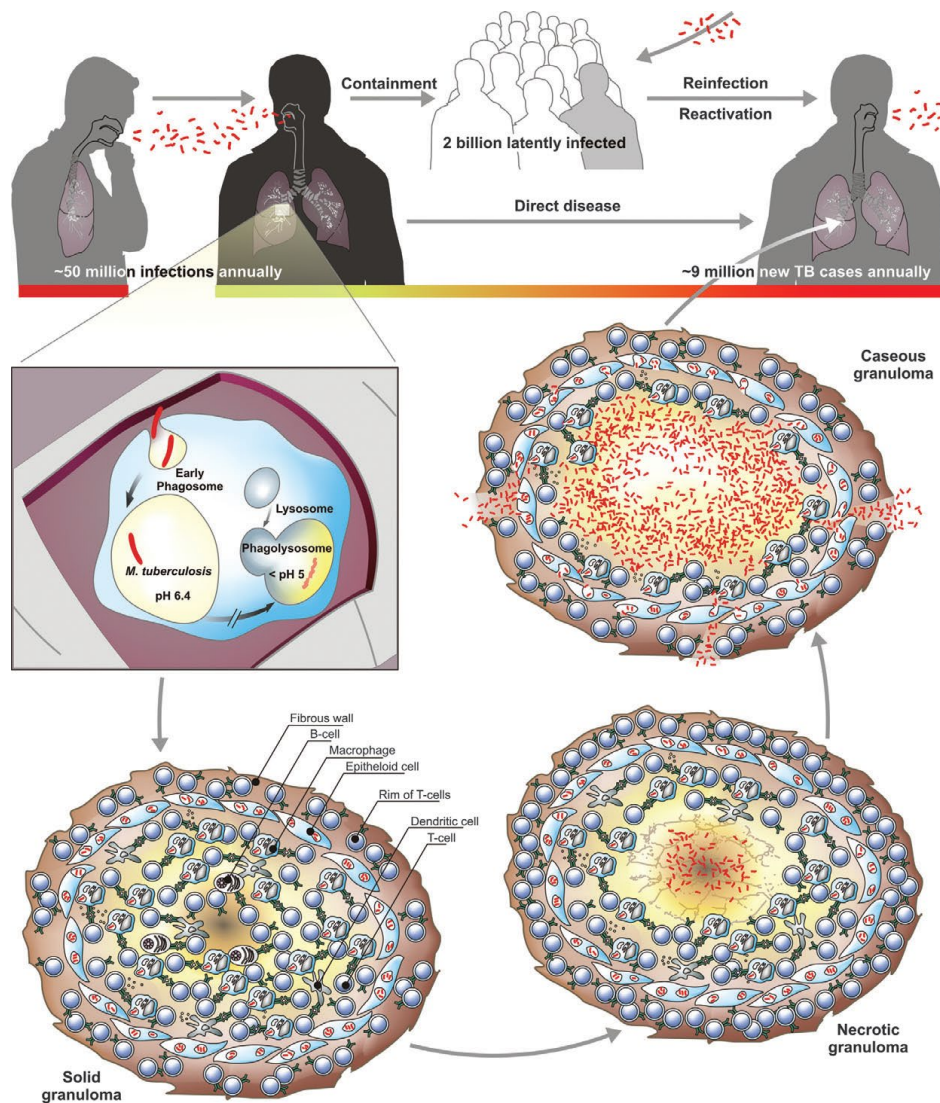


Figure 4. Schematic depiction of the different granuloma phenotypes observed in humans (Source: Gengenbacher/Kaufmann, 2012)

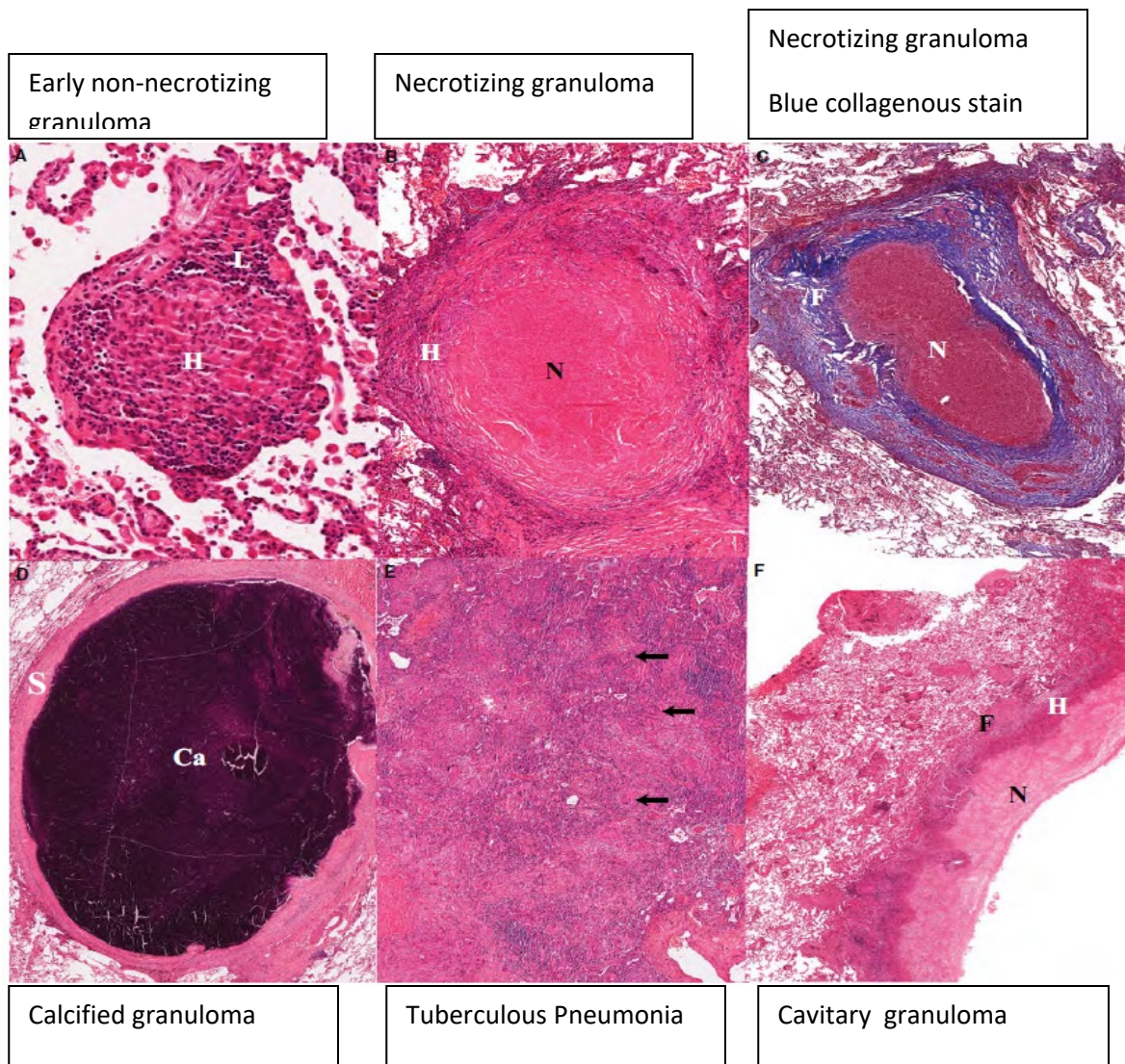


Figure 5 Tissue sections displaying human granuloma heterogeneity (Source: Lenaerts/Barry/Dartois, 2015)

Details on the various animal models (39) used to recapitulate lung granuloma development in consideration of the parameters stated in Table 1 have been summarized in the following paragraphs.

Infection route	Aerosol, intratracheal or intradermal
Inoculum size	Ultra-low dose: 15 bacilli – 30 bacilli Low to mid dose: 100-250 colony forming unit (CFU) high dose: 1000 CFU - 10 ⁶ bacilli
Bacterial strain	Mtb lab strain H37RV or Erdman, Mtb clinical isolate Beijing or CDC1551, <i>M. africanum</i> , <i>M. bovis</i> , <i>M. marinum</i> , <i>M. caprae</i>
Animal model	Mouse, guinea pig, rabbit, zebra fish, cattle or non-human primate
Mouse strain	C57BL/6, Balb C, Nos2 ^{-/-} , C3HeB/FeJ

Table1. Factors to consider in Mtb lung granuloma development studies

Non-human primates

Non-human primates (NHPs) have been used in TB research for many years' especially in regards to natural outbreaks, vaccine and drug efficacy studies. The cynomolgus macaques and common marmoset are two of the most commonly used NHP species. The NHP is the model out of all the animal models that best mimics the spectrum observed in human tuberculosis. These NHPs upon infection by using a bronchoscope or fitted air mask (15-250 CFU) develop a range of lesion types similar to that observed in human disease (39, 40) (Figure 7). These NHPs have been infected with lab strain Mtb Erdman, clinical isolates (Mtb Beijing and Mtb CDC 1551) and *M. africanum*. NHP infection with various bacteria strains precisely delineates differences between these strains. Due to cross specificity, human reagents can be used in NHPs studies. In

addition, NHPs can be infected with Simian Immune deficiency virus (SIV) which opens up avenues for SIV-TB co infection which is similar to HIV-TB co infection in humans (41). Diagnostic tools such as PET/CT with probes like 2-deoxy-2-(18F)-fluoro-D-glucose (FDG); can be employed to follow one animal throughout a drug evaluation study (30). Additionally, common marmosets have a tendency to birth twins which are used to appraise the reproducibility or differences in parallel infection studies (42). Limitations to the widespread use of NHPs in tuberculosis research are; ethical constrains, expensive biosafety facilities, restrictive animal numbers and lack of dedicated veterinarian staff.

Guinea pig and rabbit

Similarly to NHPs, guinea pigs and rabbits (43, 44) have been used in TB research for several years but due to a rareness of immunology reagents their use has been limited. Nevertheless, guinea pigs and rabbits are used to study lung pathology upon Mtb infection as they produce human-like necrotic granulomas (Figure 7). Guinea pigs are highly susceptible to Mtb (aerosol dose of 20 CFU) while rabbits are quite resistant (aerosol dose of 10^6 bacilli). In guinea pigs, the caseum remains hard, while the caseum of rabbit granulomas undergoes softening or liquefaction as observed in human granulomas (45). Pathological differences caused by different Mtb clinical strains are also observed in the guinea pig and rabbit (46, 47).

Cattle

In natura, *Mycobacterium bovis* (*M. bovis*) is the etiological agent responsible for tuberculosis in cattle. Other mammalian livestock such as goats and sheep get infected with *Mycobacterium caprae* (48). Therefore, in addition to natural transmission studies, cattle in experimental conditions have been used to study necrotic granulomas as these are similar to human granulomas caused by Mtb (49).

Zebra fish

As *M. bovis* is a more natural way to infect cattle, likewise, *Mycobacterium marinum* (*M. marinum*), an aquatic genetic relative to Mtb is used to infect zebrafish embryos. Necrotic granulomas which appear to recapitulate human caseous granulomas develop (45). Moreover,

zebrafish embryos are transparent, which provides a means by which the dynamics of primary granuloma formation and dissemination to generate new secondary granulomas during the innate immunity phase of the infection can be visualized in real time (50). Limitations of the zebrafish embryo model are the lack of lymphocytes and hence lack acquired antigen specific immunity and lack of lung structure.

Mouse

Mice as experimental animals are inexpensive, easy to handle, have a vast range of genetic variant strains (36) and have a large number of immunological tools and reagents (35). Even though the mouse is not a natural host for *Mtb*, two of the common mouse lab strains used in TB research are the C57BL/6 and BalbC mouse. In order to investigate lung pathology, these mouse strains have been infected via aerosol or intratracheally with 100 CFU to 4000 CFU of lab or clinical *Mtb* strains. The granuloma that develops in the C57BL/6 and BalbC mouse is a loose aggregate of macrophages and T cells and does not have a caseous necrotic center (51) (Figure 6 and Figure 7).

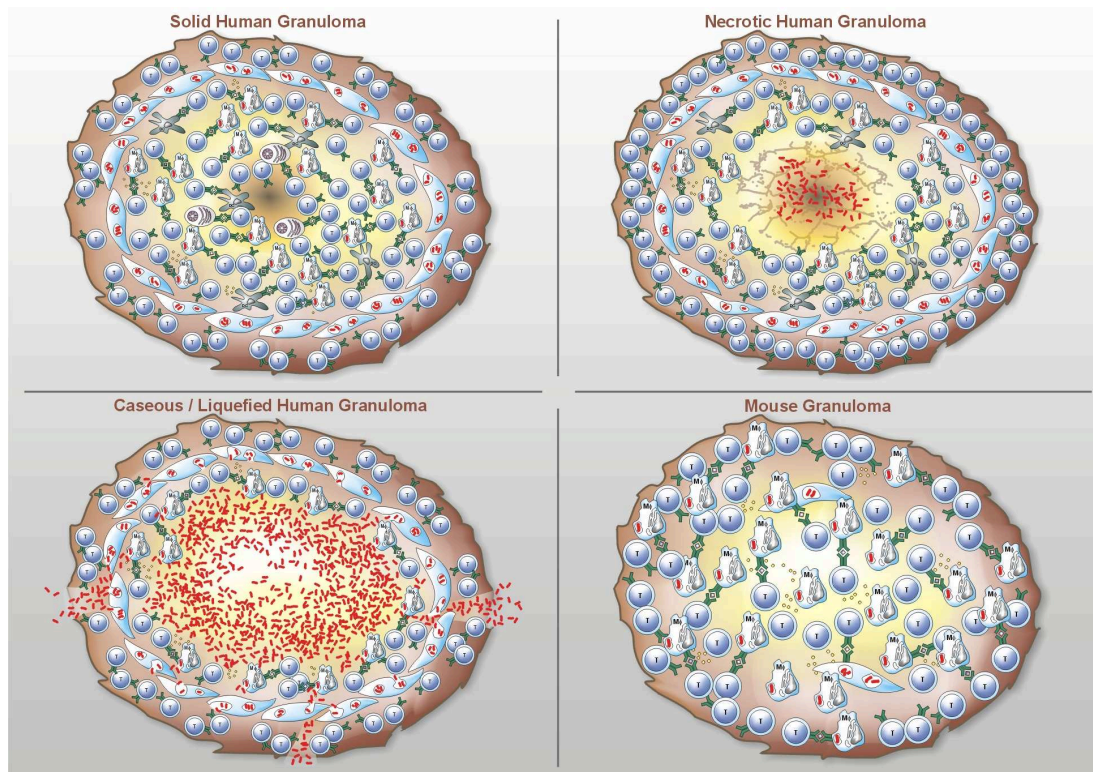


Figure 6. Schematic depiction of the different granuloma phenotypes observed in humans and in the common laboratory mouse (Source: Courtesy of Professor S.H.E. Kaufmann)

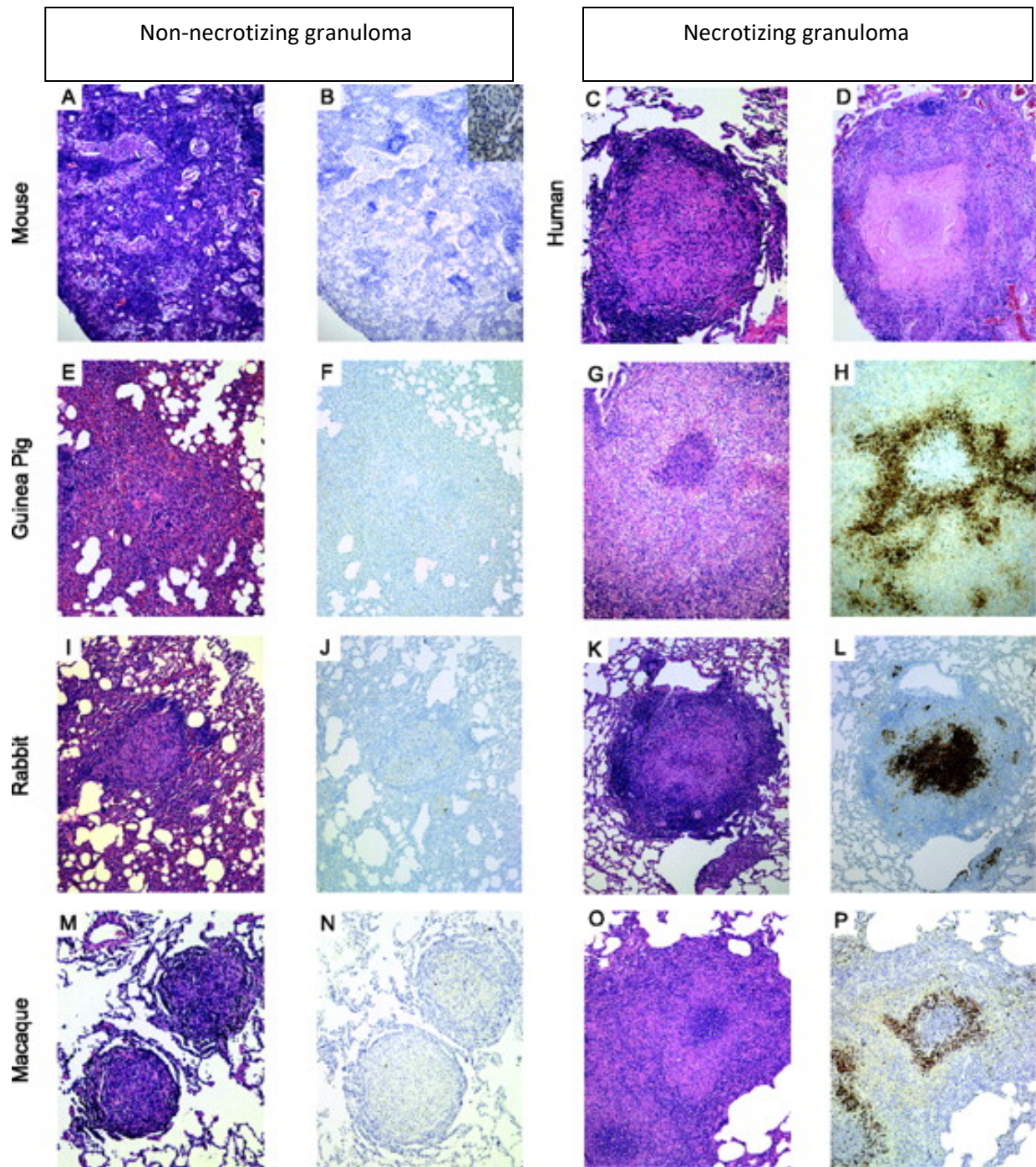


Figure7. Haematoxylin and eosin TB granuloma tissue sections from various animal models in comparison to human samples. First two columns represent non-necrotizing granulomas. Last two columns represent caseous necrotic hypoxic (brown stain) granulomas. (Source: Flynn/Barry, 2012)

In light of this, certain mouse strains that could develop necrotic granulomas similar to ones that are observed in humans have been subsequently generated. These are IL-13/IL-4ra transgenic mouse (257), interferon-gamma knock out mouse (259), I/st mouse strain (260), CBA/J mouse (258), Nos2 knockout mouse (54) and the C3HEB/FeJ (53) mouse which is a descendant strain from the CBA/J mouse. All these strains with certain perturbations develop necrotic granulomas. For example Reece S. and colleagues from the Kaufmann laboratory established a mouse TB model by using the mouse strain Nos2^{-/-} which is deficient in inducible nitric oxide (iNOS). This mouse strain upon ear intradermal infection (10^4 Mtb H37RV) and blockage of tumor necrosis factor alpha (TNF- α) or IFN- γ , develops caseous hypoxic lung granulomas (54, 261) (Figure 9). The more established necrotic granuloma model is the C3HeB/FeJ mouse strain which is commonly referred to as the Kramnik mouse. This is an immunocompetent strain that has a mutation of the intracellular pathogen resistance 1 (Ipr1) gene (53) of the super susceptibility to tuberculosis 1 (sst-1) locus (52). The sst-1 mutation is mostly lung specific, hence upon aerosolized Mtb Erdman (100 CFU to 2×10^4 CFU), organized caseous hypoxic lung granulomas develop (Figure 8).

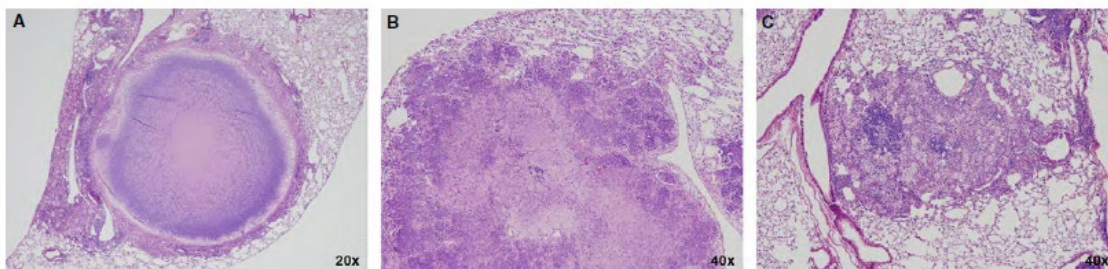


Figure 8. Haematoxylin and eosin Tuberculosis granuloma tissue sections from C3HeB/FeJ mice (Source: Lenaerts/Barry/Dartois, 2015)

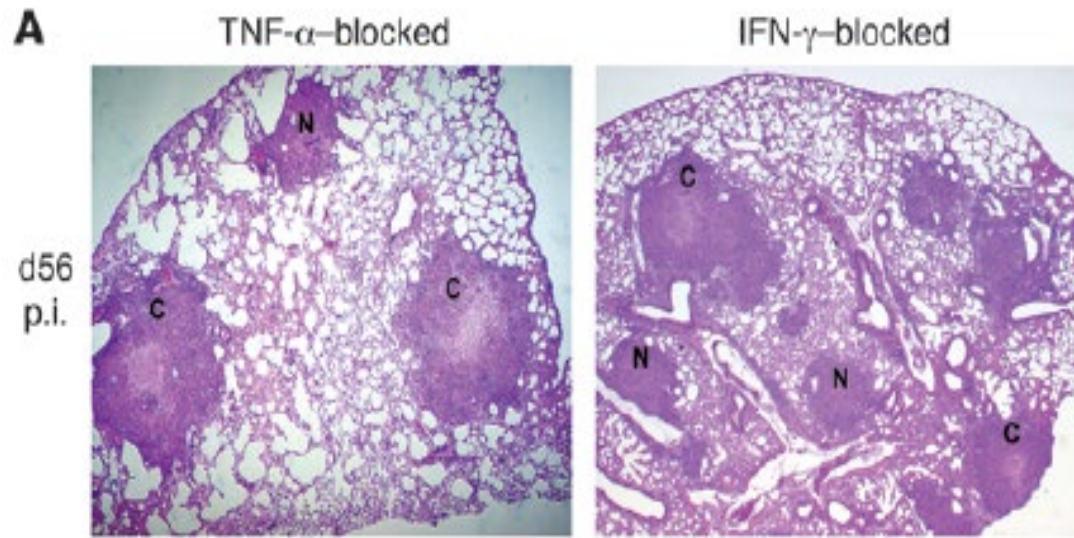


Figure9. Hematoxylin and eosin Tuberculosis granuloma tissue sections from TNF- α and IFN-g blocked *Nos2*^{-/-} mouse (Source: Reece/Kaufmann, 2010)

Even though granuloma pathology similar to that observed in humans develops, one limitation is that the immune system is still murine. Therefore, these mouse models are unable to elucidate human specific immune responses that have been observed from human clinical samples.

1.3 Immune response to TB

Although animal models have certain limitations, they have provided information on the pathology of TB and on major cellular-molecular mechanisms of the immune response to TB (55). Some of these mechanisms have been confirmed in studies of rare human genetic conditions (56), on human clinical samples and from HIV- associated TB. In relation to the pathology of the disease, using a reductionist approach, these immune mechanisms can be divided into three stages (82).

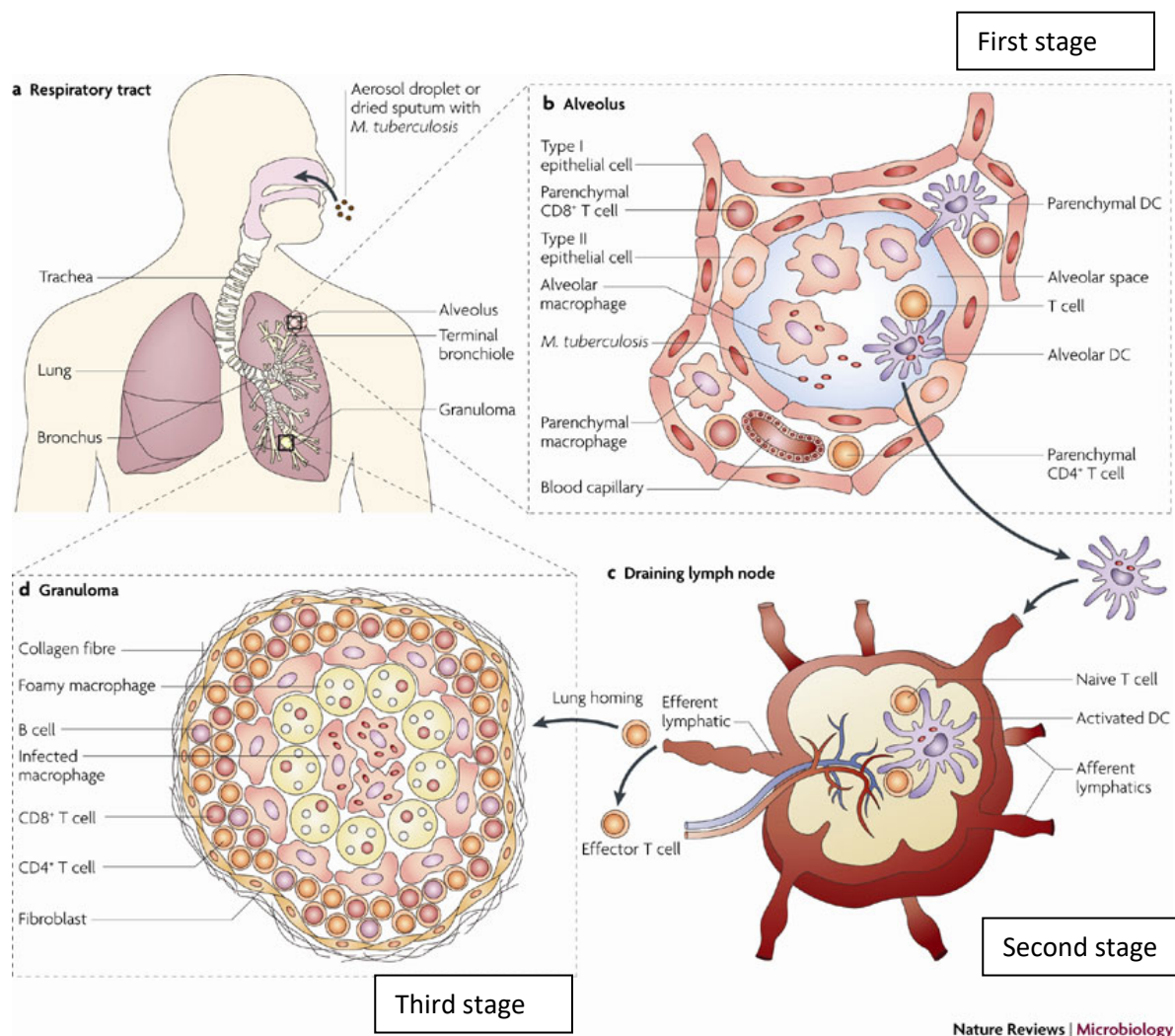


Figure10. Schematic depiction of the first three stages of the immune process in Mtb infection and granuloma formation (Source: Griffiths/Nyström/Sable/Khuller, 2010)

First stage

Commencing from the 1920s, Florence Sabin and her colleagues determined that pulmonary alveolar macrophages were the primary immune cell that phagocytoses Mtb upon inhalation in rabbits (57). Phagocytosis is initiated by Mtb pathogen-associated molecular patterns (PAMPs) such as lipomannan (LM), mannose-capped lipoarabinomannan (ManLam) and phosphatidylmyo-inositol mannosides (PIMs) engaging a gamut of surface macrophage pattern recognition receptors (PRRs). PRRs consist of Toll like receptors (TLRs), complement receptors (CRs), mannose receptors (MRs), scavenger receptors (SRs), dectin, mincle and dendritic cell (DCs)-specific intracellular adhesion molecule-3-Grabbing non-integrin (DC-SIGN) (58). A specific example of PAMPs-PRRs interaction is LM binding on TLR2-TLR1 heterodimers (59). Cholesterol serves as an anchor that promotes interactions between mycobacterial PAMPs and surface PRRs (60). PAMPs and surface PRRs interactions initiates the first steps leading to the intracellular killing of the bacteria, intracellular signaling cascade and cytokine/chemokine production by alveolar macrophages. The importance of specific TLRs has been shown in studies such as those conducted in TLR 2- deficient mice (61) and further confirmed in patients with polymorphisms in TLR2 (62). Both species, exhibited increased susceptibility to TB.

The secondary cell types that phagocytize Mtb upon inhalation are airway epithelial cells (AECs) and alveolar Type II pneumocytes (Figure 10b). These cell types in conjunction with Mtb infected alveolar macrophages produce cytokines and chemokines that affect the cellular microenvironment; leading to an influx of monocytes, macrophages, DCs and neutrophils from neighboring capillaries (63, 71). First stage cytokines that include TNF- α , IFN- γ , IL-1 α , IL-1 β and IL-18, are produced concurrently with first stage chemokines such as chemokine (C-C motif) ligand 2 (CCL2), CCL5, C-X-C motif chemokine 5 (CXCL5) and CXCL8. Nouailles G. and colleagues from the Kaufmann laboratory observed that upon TLR-2 ligation AECs, secrete CXCL-5 that interacts with chemokine receptor 2 (CCR2) which prompts the recruitment of neutrophils in Mtb infected mice (72). In another study, patients from northern Spain that had CCL5 polymorphisms were linked to susceptibility to TB (73). These two studies and others (71) lend support to the importance of various chemokines in the early TB stage working in tandem with early stage cytokines.

TNF- α in particular, is a key cytokine necessary for controlling Mtb infection in phagocytic cells (78). The importance of TNF- α to Mtb control, was also demonstrated in rheumatoid arthritis and Crohn's disease patients that developed reactivated TB upon anti-TNF treatment (64). TNF- α works in concert with IFN- γ activated macrophages, thus launching the mechanisms required to INHIBIT Mtb as shown by Flesch IE and colleagues from the Kaufmann Laboratory (65). The importance of IFN- γ in humans in controlling mycobacterial infection has been confirmed in studies examining children with mutations in interferon- γ -receptor gene. These children had a greater susceptibility to mycobacterial infections (66).

Some mechanisms used by activated macrophages to destroy Mtb at this stage are; generation of reactive oxygen intermediates (ROI), generation of reactive nitrogen intermediates (RNI), acidification of phagosomes, secretion of lysosomal enzymes and production of defensins (38). Almost all of the above mechanisms mentioned have been confirmed in human TB studies, but the role of iNOS, nitrogen oxide (NO) and RNI is still controversial (68). Murine TB research (67) and Zebrafish *M. marinum* research (77), supports a protective role for iNOS/NO whereas in human TB research no clear role has been assigned. What is definitely known is that firstly, human peripheral blood monocytes produce NO upon Mtb infection (69); secondly, iNOS expression has been detected on active TB granulomatous tissue (70) and lastly, alveolar macrophages from active TB patients have a higher level of iNOS protein expression compared to healthy donors (71).

In this first stage, some Mtb does escape macrophage killing mechanisms by hindering the fusion between the phagosome and lysosome (74), and by the use of protein secretion systems. Mtb protein secretion systems located in RD1 are commonly referred to as early secreted antigen 6 kilodaltons (ESAT-6) secretion system (ESX). ESAT-6 in juxtaposition with CFP-10 deliver virulence factors into host macrophages in order to further prevent the bacteria from being destroyed leading to necrotic death of the macrophages (76). In addition, RD1 acts on neighboring epithelial cells leading to the expression of matrix metalloproteinase 9 (MMP-9) in zebrafish. While in humans, it is MMP-1 that drives TB immunopathology (134). This causes more cytokines (such as IL-27 and IFN- β) and chemokines (such as CCL3 and CCL4) to be produced, prompting the recruitment of more phagocytic cells of the innate immune system

such as parenchymal lung macrophages, alveolar DCs, parenchymal DCs and neutrophils to take up evaded bacteria. This cytokine/chemokine storm and subsequent innate cell migration has also been observed in *in vivo* studies of infected rabbits (75) three hours post infection with Mtb (63, 71) (Figure 10b).

Some of the alveolar DCs, parenchymal DCs, inflammatory monocytes, and neutrophils carry bacilli into the lung parenchyma generating a primary inflammatory focus known as the Ghon complex. Simultaneously, other alveolar DCs and parenchymal DCs carry whole bacteria to the draining thoracic lymph nodes leading to the second stage of the immune process. These DCs also collect neutrophil Mtb apoptotic bodies which permit them to migrate faster to the lymph nodes compared to DCs that have phagocytized whole bacteria (110). The time frame for this first stage has been estimated to be about 8-10 days in mice and guinea pigs (79, 86), which is quite long compared to the approximately 20 hours it takes for influenza virus to be mostly killed and transported to the lymph nodes to kick off the second phase of the immune response (55). In humans, the closest anatomical confirmation of the first stage is from studies that showed that viable bacilli are present in apparently healthy lung acquired from autopsies (84). It is also estimated that, the time between infection and induction of the Ghon complex in humans is between 2 and 8 weeks (80).

Second stage

DCs are the most efficient antigen presenting cells (APCs), hence upon activation, T cells proliferate and differentiate into various types of effector T cells (87). DCs are quite heterogeneous, thus in the second stage, some DCs carry whole bacilli into the draining lymph node consequently infecting the lymph node itself. Simultaneously, other types of migratory DCs that are carrying bacilli undergo apoptosis and the mycobacterial antigenic peptides are released and picked up by uninfected activated lymph node resident DCs (Figure 10c). The resident DCs present these Mtb antigens to naive T cells in the lymph nodes (81, 85). These antigens are presented to T cells via major histocompatibility class I (MHC-I), MHC-II and CD-1 presentation. MHC I molecules interact with CD8 T cells, MHC II molecules interact with CD4 T cells and lipids interact with the CD1 reactive T cell family, respectively (87). DCs trafficking and migration is prompted by chemokines such as CCL19, 20 and 21 in association

with chemokine receptors such as CCR6 and CCR7 (95). Increased expression of adhesion molecules such as lymphocyte function-associated antigen 1 (LFA-1), also promotes DC migration into the draining lymphnode upon TB infection (96).

Recent functional homology studies have led to the correlation between human and murine DCs (97). Essentially, cluster of differentiation 103⁺ (CD103⁺) DCs in mice, are homologues to CD141^{high} (CD141^{hi}) DCs in humans. In mice, CD103⁺ DCs are the migratory DCs (98, 99) that interact with lymphnode resident CD8⁺ DCs (Humans: CD141⁺ DCs), CD4⁺ DCs (Humans: CD1c⁺ DCs) and plasmacytoid DCs (Humans: pDC). In human TB, Lozza L. and colleagues from the Kaufmann laboratory examined lymphnode tissue sections from TB patients, and observed that myeloid CD11c⁺ DCs, pDCs and CD141^{hi} DCs were in close contact with CD3⁺ T cells and CD20⁺ B cells (100). Migratory DCs, resident DCs and naïve lymphocyte contact is important in order to initiate an adaptive response. The importance of this communication is observed in studies where mice have been depleted of DCs (101) and in humans with genetic DC deficiencies (102). In mice, this depletion resulted in a significant increase in bacterial loads in the lungs and spleens due to an inability to mount an efficient CD4 T cell response, while in humans, BCG-osis and susceptibility to *Mtb kansasii* was observed (REF).

In the pre-antibiotic era, patients that suffered from lymphnode TB particularly cervical lymphnode TB (scrofula) were quite common (91, 94). Lymphnode infection has been proven by retrieving culturable bacteria and by pathological analysis of lymphnodes in murine TB (88), guinea pig TB (89), cattle TB (49) and NHP TB (90). Further evidence of lymphnode involvement in TB has been observed in NHPs (92) and latent TB (93) via FDG PET-CT. Increased inflammatory and immunological activity correlating with increased FDG uptake in the lymphnodes was observed. Currently, more research is being undertaken to understand the role of lymphnodes, lymphnode architecture, the lymphatics, lymphoid organs such as the spleen and their associated cells in TB control and dissemination (103, 228).

In mice, the time frame for the second stage is approximately 11-14 days post aerosol infection while in humans measurable adaptive immune responses appear approximately 42 days after *Mtb* exposure (79). Lung homing of the effector T cells occurs under the influence of chemokines and mediators which sets up the third stage of the immune process.

Third stage

Effector T cells originating in the draining lymphnodes migrate to the lungs through the efferent lymphatics and the pulmonary capillaries to the site of inflammation under the influence of chemokines such as CXCL13, CC19 and CCL21 (106). T cell migration through the lung parenchyma is also aided by the expression of CXCR3 and CXCR5 (107,108) and adhesion factors such as intercellular adhesion molecule 1 (ICAM-1) (104) (Figure 10c). These chemokines also lead to the further recruitment of a new set of natural killer (NK) cells, CD4⁺, CD8⁺, gamma delta T cells, CD1-restricted T cells and B cells. In the meantime, a series of third stage cytokines are released in the microenvironment. These cytokines drive the development, differentiation and functional capabilities of immune cells that are part of the bridge between the innate and the adaptive response. Hence in this stage; lymphnode effector cells, lung parenchyma effector cells and vascular effector cells in concert with innate cells are involved in a balancing act between pro-inflammatory and anti-inflammatory effects which can be illustrated as a protective state versus a pathological state (111).

In this stage, some of the recently recruited innate cells are newly infected with Mtb consequently secreting cytokines such as IL6, IL-8, IL-12 and IL-23. The importance of the IL-12/IL-23 axis and its associated components in controlling Mtb has been confirmed in patients with Mendelian susceptibility to mycobacterial disease (MSMD). MSMD patients have mutations in genes encoding for IFN γ receptor 1 (IFNGR1), IFN γ receptor 2 (IFNGR2), Signal Transducers and Activators of Transcription 1 (STAT1), the p40 subunit of IL-12 and IL-23, IL-12 receptor β 1 (IL12RB1), nuclear factor- κ B (NF- κ B) essential modulator (NEMO), Cytochrome b-245 (CYBB) and interferon regulatory factor 8 (IRF8). All these mutations have effects on mononuclear phagocyte subgroups, hence providing a link on the means by which mononuclear cells progress from tuberculous pneumonia to the classical granuloma structure at the site of the infection (109) (Figure 10d).

Simultaneously, CD4 T cell subtypes observed in this stage are T-helper 1 (Th1) cells, Th2, Th17, and regulatory T cells (T regs) (105). Naïve CD4 T cells upon stimulation by IL-12 and IFN-g differentiate into Th1 cells. Th1 cells are responsible for the production of cytokines such as TNF- α , IFN-g and IL-2. Th1 cells that simultaneously produce these three cytokines are termed

polyfunctional T cells. These polyfunctional T cells are involved in a coordinated effort with Th17 cells to act upon intracellular pathogens such as Mtb (114). Th17 cells are generated when transforming growth factor-beta 1 (TGF- β 1), IL-6 and IL-21 act on naïve CD4 T cells. Th17 cells produce cytokines such as IL-17, 21 and 22. In murine TB, it has been observed that lung IL-17 is mostly produced by gamma delta (gdTs) T cells (112) and that an IL-17 knockout mouse strain upon infection with a hypervirulent Mtb was unable to control the disease in comparison to a less virulent strain. In this study, it was observed that poor recruitment of T cells to the lung contributed to the inability of controlling the infection (113). In Human TB or NHP TB, most IL-17 studies have been performed on peripheral blood lymphocytes (PBMCs) or bronchoalveolar lavage whence, a greater number of Th17 cells were found in latent TB samples (114). In addition, in latent TB samples, gdTs in particular V γ 2V δ 2 T cells which exists only in primates and in humans are activated by Mtb (E)-4-hydroxy-3-methyl-but-2-enyl pyrophosphate (HMBPP) phosphoantigen and produce more IL-17 and IL-22 in comparison to active TB samples (115). This information thus supports the role of Th1, Th17 and gdTs as falling in the protective arm of the immune response.

The pro-inflammatory responses (protective state) generated by Th1, Th17, gdTs and pro-inflammatory innate immune cells cause a great deal of tissue damage (pathological state) in their quest to reduce the increasing bacteria numbers. Therefore, cytokines such as IL-4 and IL-2 act on naïve CD4 T cells to differentiate into Th2 cells, while TGF- β and IL-2 cause differentiation into T regs (105). Th2 cells, T regs and anti-inflammatory innate immune cells in a synchronized effort produce anti-inflammatory cytokines such as IL-4, IL-5, IL-10, IL-13 and TGF- β in order to resolve the initial tissue damage (116). However, efforts to resolve this tissue damage have been observed to contribute to reduced TB control in other words an immune suppressive state is brought about. This is carried out by T regs expressing intracellular transcription factor FoxP3 that secrete IL-10 which suppresses macrophage activation therefore reducing the macrophages ability to kill Mtb (117). This also leads to; reduced antigen presenting competence, reduced IL-1 α , IL-12 and TNF- α production by innate cells, and reduced CD4⁺ T cell and CD8⁺ T cell activation and proliferation (117). These observations were reported by Kursar M. and colleagues from the Kaufmann laboratory and other groups using the experimental mouse model for TB (118, 135). In human TB, some studies report that there is an increase of T regs in the blood and lung of

active TB patients (119) giving credence to T regs involvement in immune suppression while other studies report no increase of T regs in active TB (120). In NHP TB, animals that had a significantly higher number of T regs in the blood prior to and during early infection developed latent TB (121). In this study, it was also observed that both active and latent TB animals had decreased number of T regs in the blood later during the infection and T regs were observed in the lymphocyte cuff of the lung granuloma. Collectively, these observations support the fact that T regs have different effects on infection outcome in regards to disease status.

The main role of CD4⁺ T cells is to 'help' or augment the cytotoxic and humoral branches of the adaptive immune response. CD8⁺ cytolytic T cells (CTLs) and NK cells directly kill Mtb infected innate cells by the use of cytotoxic molecules such as perforin, granzymes and granulysin (124). Muller I. and colleagues from the Kaufmann laboratory and other groups have established a general protective role by CD8 T cells in murine TB (122, 169). This role has also been confirmed in NHP TB (123). Furthermore, in murine TB the antimicrobial role of CD8 perforin and granzyme (169), but not of granulysin has also been established. This is because; granulysin is only produced by NHP and human CTLs (125). Additionally, a more human specific function of CD8 T cells to TB is possible as CD8 T cells also include Vg2Vd2 T cells, Vα7.2 mucosal associated invariant T cells (MAITs) and lipid specific CD1 T cells (124). In humans and NHPs, the CD1 family consists of CD1a, b, c, d and e; in rabbits and guinea pigs it consist of CD1a, b and c; in cattle it is made up of CD1a, b, d and e whereas mice have only CD1d and zebrafish have none (126). Taking in account the differences in the CD1 family across the various experimental models and in humans, there is evidence that CD8-CD1 T cell activation and CD4-CD1 T cell activation by mycobacterial lipids is part of the protective branch against TB.

Even though the bulk of the immune response to TB in the third stage is made up of cell mediated immune mechanisms, humoral immunity is slowly being built up. B cells are the main components of humoral immunity and their main function upon activation is to proliferate and differentiate into plasma cells. Plasma cells produce antibodies that recognize and neutralize extracellular pathogens (128). Antibody classes are IgA found in mucosal areas such as the respiratory tract, IgD, IgE, IgG and IgM (128). B cells also act as APCs so they can activate traditional T cells and non-traditional T cells as some human B cells express CD1c and CD1d

(127). Experimental TB studies that focus on the role of B cells and antibodies in the mouse show conflicting results (136). One study that used mice that have B cells but lack secretory immunoglobulin, showed that these mice, were more susceptible to TB in comparison to wild type mice due to an increase macrophage production of IL-10, IL-6 and GM-CSF as the disease progressed (137). This suggests that B cells play a role in the last steps of the disease as the bacteria is gearing up for transmission. In another study that used mice that lacked B cells and were reconstituted with B cells from tuberculosis infected wild type mice; these mice controlled TB upon infection compared to their B cell deficient counterparts (138). This control was achieved by limiting neutrophil infiltration suggesting that B cells aid in controlling the disease during the initial infection. A murine TB study, in line with what has been observed in human TB studies showed that B cells were present as aggregates with T cells in the lung in a manner reminiscent of lymph node germinal centers (131). These lymphoid follicular like structures are created under the influence of chemokines such as CXCL13, CC19 and CCL21. Ulrichs T and colleagues from the Kaufmann Laboratory characterized these B cell aggregates in lung tissue from active TB patients (130). In addition to B cell aggregates, B cell clusters and antibodies are located in the lymphocyte cuff of the lung granuloma in NHP and human TB (139). B cells and antibodies have not been assigned a clear role in TB, but their location suggests that B cells have the opportunity to directly interact with T cells and innate cells thus having pro and anti-inflammatory functions (129).

In mice, the time frame for the third stage is approximately 28-30 days post aerosol infection while in humans the time frame of the third stage is variable (1 to 5 years post initial infection) as this is connected to each person's individual status (141).

Quality of the Human Lung Immune response to Tuberculosis

The quality of the immune response in all three stages depends on an individual's genetics, their age, their health status, their nutritional status, their exposure rate to TB, their vaccination status and the Mtb strain they encounter. Specifically, events that occur in the first stage of the immune response could have a cascade effect on the next two stages (142). These events lead to early clearance or a range of infection/pathology (133, 140).

In the first stage; it is true that alveolar macrophages, AECs and alveolar Type II pneumocytes are the first phagocytes, but neutrophils are the largest infected cell type in the airways of active TB patients (132). In an immunocompetent individual that has an optimal nutritional status, optimal health status and low exposure to TB, the neutrophils aid in early clearance of Mtb. Early clearance is defined as the successful eradication of Mtb before an adaptive response develops (133). Early clearance occurs due to the neutrophils deploying reactive oxygen species (ROS) (143), secreting antimicrobial peptides such as cathelicidin (145) and possibly via neutrophil extracellular traps (NETS) (144). Early clearance is also established when apoptotic cell death instead of necrotic cell death occurs in the alveolar macrophages and the neutrophils (146). Toxic metals such as zinc are also involved in early clearance by directly acting on Mtb in macrophages (147).

In an immunocompromised individual that has a sub-optimal nutritional status, sub-optimal health status and high exposure to virulent TB, neutrophils actually promote Mtb growth. Virulent Mtb can survive human neutrophilic ROS by inducing necrotic cell death (148) via the enhanced intracellular survival (*eis*) gene (149) and the NADH-quinone oxidoreductase subunit G (*nuoG*) gene (148). Other Mtb virulent factors that inhibit apoptotic cell death are serine/threonine kinase Pkne protein (150) and the RV3364c protein (151). Virulent Mtb also induces the production of eicosanoid lipoxin A4 (LXA4) in macrophages, which leads to necrotic cell death while inhibiting prostaglandin E2 (PGE2) which is linked to apoptotic cell death and subsequently clearance (152). In the case of toxic metals such as Zinc, Mtb up regulates the gene *ctpC* to control bacterial levels of this metal thus mitigating its effect (147).

In the situation whence innate cell clearance is not optimal; as previously mentioned in stages two and three, there is a dynamic recruitment of a vast number of innate and adaptive cells to the lung. In this vast number of recruited adaptive cells, approximately 1-30% are Mtb antigen specific T cells (153, 154). It should be noted that this frequency, depends on which part of the NHP or human lung has been sampled, which antigens (PPD, ESAT6/CFP10, antigen 85 or TB10.4) have been used for restimulation and if tetramers have been employed for more specific detection (155).

In an immunocompetent individual, with a sub-optimal nutritional status, sub-optimal health status and high exposure to virulent TB, the Mtb specific T cell response is higher in the lung thus preventing active disease from occurring and the bacterium avoids further elimination (latent/subclinical infection) (156). Continuous survival of the bacteria is also possible via the induction of the dormancy survival regulator (DosR) regulon, composed of 48 co-regulated genes (38, 157). The importance of antigenic specific T cells for Mtb survival is exhibited by the fact that the most conserved part of the Mtb genome is associated with human T cell epitopes (158). CD4⁺ T cells in particular, have a clear role in Mtb confinement in latent/subclinical granulomas, as it has been shown that direct contact of CD4⁺ T cells with Mtb infected phagocyte sub groups is necessary to contain the infection in murine TB (159). Furthermore, CD4⁺ T cell depleted NHPs suffer from exacerbated disease (160, 161) and SIV infection of latently TB infected NHPs causes reactivated TB (162). This gains clinical significance on examining HIV+ patients who are more susceptible to tuberculosis and are more likely to have disseminated TB with disorganized granulomas (163).

In an immunocompromised individual; such as patients undergoing anti TNF α therapy, the immune response cannot contain the infection leading to liquefaction and caseous necrotic granuloma formation (164). The extra layer of neutrophils, epithelioid macrophages and foamy macrophages prevent Mtb specific T cells from migrating to the priority sites and directly acting on the necessary innate cells (165). Further impairment of antigen specific T cell function, is part of the sequence that pushes caseous granulomas into cavitary TB (166, 167). Caseating granulomas are also associated with the typical symptoms of active disease such as a productive cough, fever and weight loss. Other forms of tuberculosis that can occur in an immunocompromised situation are disseminated/miliary tuberculosis and meningeal tuberculosis.

2 Humanized mice

2.1 History of Humanized mouse

Humanization is defined as endowing human characteristics or attributes to an object or animal. In biological research, humanization of mice can either be cellular-tissue humanization or genetic humanization. Genetic humanization involves replacing mouse genes with the corresponding human gene (170) while cellular-tissue humanization involves the transplantation of human cells and tissues (171). There were three major developments that occurred in the 1980s to 1990s which led to the reduction of certain barriers to cellular-tissue humanization (183).

Firstly, in 1983, a spontaneous severe combined immunodeficiency mutation (SCID) was observed in CB17 mice (172). These mice were subsequently used to engraft human PBMCs and various human stem cells (173, 174). Engraftment occurred but at suboptimal levels due to certain limitations such as T and B cells reappearing while the mouse aged, high numbers of NK cells and sufficient mouse innate activity that circumvented the ability of human cells or tissues to engraft (Figure 11).

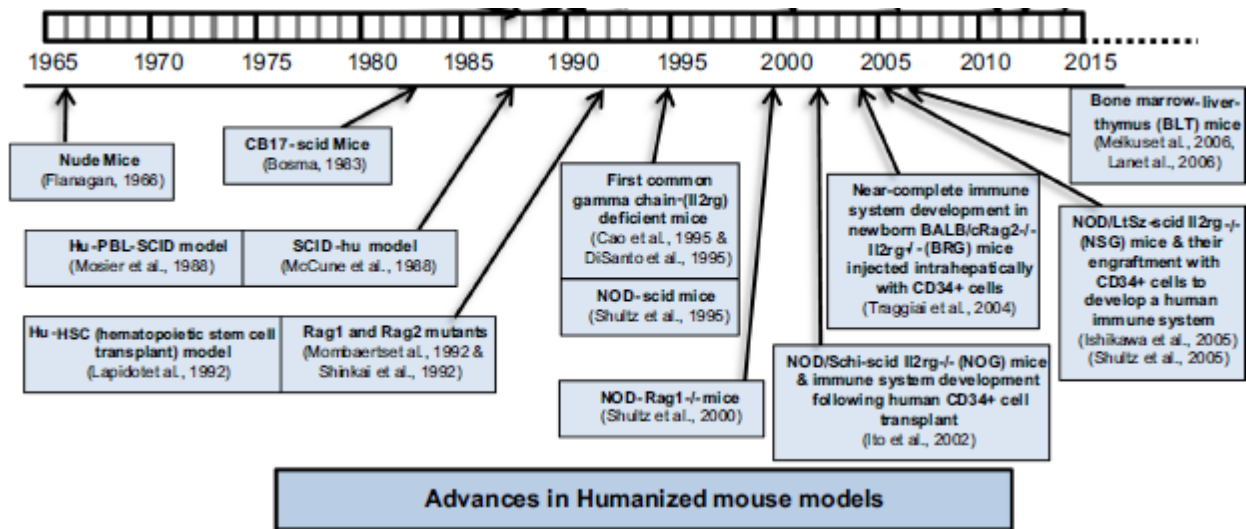
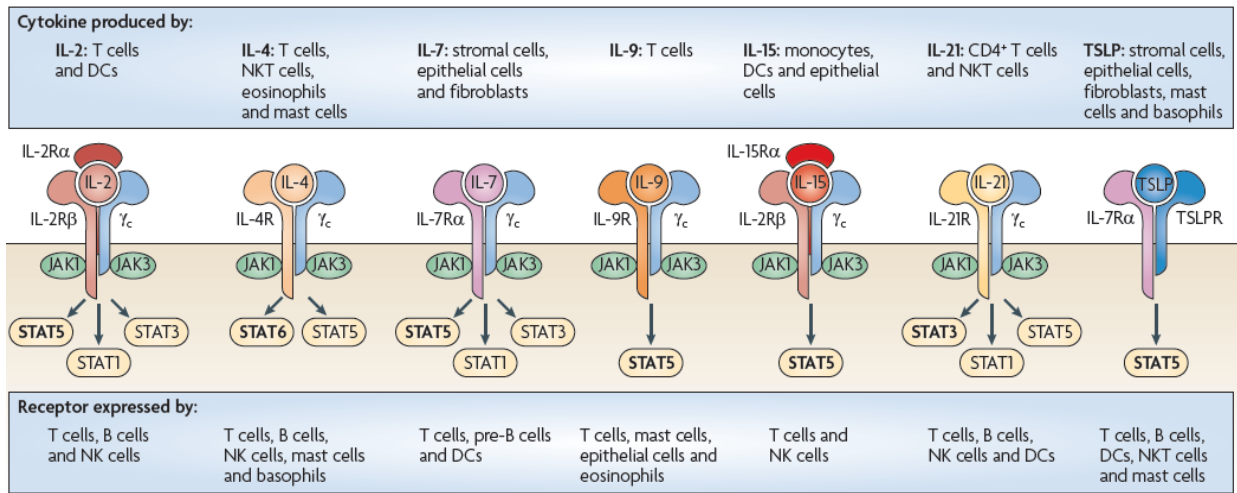


Figure 11. Timeline describing some significant advances in humanized mouse models (Source: Marsden/Zack, 2015)

Secondly, the development of immunodeficient non-obese diabetic (NOD) SCID mice led to further reduction of murine NK cell, reduced immune cell activity and radiosensitivity leading to

a slight improvement of human engrafted rates (175). Concurrently, targeted mutations at the recombination-activation gene 1 (Rag1) and Rag 2 were also developed (176, 177). This led to lower numbers of murine T and B cells, but no radio sensitivity and high numbers of NK cells hence the human cell engraftment rates was still suboptimal. Thirdly, in 1995, mice with targeted mutations in the interleukin 2 receptor gamma chain (IL-2Rg) locus were generated (180, 181). The IL-2Rg chain is a major component of the receptors IL-2, IL-4, IL-7, IL-9, IL-15 and IL-21 (182). This leads to a further reduction in murine T, B and NK cell development (Figure 12).



Nature Reviews | Immunology

Figure12. Schematic depiction for receptors for gamma chain cytokines and thymic stromal lymphopoietin (Source: Rochman/Spolski/Leonard, 2009)

These three major developments led to the generation of the BalbC Rag2 null IL-2R gamma null (BRG) mouse, the NOD SCID IL-2 receptor gamma null (NSG) mouse and the NOD Rag1 null IL-2 receptor gamma null (NRG) mouse. These mouse strains have been observed to have up to a fivefold higher level of human CD34⁺ hematopoietic stem cell (HSCs) engraftment compared to the previously described mouse strains (178, 179) and are therefore being used as a platform to further investigate the human hematopoietic system. Details on the main variables to consider while generating a Human Immune System (HIS) mouse model listed in Table 2 and are summarized in the following paragraphs.

Strain background	NSG, NRG or BRG
Age of the recipient	Newborn, juvenile or adult

Source of human cells or tissue	Fetal liver stem cells, cord blood stem cells, bone marrow, mobilized PBMCs
Injection route	Facial vein, intracardiac, intrahepatic, intrafemoral, intravenous , surgical graft
Conditioning	Irradiation

Table2. Factors to consider in HIS mouse model generation

Although the NSG, NRG and BRG mouse strains all have targeted mutations in the IL2r common gamma-chain, the NSG and the NRG mice develop higher levels of human engraftment due to the NOD background (184). In particular, the NOD signal regulatory protein alpha (SIRPa) recognizes human CD47 which allows NOD mouse macrophages to stop phagocytosis of human cells (185). Despite their profound immunodeficiency, these mice need a preparative regimen in order to permit engraftment of human HSCs. Sub lethal irradiation of these mice results in the depletion of murine HSCs thus creating space in the bone marrow and increased concentrations of chemokines such as stromal derivative factor 1 (SDF-1). This pulls human stem cells into the bone marrow in a CXCR4 dependent manner (186). Furthermore, the HIS engraftment levels specifically the human T cells, are higher in NSG newborns (1-2 days) compared to adults (5-7weeks) due to the fact that newborn mice do not suffer from thymic dysplasia like the adults. This allows the human CD34+ cells to contribute to thymus organogenesis (184).

HIS engraftment levels are also affected by the source of the CD34⁺ stem cells. Human fetal liver and umbilical cord blood HSCs delivered via intracardiac or intrahepatic injection to sublethally irradiated newborn NSGs (Hu-HSC, figure 9) have a greater level and breadth of engraftment compared to HSCs generated from mobilized adult blood or peripheral blood leukocytes (Hu-PBL-SCID, figure 9) (187). Human fetal liver HSCs in general also confer higher engraftment rates compared to cord blood HSCs possibly due to the fact that fetal liver HSCs are more primitive progenitors with a greater repopulation capacity (188). Intracardiac, intrahepatic and facial vein injections are the preferred injection route for newborns while intrafemoral and intravenous are the preferred route for juveniles and adults. Another engraftment route for adults is by surgical graft of fragments of fetal liver and fetal thymus under the mouse kidney capsule

followed by the intravenous injection of human HSCs preferably from the same donor. These mice are termed bone marrow-liver-thymus (BLT) mice (Figure 13).

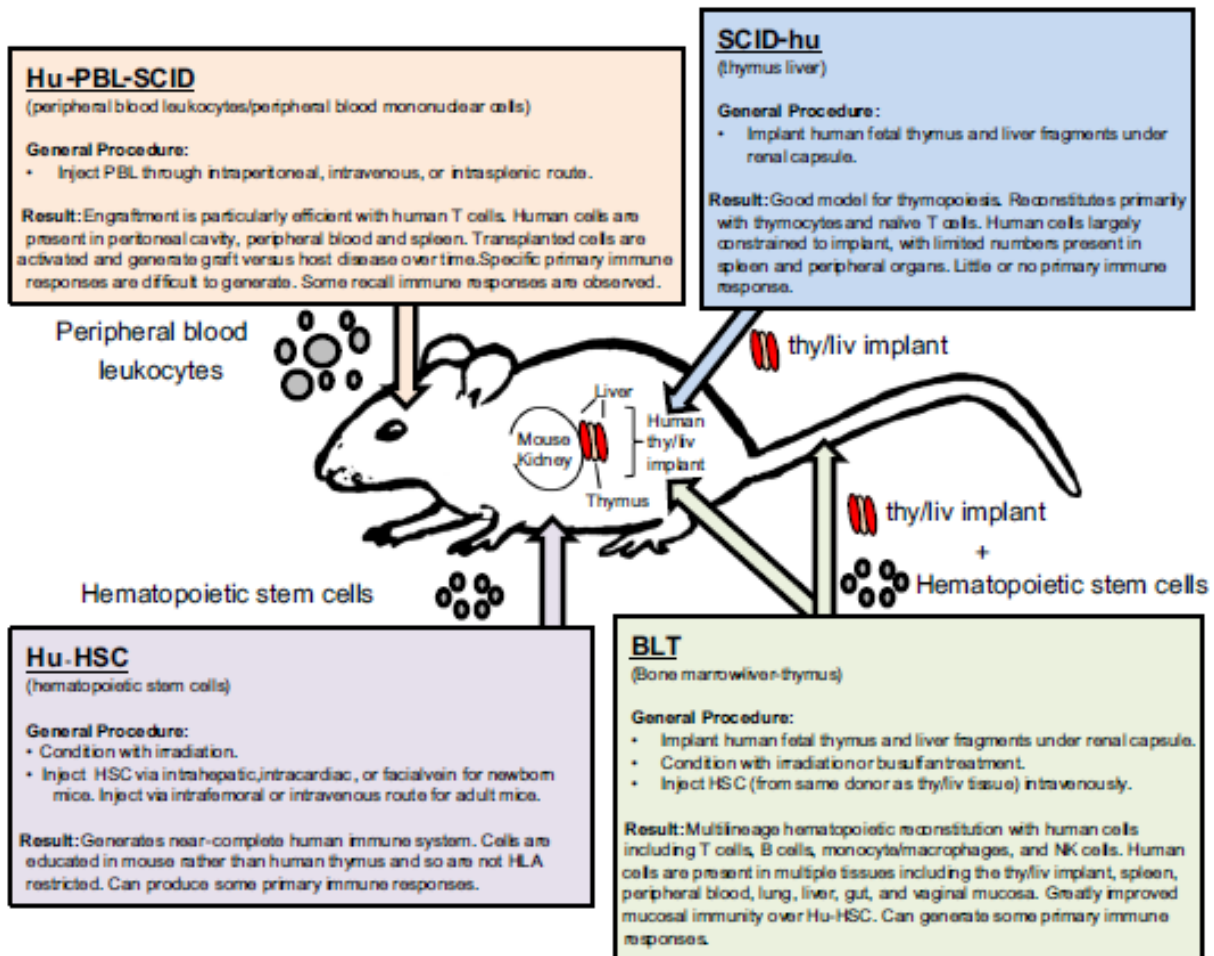


Figure 13. Overview of the major humanized mouse models used in hematopoietic and infectious disease research (Source: Marsden/Zack, 2015)

Upon engraftment of CD34⁺ HSCs, the Hu-HSC mice also known as HIS mice have been observed to develop all lineages of human hematopoietic cells in the blood and other organs (Figure 14). These cells are the T cells, B cells, NK cells, DCs, monocytes/macrophages, granulocytes, erythrocytes, megakaryocytes and platelets (189). HIS mice in particular the HIS NSG mice, have been observed to have a sufficient pool of human HSCs greater than 10 weeks post engraftment in the bone marrow which aids in the maintenance of long term hematopoiesis (262). HIS NSG bone marrow has also been observed to be morphologically and phenotypically similar to

human bone marrow aspirates (263). Furthermore, the different human immune subsets that have been observed in various organs of the HIS NSG mice have been shown to share basic phenotypic and functional characteristics with cells obtained from human volunteers. These human immune cells are also present for greater than 9 months post-transplantation.

The human myeloid cells in the HIS NSG mouse have been shown to phagocytize beads and pathogens. They also respond to cytokines and secrete cytokines via TLR2 and TLR4 (264, 265). Additionally, HIS NSG mice that have been engrafted as pups with HSCs from cord blood have been observed to have human myeloid cells that are phenotypically immature with a reduced ability to stimulate T cells in comparison to HIS NSG mice that have been engrafted as adults with HSCs from human adult peripheral mobilized blood (266). This immature phenotype with limited T cell stimulating capability in neonate engrafted HIS NSG mice is thus similar to the human newborn innate immune system (267). The human adaptive system that develops in neonate engrafted HIS NSG mice is also similar to a human newborns' adaptive immune system (268). HIS NSG mice have conventional and non-conventional T cells that develop with a diverse T-cell repertoire (269, 270), but have lower functional capabilities in comparison to human adult T cells (271). The B cells that develop are mostly CD5⁺ B cells which are classified as immature B cells and have a reduced ability to respond to antigens (271, 272), but these B cells do have a diverse B-cell repertoire similar to what has been observed in humans (273, 274).

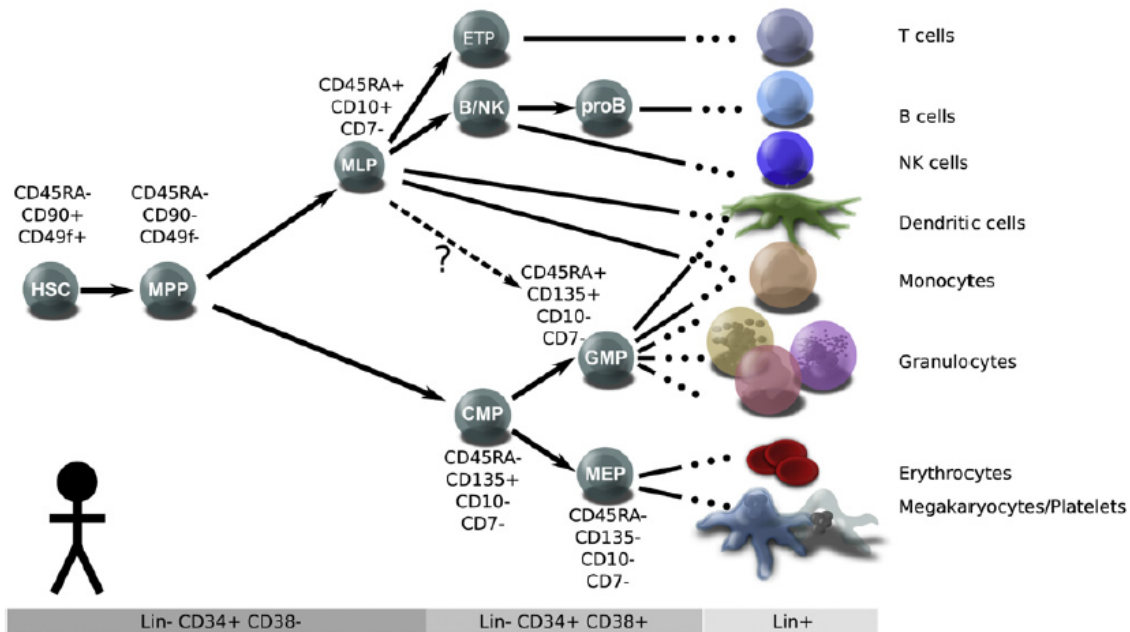


Figure 14: Schematic of current model of lineage determination in the Human hematopoietic hierarchy (Source: Doulatov/Notta/Laurenti/Dick, 2012)

HIS mice have some limitations as they are a chimera of human and mouse. Some of these limitations are; most of the mouse cytokines and growth factors cannot act on the human immune cells causing sub-optimal development and function; the endothelium, epithelium and stroma are still murine which could influence interactions with the human immune cells; the mouse innate system is albeit sub-optimal in function, but it is still present; and there is no human leukocyte antigen (HLA) so there is poor communication between human APCs and human T cells that develop (190). Poor communication between human immune cells also leads to a suboptimal humoral immune response with lower levels of antibody production in comparison to what is observed in an immune-dominant situation. Immunoglobulin class switching is also compromised. Since murine T cells and B cells are absent, there is no scaffold for proper lymphnode development and the accompanying germinal centers (190, 275). Despite these limitations, HIS mice have been used in various research fields such as basic immunology, tumor immunology, therapeutic development and infectious diseases (191).

2.2 Humanized mice and Infectious disease

Some of the infectious diseases studies that have used the HIS NSG mice to investigate the pathology and immune response using a more natural route of infection are listed below (192).

Pathogen category	Pathogen	Reference
Virus	HIV	207, 208, 209
	Epstein Barr	204, 205, 206
	Hepatitis C	203
	Dengue	200, 201, 202
	Ebola	193
	Protozoan	<i>Plasmodium falciparum</i>
	<i>Leishmania</i>	195
Bacteria	<i>Salmonella typhi</i>	196
	Sepsis	197, 198, 199
	<i>Staphylococcus aureus</i>	276, 277
	<i>Borrelia hermsii</i>	278

Table3. HIS mouse Infectious disease studies

2.3 Rationale for undertaking this thesis project

There are more than 80 differences between the mouse and human immune system. These differences do have a certain impact on translating research carried out in mice to humans. These differences arose as the two species evolutionarily diverged 65 to 75 million years ago; in respect to their living environment, body size, day-night cycle, pathogens encountered and lifespan (210). These differences include; differential expression of TLR2/3/9/10, different antibody isotypes and different FCR receptors. As previously mentioned in this thesis introduction, there are differences in CD1 genes between mice and humans. There are also human specific classifications of certain cells such as gamma delta T cells, CD8 granulysin T cells, CD8 MAIT cells and neutrophil defensins. Broader differences between mice and humans are exhibited in physiological/anatomical sites such as the blood whence humans are neutrophilic

rich (50-70% neutrophils, 30-50% lymphocytes) while mouse blood is lymphocytic rich (10-25% neutrophils, 75-90% lymphocytes).

A 2013 comparative biology study examined the gene expression of serially drawn white blood cells in trauma, burns and endotoxemia in humans and mice (211). The study conclusion stated that the inflammatory gene expression patterns of the human groups correlated more with each other than with the associated mouse group. A competitor group using the same data set in 2015 but with different computational tools stated in their conclusion that the inflammatory genomic responses of humans and mice correlate with each other in their respective groups (212). These studies have spurred research that aims to harmonize or delineate human-mouse differences and their impact on immunology, inflammation, infectious disease and drug therapy. There have also been calls for properly designed and analyzed animal experiments (213); in consideration of the fact that 90% of the animal model based drug research that enter clinical trials fail (214).

An example of a failed trial that had dangerous consequences is the hepatitis B drug fialuridine. Fialuridine was administered to 15 patients in a phase 2 trial after undergoing toxicology testing in mice. Five of the patients died while two required liver transplants (215). A retrospective study done in immunodeficient mice with partially destroyed mouse liver cells and repopulated with human liver cells showed these mice died after receiving fialuridine (218). The Hu-hepatocyte (Hu-Hep) mice exhibited pathology similar to that of the human patients that died. The cause of death was linked to the drug being taken up by a transporter expressed in human mitochondria, but not in mouse mitochondria. Another example is the previously mentioned antibiotic linezolid. This antibiotic had limited activity in mouse studies (216, 217) and was subsequently sidelined until clinicians pushed for the drug to be administered to some MDR TB and XDR-TB patients (29, 30 and 230). The failure of some TB drug studies could be linked to the fact that mouse TB granulomas are not organized in a stratified manner with various immune cells as exhibited in humans. This could have an effect on drug penetration into the granuloma and the drug's mode of action in the diverse oxygen environments arising in various granulomas (231, 232). Hence the premise of my first thesis aim is to establish a HIS mouse model that develops granulomas reflective of human pathology. The fulfillment of this aim will provide the

groundwork to eventually establish a pre-clinical platform for TB drug therapy evaluation in the HIS mice.

In order to supplement animal experimentation, there has been a marked improvement in the *in vitro* or *ex vivo* handling of human primary cells and human tissue. These include more controlled authentic cell lines (219), 3D cell culture (220), tissue explants cultures (221) and organ-on-a-chip (222). In addition to this, more physiological relevant methods such as culturing cells in hypoxic chambers (223) or using different stimulants to exhibit a range of human macrophages (224) are being employed. These systems do provide valuable information, but are limited as dynamic cell interactions are not fully recapitulated and there is a challenge in acquiring lung specific cells. As previously stated, human blood is neutrophilic rich, whereas the human bronchoalveolar compartment in a “naïve” state is made of 90-95% macrophages, 5-10% lymphocytes and less than 1% neutrophils (225). In addition, human alveolar macrophages and alveolar dendritic cells are different from blood monocytes and dendritic cells on the transcriptomic level (97). This leads to differences in their interactions with the same pathogen. In regards to TB, human alveolar macrophages infected with *Mtb in vitro* produce more TNF- α , IFN-g, IL-12 and chemokines than blood monocytes (226, 227). Furthermore, human alveolar macrophages have greater phagocytic capabilities than peripheral blood-derived macrophages (227, 229). Hence the premise of my second thesis aim is to perform a comprehensive analysis of human *in vivo* immune responses to TB at the site of infection- the lung, as the disease progresses.

A great number of the major infectious pathogens exhibit host restriction. Host restriction or specificity is defined as the ability to colonize or infect a host (233). Host specificity arises due to certain molecular factors or receptors that are required by the virus, bacteria or parasite to invade a host (234). As human specific pathogens cause the greatest disease burden worldwide, alternative species have been used in order to understand immunopathology and generate drugs and vaccines. These alternatives are illustrated by the use of SIV or SHIV instead of HIV in NHPs, *Plasmodium berghei* instead of *Plasmodium falciparum* in mice and *Salmonella typhimurium* instead of *Salmonella typhi* in mice. Other alternatives include the murinazation of the Hepatis C virus (235) and the murinazation of the bacteria *Listeria monocytogenes* in order

to cause oral listeriosis (236). For TB, options include as previously mentioned, *M. marinum* instead of Mtb in zebrafish, *M. bovis* instead of Mtb in cattle and BCG in human *in vitro* systems. Mtb does infect a range of vertebrates as shown by Robert Koch and various scientists till present date, but only humans are naturally infected with Mtb as modern humans coevolved with Mtb 70,000 years ago. Therefore, Mtb has shaped the human immune system and concurrently the human immune system has shaped Mtb (237). Hence the supportive premise of my second thesis aim is to perform a simultaneous analysis of the host and bacteria as the disease progresses. Fulfilling this aim will provide a framework to understand other human specific bacteria such as *Neisseria gonorrhoeae*, *Neisseria meningitides* and *Mycobacterium leprae* and human specific viral-bacteria co infections such as HIV-TB.

As previously mentioned, a good number of the HIS mouse studies have been done for viruses (191, 192). Viruses and bacteria trigger different immune responses and subsequently different killing mechanisms and pathology even if they infect the same site such as the lung. For instance, in a Hu-PBL BRG mouse aerosol influenza study, the mice developed signs of influenza associated pneumonia (238, 239) which is pathologically different from TB granulomas. HIS mouse studies done that are done with bacteria such as *Salmonella typhi* (196, 240), sepsis (197, 198, and 199) and Borelia (278) exhibited some of the specific disease associated clinical features seen in human patients. For Borelia, this was recurrent bacteremia which is associated with relapsing fever and for sepsis this was a cytokine storm. These studies further support my first thesis aim of establishing a HIS mouse model that develops human TB clinical features and TB pathology.

Recently, there have been three groups that used the NSG mouse as a platform to investigate mycobacteria. Heuts and colleagues engrafted newborn NSG mice with cord blood derived stem cells (241), whereas, Calderon and colleagues (242) and Lee and colleagues (243) generated BLT NSG mice. Heuts et al administered BCG intravenously, and they observed granulomas containing human cells in the liver. Lee et al administered BCG via the intra tracheal route and they observed lung lesions containing human cells. Both these studies did not exhibit caseous necrotic lung granulomas as BCG lacks RD1 a key virulence factor of TB that directs the macrophages to begin granuloma organization (76, 247). Heuts et al used an infection route

that gave pathology in the liver and not the lung which is the main site of infection in TB. Furthermore, there are some differences between Kupffer liver macrophages and lung alveolar macrophages which could influence the results observed (244, 245). Calderon et al administered intra nasally 250 CFU to 10^6 Mtb bacteria. In their study; at 6 weeks post infection, they did observe large caseous necrotic lung granulomas with a CD3⁺ T cell outer rim similar to that observed in active TB. The human infectious dose is estimated to be less than 10 bacilli (246); which is much lower than the traditionally administered dose used in various experimental models. Therefore the additional premise to my first thesis aim is to establish a Human Immune system (HIS) mouse model using a more natural dose and route of infection.

Aims of this PhD project

The main aims of this study are thus:

- 1) Establish a Human Immune system (HIS) mouse model that develops granulomas reflective of human pathology upon ultra-low dose aerosolized Mtb infection
- 2) Perform a comprehensive analysis of human *in vivo* immune responses to TB as the disease progresses

Materials and Methods

Ethics

All animal experiments were conducted according to German animal protection law (Landesamtes für Gesundheit und Soziales Berlin G03070/12 and G0081/09). All human material received approval from Charite Medical hospital, Berlin.

All protocols implemented are courtesy of the Kaufmann Lab Max Planck Institute of Infection Biology Berlin, Munz Lab University of Zurich, European core facilities and US core facilities.

Statistical analysis

Statistical analysis was performed using GraphPad Prism software for Windows. When two groups were compared, the following tests were used: unpaired or paired t-test (parametric analyses) or Mann-Whitney test or Wilcoxon Rank-Sum test (non-parametric analyses). When more than two groups were compared, one of the following tests was used: ANOVA (parametric analyses) or Kruksal-Walis test and Dunn's post-test (non-parametric analyses).

Preparation of Human stem cells

Human fetal liver (15-22 weeks) was obtained from Advanced Bioscience Resources. The tissue was minced and treated with 2 mg/mL collagenase D (Cat #: 1088882001; Roche Diagnostics) in Hanks balanced salt solution with CaCl₂/MgCl₂ (Cat #: 24-020-117; Gibco) for 30 minutes at 37°C in a 5% CO₂ incubator followed by filtering through 70-µm nylon cell strainers (Cat #: 352350; BD Biosciences). 30 ml of Hanks/collagenase liver cell slurry was carefully layered on 15ml ficoll (Cat #: L6115; Biochrom) in a 50 ml falcon tube (Cat #: 62.547.254; Sarstedt) and centrifuged at 2000 rpm, room temperature (RT) for 30 minutes with no break. After centrifugation, the mono-nuclear cell layer (MNC) was collected using a 10 ml pipette (Cat #: 86.1251.025; Sarstedt) and transferred into a fresh 50 ml tube. 25 ml of cold Phosphate Buffer solution (PBS) (Cat #: 10010023; Gibco) was added to the MNC and underwent centrifugation of 1200 rpm at 4°C for 10 minutes.

The cell pellet was resuspended in 20 ml of MACS buffer that was composed of PBS, 2mM EDTA

(Cat #: 15575020; Life technologies), 0.5% bovine serum albumin (BSA) (Cat #: 130-091-376; Miltenyi Biotech) and underwent centrifugation of 1200 rpm at 4°C for 10 minutes. An aliquot was taken to determine cell numbers with Trypan blue solution (Cat #: 15250061; Life technologies) using a Neubauer counting chamber and a light microscope. CD34⁺ human hematopoietic stem and progenitor cells (HSPCs) were isolated from the MNC using the direct CD34 MicroBead human ultrapure kit (Cat #: 130-100-453; Miltenyi Biotec). The MNC was resuspended in MACS buffer at 300ul for 10⁸ MNC in a 15 ml falcon tube (Cat #:62.554.502; Sarstedt). 100ul of CD34 and 100ul FC block per 10⁸ MNC was added. The cell bead mix was incubated for 30 minutes at 4°C. At the end of the incubation, 10 ml of MACS buffer was added to the cell bead mix and underwent centrifugation of 1200 rpm at 4°C for 5 minutes. The supernatant was decanted and the cell pellet was resuspended in 300 ul per 10⁸ of MACS buffer. A MACS LS (Cat #: 130-042-401; Miltenyi Biotech) column was placed in a magnetic MACS separator (Cat #: 130-042-302; Miltenyi Biotech). The LS column was rinsed with 3 ml of MACS buffer and allowed to empty out by gravity flow. 3 ml of cell bead mix was applied to the column and allowed to empty out by gravity flow into a fresh 15 ml tube. The column was rinsed with two subsequent 3 ml MACS buffer washes.

The column was removed from the separator and the CD34⁺ fraction was flushed out by using a plunger and 6 ml MACS buffer. The CD34⁺ fraction underwent centrifugation of 1200 rpm at 4°C for 5 minutes and was reapplied on a fresh LS column in order to increase the purity as previously described. A 20ul aliquot of the CD34⁺ fraction was taken to determine cell numbers and purity via flow cytometric analysis. The CD34⁺ HPCs were frozen in StemMacs Cryo-Brew solution (Cat #: 130-109-558; Miltenyi Biotech) in Nalgene cryotubes first overnight at -80 °C in Nalgene freezing containers and then stored in liquid nitrogen at -178 to -150°C.

Generation of Human Immune system mice

NOD. *Cg-Prkdc^{scid} Il2rg^{tm1Wjl}/SzJ* (NSG) mice were obtained from The Jackson Laboratory (Cat #: 005557) and were kept and bred under specific pathogen-free conditions at the Max Planck Institute of Infection Biology, Berlin (MPIIB). CD34⁺ HPCs frozen cryovials were submerged in a 37°C water bath and were gently swirled back and forth until 90% of the cells were thawed. The CD34⁺ HPCs were gently decanted into 5ml of PBS and underwent centrifugation of 1200 rpm at

4°C for 5 minutes. The CD34⁺ HPCs were filtered over a 70-µm filter and resuspended in PBS. Cell viability and cell numbers were determined using Trypan blue and a light microscope. One- to three day-old NSG mice were irradiated with 100 cGy and injected intrahepatically (Hamilton glass syringe, Cat # 81001; Hamilton microneedle, Cat #: 7748-16) with $1-2 \times 10^5$ CD34⁺ HPCs in 25ul of PBS 24 hours after irradiation. In specific experiments, some mice were injected with 50ul of PBS as a control.

Human immune reconstitution determination

Flow cytometry analysis

100 to 200ul of blood was collected from the tail vein by tail cut and placed in a 1.5 ml tube that contained 100ul of heparin (Cat #: N65542.03; Ratiopharm). The heparinized blood underwent centrifugation of 3000 rpm at RT for 5 minutes. The plasma fraction was collected and placed in a fresh 1.5 ml tube. This plasma fraction was frozen at -20°C. The blood pellet was resuspended in 100ul of staining mix made of the components in the table below (Table 4). The blood pellet mixture was incubated at 4°C in the dark for 30 minutes. 1 ml of 1:10 diluted water BD biosciences Lysing fix buffer (Cat #: 349202) was added to blood pellet mixture and the sample was incubated for an additional 10 minutes at RT in the dark. At the end of the incubation period, the sample underwent centrifugation at 1700rpm for 5 minutes at 4°C. The supernatant was decanted and 100ul of PBS was added. The peripheral leucocytes were then analyzed by fluorescence-activated cell sorting (FACs) on a BD LSR II flow cytometer to check for the level of reconstitution of the human immune system. The gating strategy implemented and visualized using FlowJo software was done taking into account isotype stains and fluorescent minus one (FMO) stains.

Ab	FLUOROPHORE	clone	Catalog number	Company
Anti- human CD4 Helper T cells	A488	OKT4	317420	Biolegend
Anti- human CD19 B cells	PE	HIB19	302208	Biolegend
Anti- human CD3 T cells	PerCp	UCHT1	300428	Biolegend
Anti- human CD45 leukocytes	Brilliant violet 510	H130	304036	Biolegend
Anti-mouse CD45	Alexa Fluor700	30-F11	103128	Biolegend

leukocytes				
Anti- human CD8 Cytotoxic T cells	Brilliant violet 421	SK-1	344748	Biolegend
Mouse FC block clone 2.4 G2	None	93	101320	Biolegend
Human FC block	None	None	422302	Biolegend
Cell staining buffer	None	None	420201	Biolegend

Table4. Peripheral blood FACS panel

Infection with *M. tuberculosis*

The *M. tuberculosis* strain H37Rv (Cat #: 27294; ATCC) was cultured in Middlebrook 7H9 broth (Cat #: 271310; BD biosciences) supplemented with 0.05% (v/v) Tween 80 (Cat #: P4780; Sigma Aldrich) and Middlebrook ADC Enrichment (Cat #: 211887; BD biosciences) until mid-log phase (OD_{600 nm} 0.6–0.8). Bacteria were harvested, resuspended in PBS, and frozen at –80°C until use. For aerosol infection, mice received a dose of approximately 15-30 CFU *M. tuberculosis* in the lung, using whole body aerosol exposure system (Glas-Col). Aerosol particles were generated using a three-jet Collison nebulizer (BGI Inc, Waltham MA) fitted with a fluid reservoir. Mtb aerosol particles were dispersed under positive pressure over unrestrained mice that were placed in a stainless steel mesh cage capable of holding up to 250 mice. All infected mice were kept under bio-safety level 3 and under specific pathogen-free conditions at the Max Planck Institute of Infection Biology, Berlin (MPIIB).

Organ harvesting

Mice were sacrificed at specific time points by cervical dislocation and the organs were aseptically removed. These organs were the blood, lung, spleen, liver, kidney, whole bone, lymph nodes, heart, brain and spine. These organs were processed for various analyses under bio-safety level 3 conditions and were transferred for further analyses under bio-safety level 2 environment after Mtb inactivation.

Cell isolation for bacterial burden enumeration

Soft organs such as the lung, spleen, liver and kidney were directly homogenized in 1 ml PBS containing 0.05% Tween 80 (v/v). Bone marrow homogenates were obtained by flushing out snapped femur and tibiae by using an insulin syringe (Cat #: 34900232; BD biosciences)

containing 1 ml PBS 0.05% Tween 80 (v/v) and was pressed through a 70- μ m cell strainer using the plunger from a 2 ml syringe (Cat #: 300186; BD biosciences). Homogenates were then diluted in PBS containing 0.05% v/v Tween 80 and plated onto Middlebrook 7H11 agar plates supplemented with Middlebrook OADC Enrichment (BD). Bacteria colonies were counted after 3 to 4 weeks of incubation at 37°C and reported as the median Log CFU.

Cell isolation for phenotypic analysis

After aseptic removal, the lungs, spleen, femur and tibia were transferred to a 15ml tube containing 10ml of hypothermosol storage media (Cat #: 101102; Biolife solutions). Organs were subsequently processed in cold complete RPMI medium (cRPMI). Complete RPMI medium consisted of 500 ml RPMI medium 1640 (Cat #: 31870-025; Gibco), 5 ml of 200 mM L-glutamine (Cat #: M11-004; PAA), 5 ml of 1M HEPES (Cat #: S11-001; PAA) , 500ul of 50 mM β -mercaptoethanol (Cat #: 31350-010; PAA), 50 ml of heat-inactivated fetal bovine serum (Cat #: 10270-106; Gibco) and 5 ml of 10000 U/ml penicillin- 10000 μ g/ml streptomycin solution (Cat #: P11-010; PAA). The medium was filtered through a 0.22- μ m filter unit (Cat #: SCGPS05RE; Millipore).

The lungs were transferred to a sterile petri dish containing 10 ml of a collagenase cRPMI mixture. This collagenase mixture consisted of collagenase IV (0.7mg/ml) (Cat #: C5138; Sigma Aldrich) and collagenase D (0.3mg/ml) dissolved in cRPMI. The lungs were minced with surgical scissors and treated in the collagenase mixture for 30 minutes at 37°C in a 5% CO₂ incubator followed by mashing through 40- μ m nylon cell strainers (Cat #: 352340; BD biosciences) with a sterile 2ml syringe plunger. The cell strainer was then washed with 10 ml of cRPMI and the cell mixture was transferred to a 50 ml falcon tube. The lung sample underwent centrifugation at 1500rpm for 5 minutes at 4°C. The supernatant was decanted and the cell pellet was loosened by flicking the bottom of the tube. 2 ml of diluted red blood cell (RBC) lysis buffer (Cat #:420301; Biolegend) was added to the lung cell sample. The lung cell sample was incubated at RT for 2 minutes. At the end of the incubation period, the lysing was quenched by adding 10ml of cRPMI. The lysed lung cell samples underwent centrifugation at 1300 rpm for 5 minutes at 4°C. The supernatant was decanted and the cell pellet was resuspended in 1ml of cRPMI and filtered

over a 30- μ m cell filter (Cat #: 130-041-407; Miltenyi biotech). An additional 1ml of cRPMI was used to rinse the filter. The lung cell sample was stored at 4°C prior to further analysis.

The spleen was transferred into a 70- μ m cell strainer in a sterile petri dish and pushed through with a 5 ml syringe plunger in 1 ml of cRPMI. The cell strainer was washed with 9 ml cRPMI and transferred into a 15 ml tube.

For the bone, each end of the femur and tibia was snipped in a sterile petri dish. An insulin syringe containing 500ul of cRPMI was used to flush out the femur. An additional 500ul cRPMI was used to flush out the tibia. The bone marrow was flushed unto a 70- μ m cell strainer and pushed through using a 2 ml syringe plunger. The cell strainer was washed with 5 ml cRPMI and transferred into a 15 ml tube. The spleen and bone marrow samples underwent centrifugation at 1500rpm for 5 minutes at 4°C. The supernatant was decanted and the cell pellet was resuspended in 2 ml of RBC lysis buffer at RT for 2 minutes. At the end of the incubation period, the lysing was quenched by adding 10ml of cRPMI.

The lysed spleen and bone marrow samples underwent centrifugation at 1300 rpm for 5 minutes at 4°C. The supernatant was decanted and the cell pellet was resuspended in 2 ml of cRPMI and filtered over a 70- μ m cell filter (Cat #: 130-095-823; Miltenyi biotech). An additional 3 ml of cRPMI was used to rinse the filter. The spleen and bone marrow samples were stored at 4°C prior to further analysis.

An aliquot from the lung, spleen and bone marrow was taken to determine cell numbers and cell viability with Trypan blue solution using a Neubauer counting chamber and a light microscope.

Cell phenotypic analysis by flow cytometry

Lung cells, splenic cells and bone marrow cells in single cell suspension were incubated at room temperature in the dark for 15 minutes in antibodies specific for human and mouse cell surface markers in a 96 round bottom plate (Cat #: CLS3799; Corning Costar). Human and mouse FcR blocking reagents were added in order to optimize the fluorescent stain. Two different panels were used, one labeled innate (Table 5) and the other labeled adaptive (Table 6). At the end of

the incubation period, 100ul of PBS was added to each sample. The samples underwent centrifugation at 1200 rpm for 3 minutes at 4°C. The supernatant was decanted 4% paraformaldehyde (PFA) (Cat #: 158127; Sigma Aldrich) was added. The samples were incubated for 20 minutes at room temperature in the dark. At the end of the incubation period, 100ul of PBS was added to dilute to 2%PFA and incubated overnight at 4°C in the dark. The next day, the samples underwent centrifugation for 3mins at 1500rpm. The supernatant was discarded and the cells were resuspended in 100ul clean PBS and transferred to a fresh TB free 96 well plate. The leucocytes were then analyzed by fluorescence-activated cell sorting (FACS) on a BD FACS CANTO II. The gating strategy implemented and visualized using FlowJo software was done taking into account isotype stain and fluorescent minus one (FMO) stains.

Ab	FLUOROPHORE	clone	Catalog number	Company
Anti- human CD45 leukocytes	Brilliant violet 510	H130	304036	Biolegend
Anti-mouse CD45 leukocytes	Alexa Fluor700	30-F11	103128	Biolegend
Anti- human CD66a/c/e+66b neutrophils	PE	ASL-32 G10F5	342303 305105	Biolegend
Anti- human HLADR	PECF 594	G46-6	562304	BD
Anti- human HLA-ABC	PERCP CY5.5	W6-32	311419	Biolegend
Anti-mouse CD123 plasmacytoid DCs	PE CY7	6H6	306009	Biolegend
Anti- human CD33 myeloids	APC	WM53	303407	Biolegend
Anti- human CD14 monocytes	APC H7	M5E2	561384	BD
Anti- human CD11c Conventional DCs	Brilliant violet 421	Bu15	337225	Biolegend
Mouse FC block clone 2.4 G2	None	93	101320	Biolegend
Human FC block	None	None	422302	Biolegend
Cell staining buffer	None	None	420201	Biolegend

Table5. Organ innate FACS panel

Ab	FLUOROPHORE	clone	Catalog number	Company
Anti- human CD45 leukocytes	Brilliant violet 510	H130	304036	Biolegend
Anti-mouse CD45 leukocytes	Alexa Fluor700	30-F11	103128	Biolegend
Anti- human CD19 B cells	PE	HIB19	302208	Biolegend
Anti-human CD45 RA naïve T cell marker	PECF 594	HI 100	562298	BD
Anti-human CD197 (CCR7) memory T cell marker	PERCP CY5.5	150503	561144	Biolegend
Anti- human CD4 Helper T cells	PE CY7	SK3	355612	Biolegend
Anti- human CD20 B cells	APC	2H7	302310	Biolegend
Anti- human CD8 Cytotoxic T cells	APC H7	SK1	560273	BD
Anti- human CD3 T cells	Brilliant violet 421	Ucht1	300434	Biolegend
Mouse FC block clone 2.4 G2	None	93	101320	Biolegend
Human FC block	None	None	422302	Biolegend
Cell staining buffer	None	None	420201	Biolegend

Table6. Organ adaptive FACS panel

Cell isolation for biomolecules characterization

After aseptic removal, the lungs and spleen were transferred into sterile M tube (Cat #: 130-093-236; Miltenyi Biotec) containing 1 ml of homogenate mix. The homogenate mix recipe used was 50 ml PBS/Tween 20 0.5% (Cat #: 9005-64-5; Sigma Aldrich) in which one protease inhibitor tablet (Cat #: 04693159001; Roche) was dissolved. A mechanical tissue dissociator (gentleMACS™ Miltenyi) on a protein program was used to make single cell homogenates. The M tubes underwent centrifugation at 1500rpm for 5 minutes at 4°C in order to retrieve more sample material. The homogenate was transferred into 1.5 ml screw cap tube (Cat #: 72.692.005; Sarstedt) and underwent centrifugation at 20,000 rpm for 2 minutes. The supernatant was transferred into two separate spin-x tubes (Cat #: CLS8160; Corning Costar) and underwent centrifugation at 8000 rpm for 5 minutes at 4°C to remove Mtb bacteria. The

flow through was transferred into fresh sterile 1.5 ml screw cap tubes, the outside wiped down with 4% Melsept and stored at -80°C in the biosafety level 2 until further analysis.

Biomolecules characterization

The cytokine and chemokine concentrations in the plasma and cell homogenates were measured using the Bio-Rad Bio-Plex Pro Human Cytokine 27-plex Panel (Cat #: M50-0KCAF0Y) and the Bio-Rad Bio-Plex Pro Mouse Cytokine 23-plex Panel (Cat #: M60-009RDPD). The isotype concentrations in the plasma and cell homogenates were measured using Bio-Rad Bio-Plex Pro Human isotyping (Cat #: 171A3100M). In all multiplex assays, the volume of the coupled beads, detection antibodies and streptavidin-PE conjugate was halved and capped up with the appropriate buffer to the required volume. Then the assays were performed according to the manufacturer's instructions. Assay plates were read using the Bio-Rad Bio-Plex 200 system.

Preparation of Organ histology blocks

Paraffin blocks

Organs were fixed in 50 ml tubes containing 30 ml 4% w/v PFA for 24 hours at 4°C. These organs were placed in embedding cassettes and were dehydrated sequentially in 30%, 50%, 70%, 80%, 90%, 95% and 100% ethanol (EtOH) (Cat #: 459836; Sigma Aldrich) for 2 hours each. The organs were subsequently incubated in xylol (Cat #: 296325; Sigma Aldrich) for 1 hour. The organs were then placed in melted paraffin (Cat #: 03897; Sigma Aldrich) at 56-58°C for 2 hours and were then transferred into a new paraffin bath for an additional 2 hours. The next day, the organs were placed in an embedding mold and submerged in melted paraffin to form histology blocks. The paraffin tissue blocks were cooled on -20°C ceramic slab for 4 hours. The blocks were stored at room temperature until sectioning. Histology blocks were first trimmed then were cut to two- to three- μ m thick sections on a microtome (Leica). Sections were floated in a 42°C water bath and were fished out using super frost microscopy slides (Cat #: 10143351; Thermo Fisher). The slides were then dried for 24 hours in a 37°C incubator. Paraffin sections were deparaffinized sequentially in xylol, xylol, 100% EtOH, 95% EtOH, 80% EtOH, 70% EtOH, 50% EtOH and water for 10 minutes each in order to begin the various histological stains.

Pathological analysis

Hematoxylin and eosin stain

The deparaffinized sections were transferred from water and immersed in Harris hematoxylin solution (Cat #: HHS128; Sigma Aldrich) for 5 minutes at RT. The slides were rinsed in cool running water for 5 minutes. The slides were then repeatedly immersed in 0.3% acid alcohol for 30 seconds and then rinsed in cool running water for 1 minute. The slides were then immersed in Eosin Y solution (Cat #: 230251; Sigma Aldrich) for 2 minutes at RT. The slides were repeatedly immersed in cool running water for 1 minute. The slides were then dehydrated sequentially in 30%, 50%, 70%, 80%, 90%, 95%, 100% ethanol and xylol for 5 minutes per solution. Coverslips (Cat #: 1014355123NR15; Thermo Fisher) were affixed to the slides with mounting medium (Cat #: SP15; Thermo Fisher) to protect the tissue sections.

Ziehl-Neelsen stain

The deparaffinized sections were transferred from water and immersed in a working solution of fuchsin from the Roth Ziehl-Neelsen staining kit (Cat #: 8276.1) that had been pre-heated at 58-60 °C in a coplin jar placed in a water bath. The slides were kept in the heated solution for 15 minutes. The slides were removed from the coplin jar and were rinsed in cool running water for 1 minute. The slides were then repeatedly immersed in 3% hydrochloric acid in 95% ethyl alcohol for 1 minute. The slides were rinsed in cool running water for 3 minutes and then immersed in hematoxylin gill number 2 (Cat #: GHS216; Sigma Aldrich) for 30 seconds. The slides were repeatedly immersed in cool running water for 1 minute. The slides were then dehydrated sequentially in 30%, 50%, 70%, 80%, 90%, 95%, 100% ethanol and xylol for 5 minutes per solution. Coverslips were affixed to the slides with mounting medium to protect the tissue sections.

Immunohistochemistry

The deparaffinized sections were then subjected to a heat-induced epitope retrieval step by steaming under high pressure for 3 minutes in Target retrieval solution, pH 9 (Cat #: S236784-2; Dako Agilent Technologies). The sections were cooled in the buffer for 30 minutes and further rinsed in cool running water for 10 minutes. Endogenous peroxidase was blocked by incubating the sections in 3% H₂O₂ (Cat #: 95299; Sigma Aldrich) for 10 minutes at RT. The sections were

rinsed under cool running water for 5 minutes and then further washed in Tris-buffered saline Tween 20 (TBST) for 5 minutes. The sections were blocked in rodent block M (Cat #: RBM961; Biocare) for 1 hour at RT in a moistened chamber. The blocking agent was decanted, and the sections were incubated with the following individual primary antibodies for 1 hour at RT. Antibody specificity was confirmed by using isotype controls.

Ab	clone	Catalog number	Company
Anti- human CD20 B cells	L26	M0755	Dako Agilent
Anti- human CD3 T cells	F.2.38	M7254	Dako Agilent
Anti- human CD15 neutrophils	KP1	M0814	Dako Agilent
Anti-human CD68 macrophages	None	559045	BD biosciences
Anti- human CD4 Helper T cells	4B12	NCL-L-CD4-368	Leica biosystems
Anti- human CD8 Cytotoxic T cells	4B11	NCL-L-CD8-4B11	Leica biosystems

Table7. Organ immunohistochemistry antibodies

At the end of the primary antibody incubation period, the sections were washed in TBST thrice for 5 minutes each. The sections were then incubated for 10 minutes at room temperature with MACH 4 universal AP probe from the MACH 4 Universal AP Polymer kit (Cat #: M4U536; Biocare) with another incubation of 10 minutes at RT with the MACH 4 MR AP Polymer from the kit. The sections were washed in TBST thrice for 5 minutes each and then incubated in 100ul of DAB substrate (Cat #: K3468; Dako Agilent) for less than 1 minute at RT. The sections were quickly immersed in cool running water and counterstained with hematoxylin for 40 seconds. The slides were washed in cool running water for 10 minutes and then slides were then dehydrated sequentially in 30%, 50%, 70%, 80%, 90%, 95%, 100% ethanol and xylol for 5 minutes per solution. Coverslips were affixed to the slides with mounting medium to protect the tissue sections.

Tissue sections were imaged using a Leica DRMB microscope with a ProgResC12 (Jenoptik) Camera. Lung tissue sections were scanned using Aperio AT2 Leica slide scanner.

Donor/Infection	HIS NSG	PBS NSG	B6	Analysis
FL8730 24 CFU	11 mice %CD45 18-38	7 mice	6 mice	Weight, survival, bacterial burden and histopathology
FL4250 15 CFU	10 mice %CD45 27-50	10 mice	6 mice	Weight, survival, bacterial burden and histopathology
FL4390 23 CFU	10 mice %CD45 13-41	10 mice	10 mice	Weight, survival, bacterial burden and histopathology

Table8. Cohort for model establishment

Donor/Infection	HIS NSG D14	HIS NSG D21	HIS NSG D28	Analysis
FL4397 %CD45 5-50 24 CFU	6 mice	6 mice	6 mice	Bacterial Burden Cell phenotypic analysis Immunohistopathology
FL3008 %CD45 8-54 15 CFU	6 mice	6 mice	6 mice	Bacterial Burden Cell phenotypic analysis Immunohistopathology Biomolecules characterization
FL9129 %CD45 10-52 23 CFU	10 mice	6 mice	6 mice	Bacterial Burden Cell phenotypic analysis Immunohistopathology

Table9. Cohort for disease kinetics

Results

Establish the model

Human immune reconstitution of NOD/SCID/IL2r^γnull mice

Newborn (1-3 days old) NOD/SCID/IL2r^γnull (NSG) mice received human fetal liver CD34⁺ HSCs via intra-hepatic injection after undergoing sub lethal irradiation of 100 cGy. The mice were bled 10 weeks post engraftment and peripheral leukocytes were analyzed via flow cytometry to assess the reconstitution of the human immune cells in comparison to human donor blood.

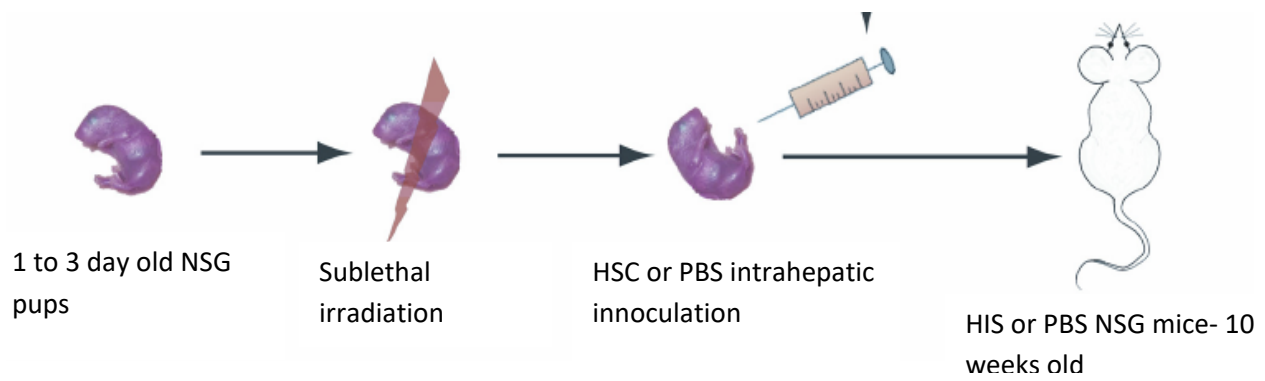


Figure15. Generation of Human Immune System mice. Newborn NSG pups were sublethally irradiated and subsequently injected with HSCs or PBS. At 10 weeks post-injection, human immune reconstitution levels was checked in the peripheral blood via flow cytometry analysis for common leukocyte marker CD45.

Frequencies of human CD45 pan-leukocytes exceeded 2% in the blood by 3 months and were quite variable between each mouse (2-80%) and each donor graft (> 9 donors). Peripheral blood human CD45⁺ cells developed into granulocytes, monocytes and lymphocytes (Figure 16). The lymphocytes consisted CD4⁺ helper T cells, CD8⁺ cytotoxic T cells and CD19⁺ B cells (Figure 17). In my hands, in line with previous findings, reconstitution of the human immune system was successfully achieved and these mice were termed HIS NSG (204). Depending on the size and age of the fetal liver (16-24 weeks), cohorts of 10-50 mice were generated per individual donor graft. Simultaneously, some of the NSG littermates underwent the same conditioning but were injected with phosphate buffer saline (PBS). These mice were termed PBS NSG and were used as controls.

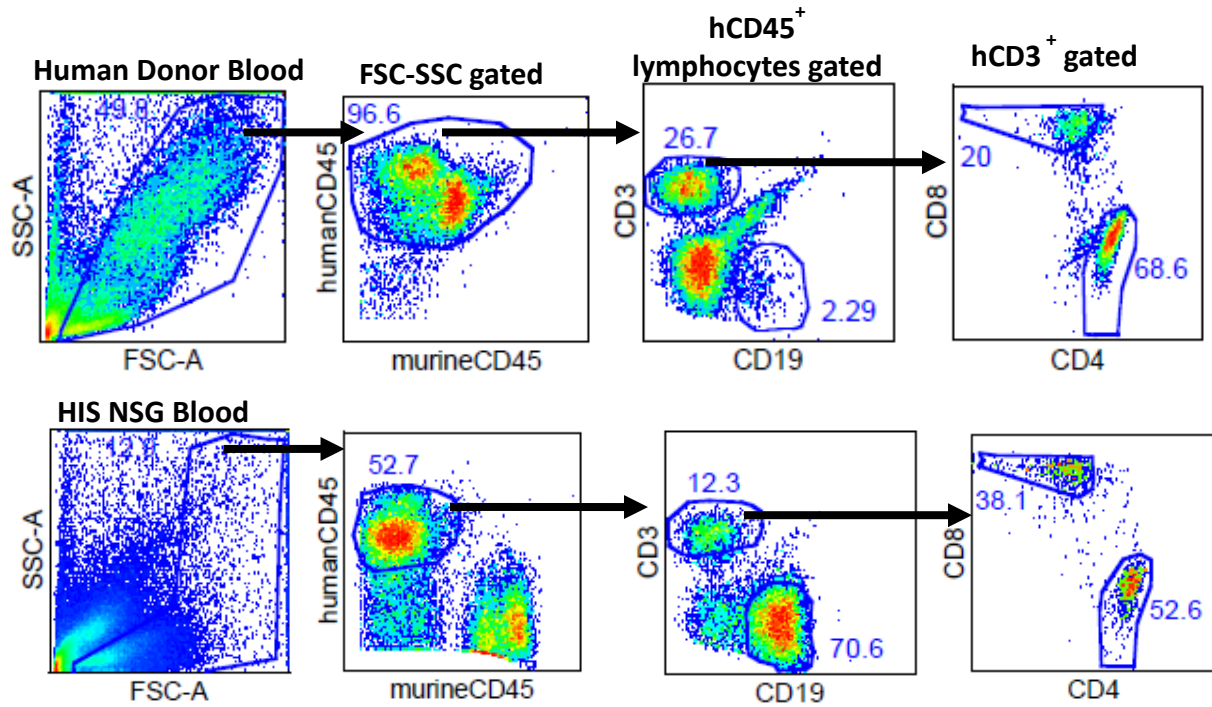


Figure16. Human immune cells reconstitution in peripheral blood. Representative dot plots of human CD45 and mouse CD45 cells. Dot plots show flow cytometric gating strategy applied to identify human leukocytes populations (FSC/SSC leukocytes → human CD45⁺ leukocytes → human CD3⁺ T cells/human CD19⁺ B cells → human CD4⁺ helper T cells and human CD8⁺ cytotoxic T cells)

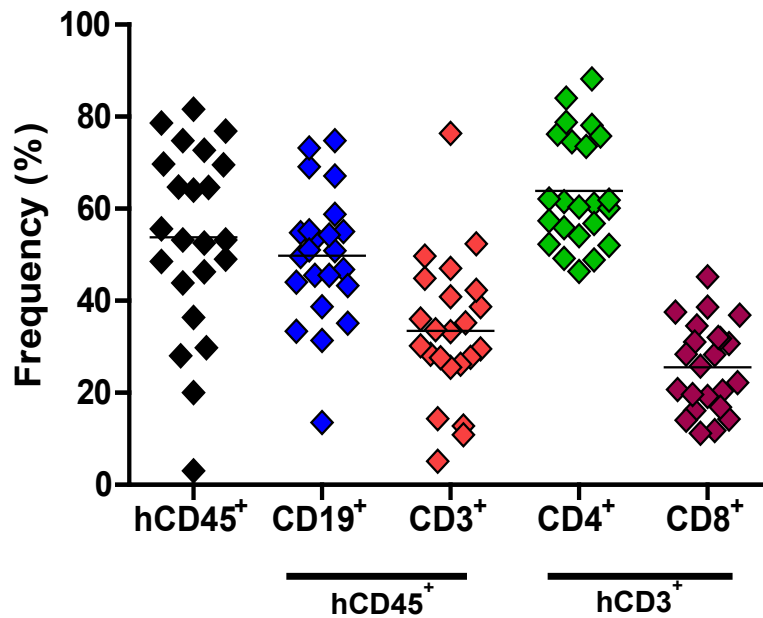
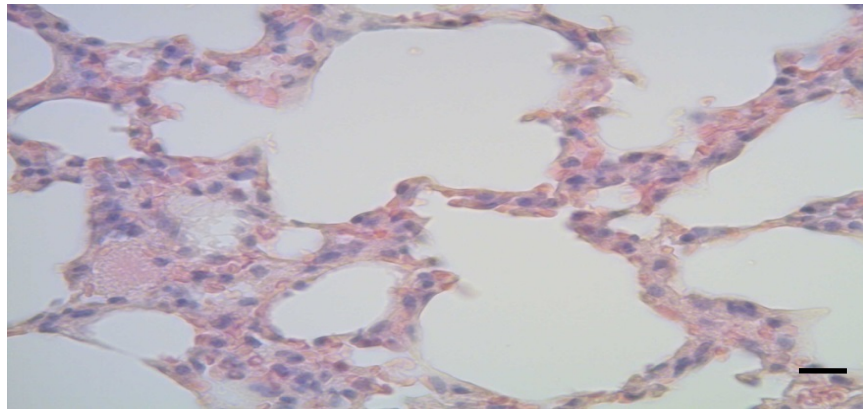


Figure17. Human immune cell frequencies in peripheral blood. Frequencies of the respective immune compartments in the peripheral blood of HIS NSG mice 10 weeks post-transplantation (n=23) reconstituted from the same donor are shown. Each symbol represents an individual mouse. Frequencies of CD3⁺ T cells and CD19⁺ B cells within human CD45⁺; and frequencies of CD4⁺ and CD8⁺ T cells within CD3⁺ cells are indicated. Horizontal bars represent means.

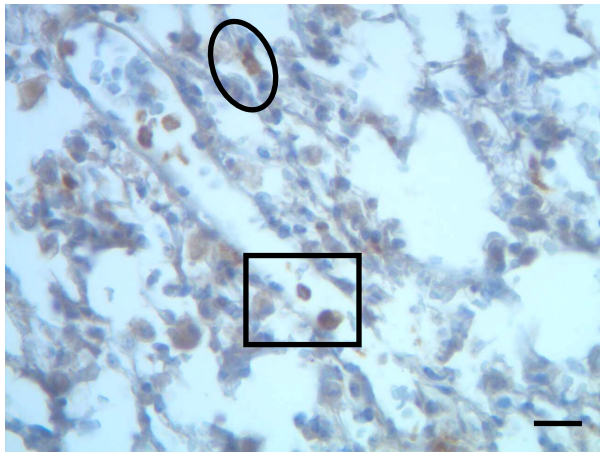
A.

HIS NSG Naïve Lung



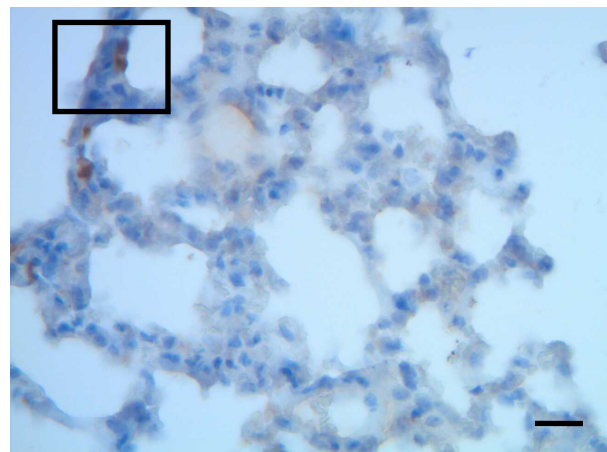
B.

CD68 macrophages



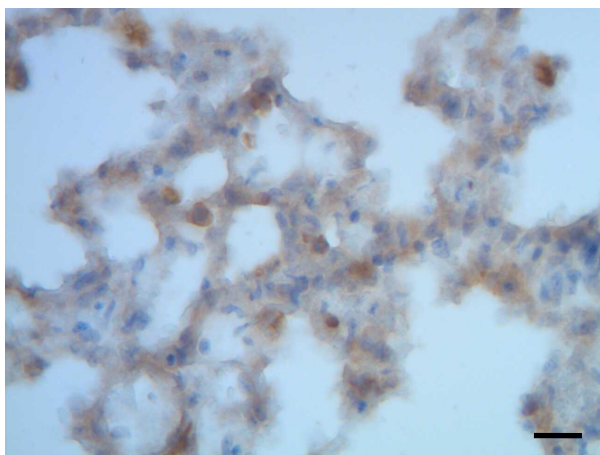
C.

CD15 neutrophils



D.

CD3 T cells



E.

CD20 B cells

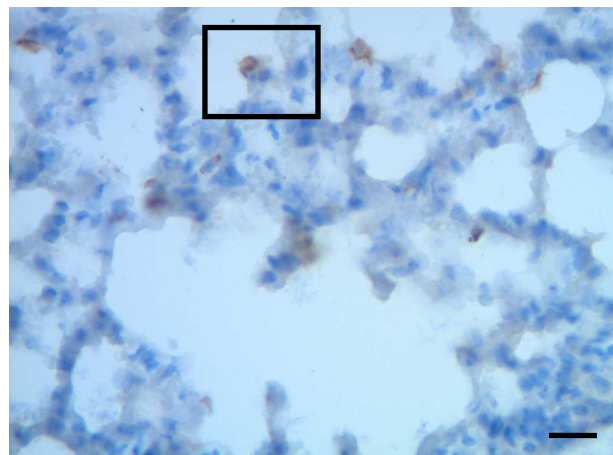


Figure18. Human immune cells reconstitution in naïve lung. Representative tissue sections of HIS NSG mice lung 10 weeks post-transplantation. (A) Hematoxylin and Eosin 400X, scale bar=40um. Immunostaining with human CD68 (B), human CD15 (C), human CD3 (D) and human CD20 (E) at magnification of 400X, scale bar=50um

To determine the extent of human immune cell reconstitution and penetrance in the main organ of interest-the lung; some HIS NSG mice were sacrificed and immunohistochemistry using human antibodies was carried out on lung tissue sections as described in the material and methods. Naïve HIS NSG lung tissue morphology had a sponge like appearance with large alveolar spaces (Figure 18A) with a spatial distribution of alveolar CD68 macrophages (Figure 18B box) and parenchymal CD68 macrophages (Figure 18B oval). CD15 neutrophils (Figure 18C box), CD3 T cells (Figure 18D) and CD20 B cells (Figure 18E box) were also detected and these cells were located in the lung parenchyma. Collectively, these findings show that the HIS NSG mice generated in this cohort had the essential human immune cells that are necessary for *Mycobacterium tuberculosis* infection studies.

Gross characterization of *Mycobacterium tuberculosis* infection in HIS NSG mice

A cohort of 12 weeks post-engraftment HIS NSG and PBS NSG mice were infected with an ultra-low dose of aerosolized Mtb H37Rv (15-30 CFU). HIS NSG mice in this cohort had frequencies of human CD45⁺ in the peripheral blood ranging from 10-50% pre-infection. In addition, 12 week old C57BL/6 (B6) mice; the mouse strain traditionally used in TB research were simultaneously infected at this dose as a supplementary control (Figure19).

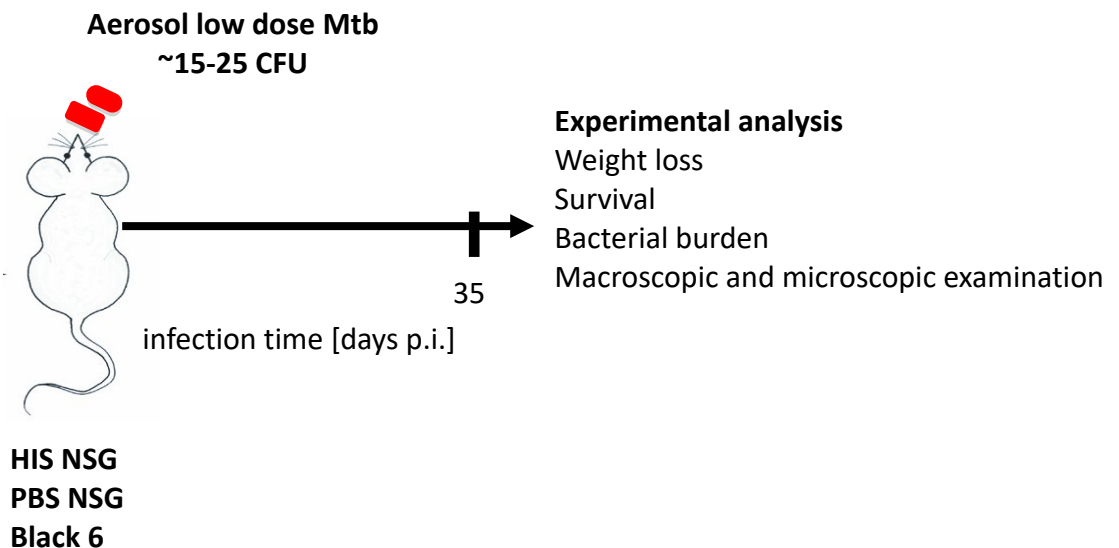


Figure19. Aerosol tuberculosis infection of HIS NSG mice. Experimental scheme of 12 weeks post engrafted HIS NSG mice with experimental readouts that were carried out on days 30-35 post infection.

All the HIS NSG and PBS NSG mice exhibited clinical symptoms such as lethargy and weight loss starting from day 25 post infection (Figure 20A). In contrast, the B6 mice maintained and even gained weight from day 25 post infection in accordance with previously published reports (257). The HIS NSG and PBS NSG mice succumbed to infection by day 33 to day 35 post infection (Figure 20B), indicating that the HIS NSG and PBS NSG mice are susceptible to an ultra-low dose of aerosolized TB.

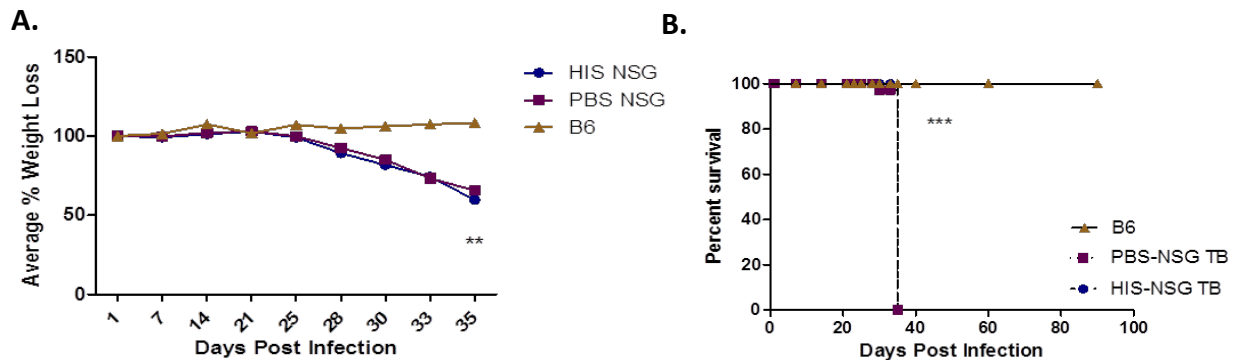


Figure 20. HIS NSG mice are susceptible to aerosolized tuberculosis. HIS NSG mice (n=10), PBS NSG mice (n=10) and B6 mice (n=10) after ultra-low dose aerosol infection with H37RV were monitored for (A) weight loss and (B) survival- Kaplan-Meier. This figure is representative of three independent experiments. (***) $p < 0.001$, ** $p < 0.01$)

Postmortem macroscopic examination was performed on major organs at day 35 post infection. All three groups were observed to have lung lesions (Figure 21C). In addition, we observed that HIS NSG and PBS NSG mice exhibited splenic lesions/granulomas (Figure 24B) and spotting on the liver and kidneys. No gross pathological changes were observed in other organs. Bacterial loads were enumerated in the lung, spleen, liver, kidney and bone marrow of HIS NSG and PBS NSG mice. The immunodeficient background of the NSG mouse precludes lymphnode development due to a lack of murine T cells and B cells; hence a comparison of HIS NSG lymphnodes to PBS NSG lymphnodes was not feasible (Figure 25D). The lung bacterial load and lung weight/body weight ratio of HIS NSG was significantly lower than that of PBS NSG by day 35 post infection (Figure 21A and B). The bacterial load in other organs such as the spleen (Figure 22A), liver (Figure 25A), kidney (Figure 25B) and bone marrow (Figure 25C) was similar in the HIS NSG and PBS NSG mice. This data indicates that there was active bacterial replication in the lung followed by bacteria disseminating to other organs of interest as the disease progressed.

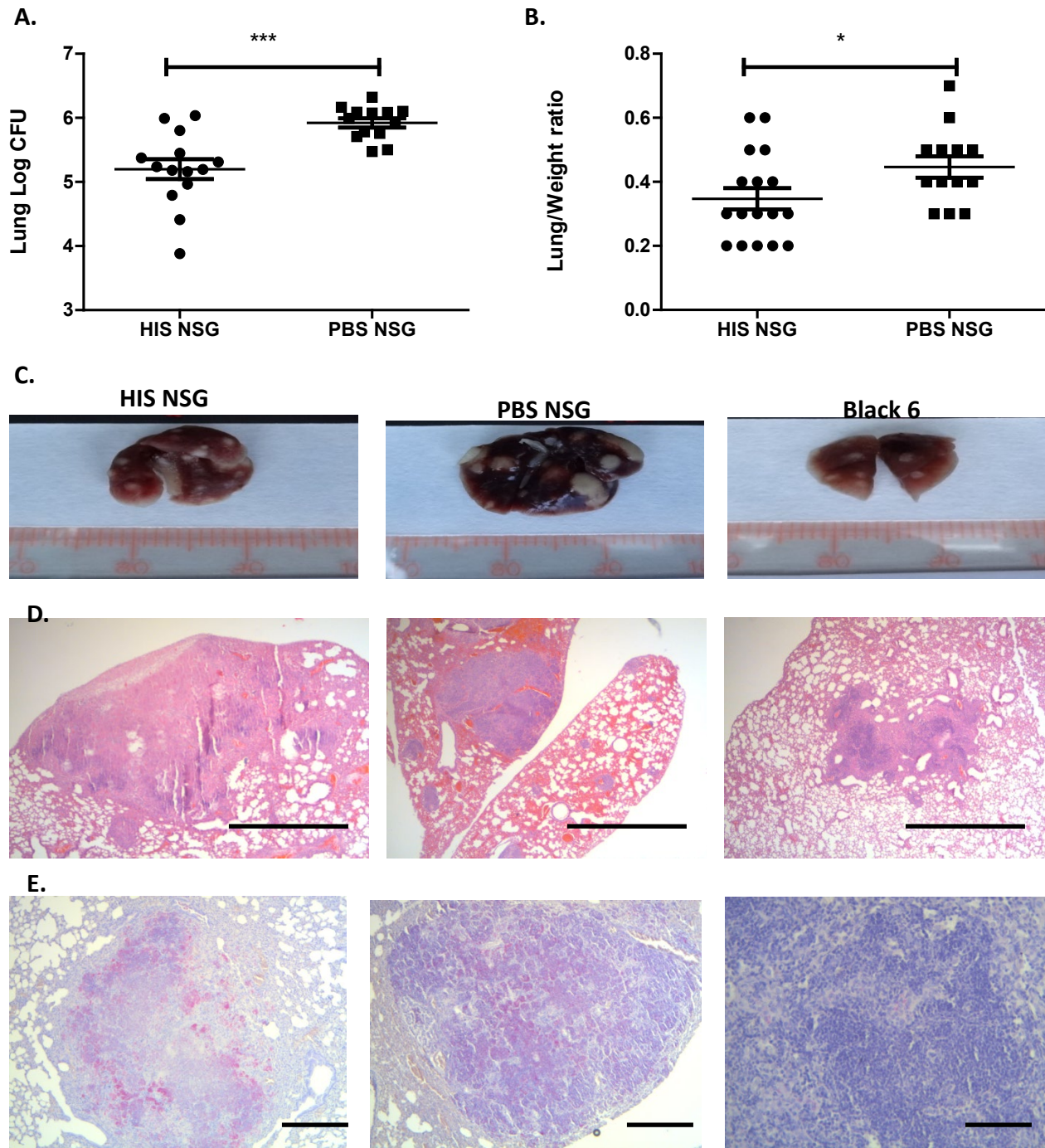


Figure 21. HIS NSG mice develop lung lesions upon Mtb infection. Bacterial burden (A) and lung/weight ratio (B) was determined at day 35 post infection. Macroscopic (C-Photographs) and microscopic analysis (D-Hematoxylin and Eosin 25X, scale bar=1000um) of lesions in representative HIS NSG, PBS NSG and Black 6 lungs was performed in addition to Mycobacterial identification (E-Ziehl-Neelssen 50X, scale bar=500um). Data was pooled from three independent experiments. (***) $p < 0.001$, (*) $p < 0.05$

In order to determine if a human like disease pathology was developed following Mtb infection, hematoxylin and eosin analysis was performed on left lung tissue sections. In B6 lungs at day 35 post infection, the lesions were comprised of non-necrotic aggregates made up of macrophages surrounded by lymphocytes (Figure 21D). Day 35 post infection PBS NSG granulomas on the other hand consisted of non-necrotic myeloid aggregates (Figure 21D). Meanwhile, HIS NSG lungs at day 35 post infection contained various granulomas which ranged from small non-necrotic myeloid aggregates, coalesced lung parenchyma and most interestingly caseous necrotic granulomas (Figure 21D and 22A). The caseous necrotic granulomas had a core that consisted of myeloid necrotic debris; an inner myeloid rim and an outer lymphocyte cuff (Figure 21D). This pathology is a characteristic feature seen in most active TB patients (Figure 22B). A characteristic of human TB granulomas called langhans giant cells which arise when epitheloid macrophages are fused, (Figure 22B arrow heads) were not found in HIS NSG granulomas.

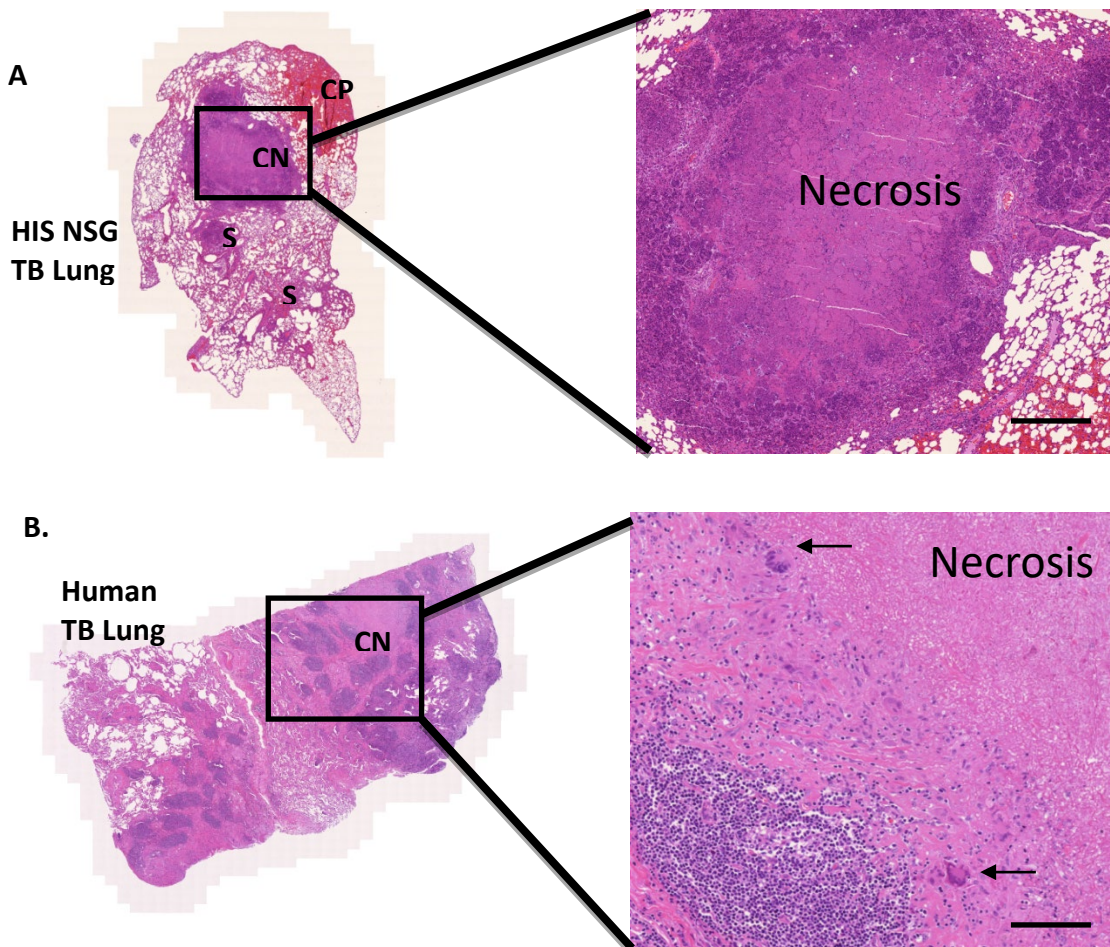


Figure22. HIS NSG mice develop human like caseous necrotic granulomas. Various lesions were observed in representative HIS NSG lung sections (A); S=solid non-necrotic granulomas, CP=coalesced parenchyma and CN=caseous necrotic granuloma. HIS NSG caseous necrotic granuloma was compared to one from a TB patient. Arrows indicate in human sample indicate giant cells. Tissue slide scan, Hematoxylin and Eosin 50X, scale bar=500um

To determine bacteria location, ziehl nielsen staining was performed on lung tissue sections. B6 and PBS NSG myeloid aggregates contained intracellular bacilli (Figure 21E) whereas the HIS NSG caseous necrotic granulomas had extracellular bacteria in the necrotic core (Figure 23) and intracellular bacteria in the myeloid inner rim (Figure 23). This data supports the speculation that Mtb is an intracellular pathogen that changes the host environment to become more extracellular in readiness for transmission.

A.

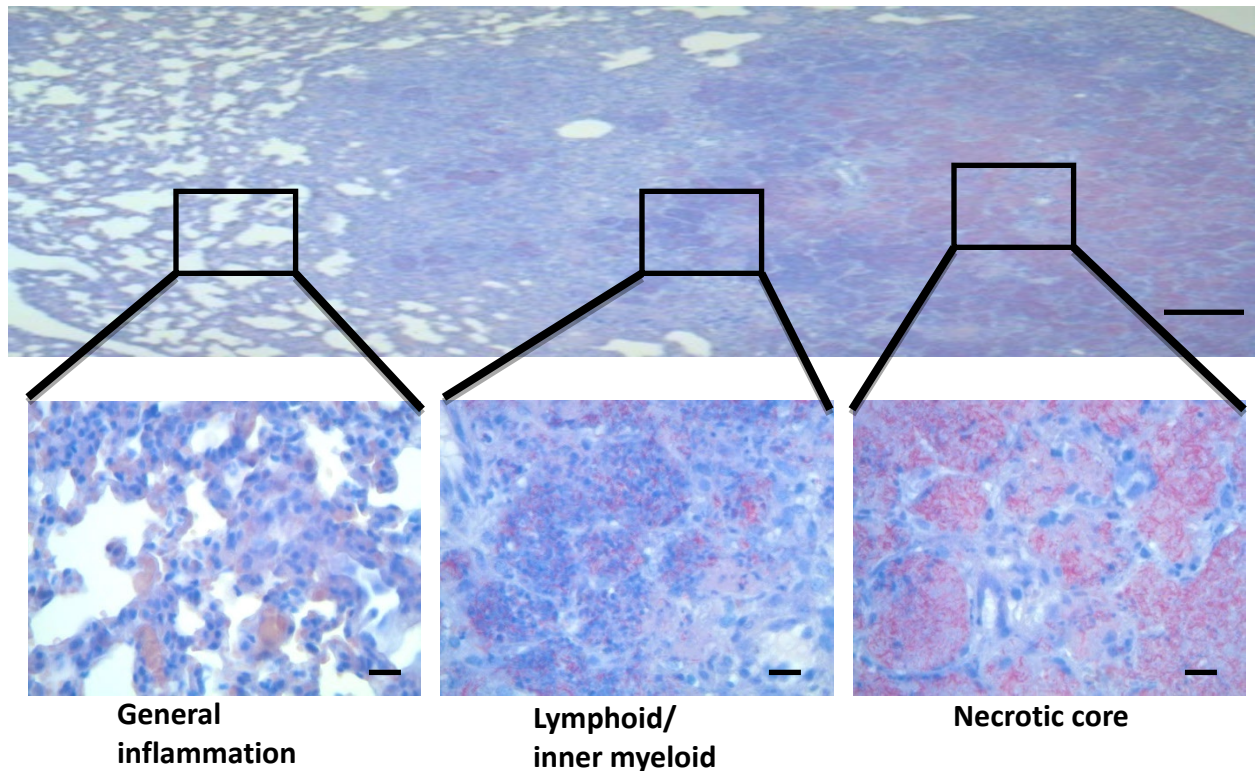


Figure23. HIS NSG mice caseous necrotic granulomas have Mtb in the center. A higher power view (B) of a Ziehl-Neelssen stain was taken of a representative HIS NSG lung (A) in order to demonstrate the zones in which intracellular and extracellular Mtb are located in caseous necrotic granulomas. (50X, scale bar=500um; 400X, scale bar=50um)

Splenic caseous necrotic granulomas whose centers were filled with extracellular bacteria were also observed in HIS NSG mice day 35 post infection (Figure 24B, C and D), whereas PBS NSG mice had non necrotic splenic aggregates that consisted of myeloid cells with intracellular

bacteria. There were no granulomas in the B6 spleen at day 35 post infection with few to undetectable intracellular bacteria. Collectively, these data suggests that the HIS NSG mouse has the ability to model active progressive disseminated TB with the associated human-like lung pathology.

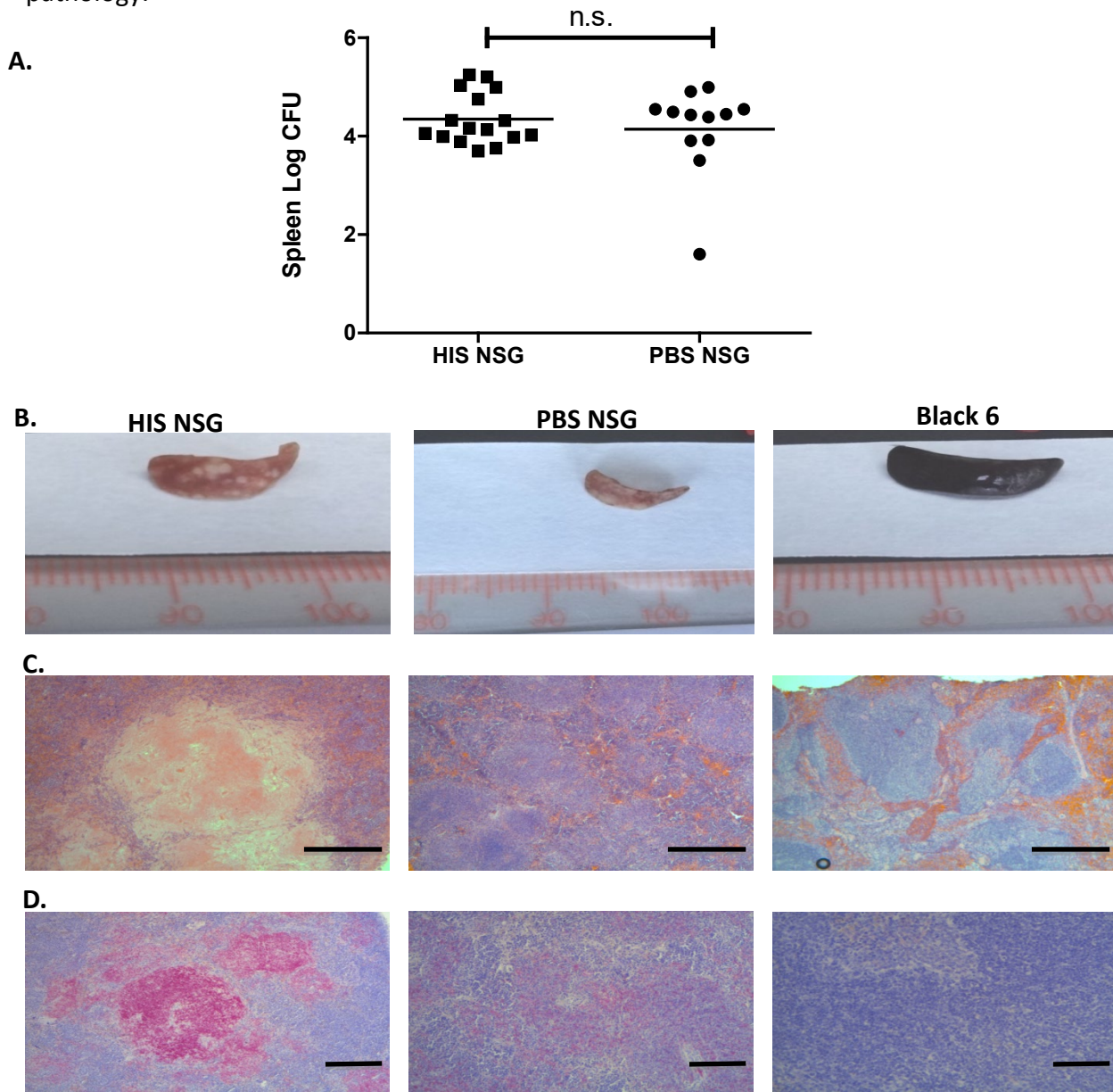


Figure 24. HIS NSG mice develop splenic lesions upon Mtb infection. Bacterial burden (A) was determined at day 35 post infection. Macroscopic (B-Photographs) and microscopic analysis (C-Hematoxylin and Eosin 50X, scale bar=500um) in representative HIS NSG, PBS NSG and Black 6 spleens was carried out in addition to Mycobacterial identification (E-Ziehl-Neelsen 100X, scale bar=200um). Data was pooled from two independent experiments. (n.s. =no significance)

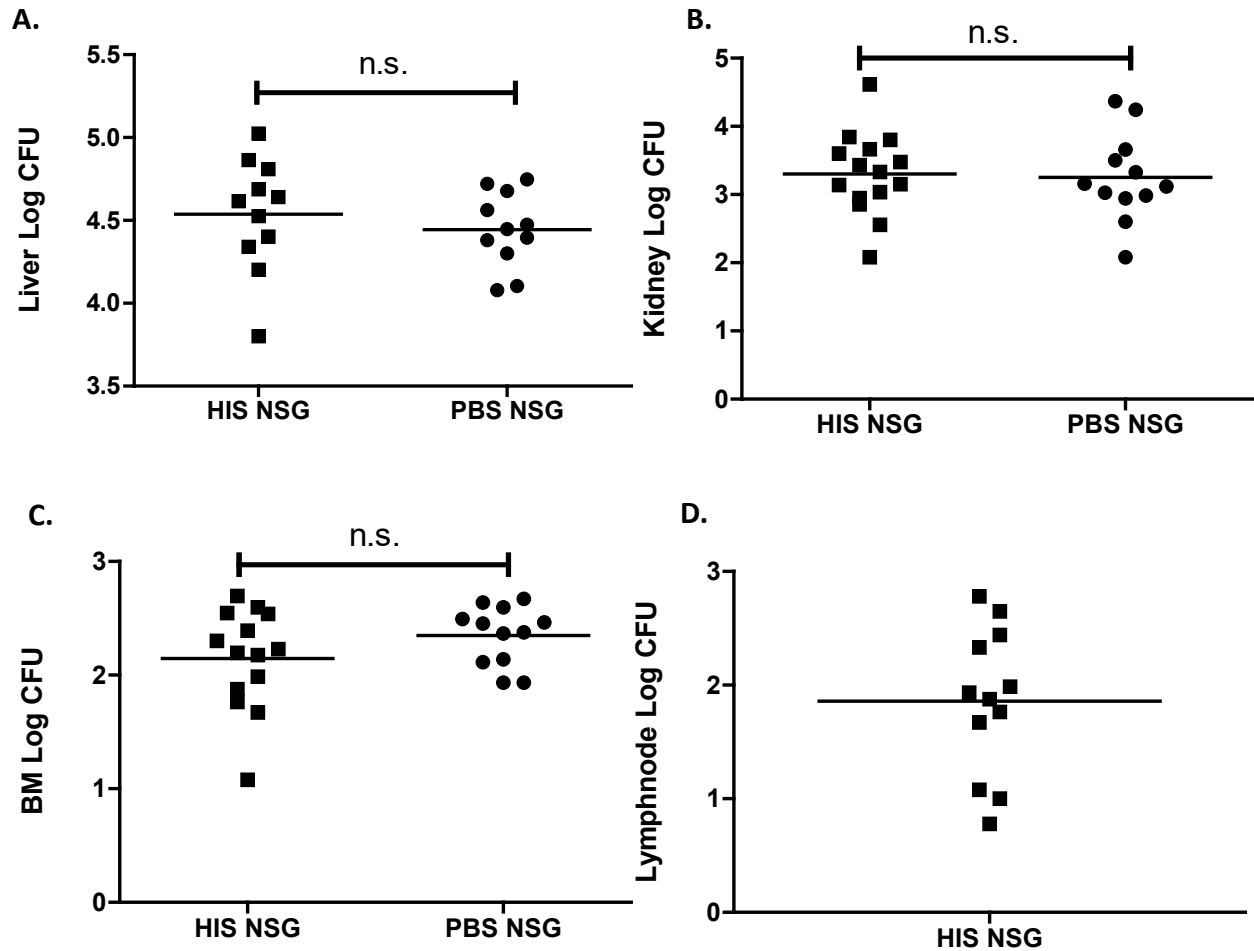


Figure 25. HIS NSG mice show signs of disseminated TB in other organs. Bacterial burden was determined at day 35 post Mtb infection in HIS NSG and PBS NSG liver (A), kidney (B), bone marrow (C) and in cervical, axial and brachial lymphnodes (D). Data was pooled from two independent experiments. (n.s. =no significance)

Kinetics of the pulmonary human immune response post Mtb infection

In order to broadly characterize the lung transformation from a myeloid spongy architecture to a myeloid/lymphoid organized biomass; minimal cell phenotype, biomolecules, bacterial burden and cellular spatio-organization was assessed in HIS NSG mice in additional cohorts at specific time points. These time points were days 14, 21 and 28 post infections (Figure 26). The HIS NSG mice in these cohorts had frequencies of human CD45⁺ in the peripheral blood ranging from 5-54% pre-infection and were aerosolily infected with 20-50 CFU Mtb.

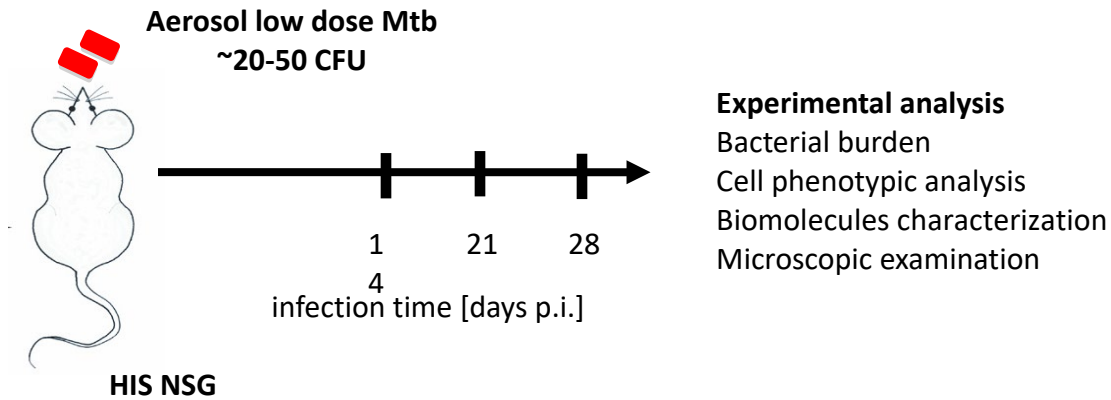
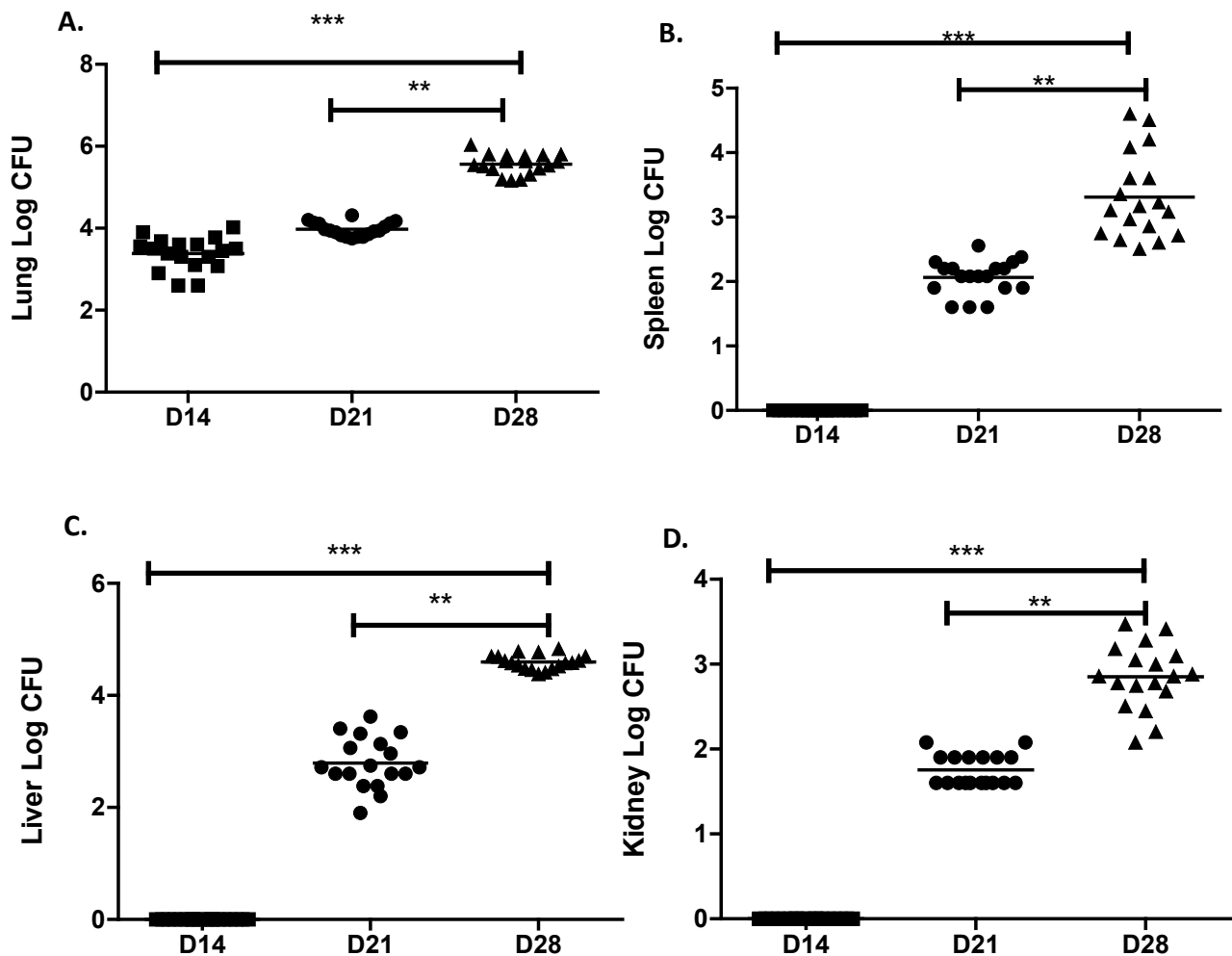


Figure 26. Aerosol tuberculosis infection of HIS NSG mice. Experimental scheme of 12 weeks post engrafted HIS NSG mice with experimental readouts that were carried out on a time course of days 14, 21 and 28 post infection.

It was observed that; at day 14 post-infection, bacteria was still contained in the lung (Figure 27A), but had disseminated to other organs such as the spleen, liver, kidney and bone marrow by day 21 post infection lung (Figure 27 B, C, D and E). There was a 2 log increase from day 14 to day 28 in the lung and from day 21 to 28 in the spleen, liver, kidney and bone marrow.



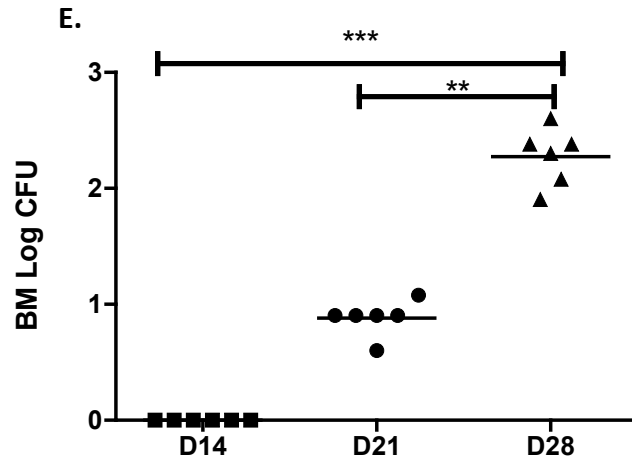


Figure 27. Tuberculosis disseminates from HIS NSG lungs as the disease progresses. Bacterial burden was determined at days 14, 21 and 28 post Mtb infection in HIS NSG lung (A), spleen (B), liver (C) kidney (D) and bone marrow (E). Data was pooled from three independent experiments for lung, spleen and kidney; n= 6 mice per time point (** $p < 0.001$, * $p < 0.05$).

Human leukocytes consisting of cells that are members of the innate and adaptive branches (Figure 28) were observed to infiltrate the lungs in increasing numbers from day 14 to day 28 post infection via flow cytometric analysis. There was a notable increase of human neutrophils defined as $CD45^+CD33^+CD66^+$, human dendritic cells defined as $CD45^+CD33^+CD11c^+$ and human monocytes/macrophages defined as $CD45^+CD33^+CD14^+$ in the lungs by day 28 post infection (Figure 29). The human $CD45^+CD3^+CD4^+$ T cells, human $CD45^+CD3^+CD8^+$ T cells and human $CD45^+CD19^+CD20^+$ B cells also increased in the lungs by day 28 post infection, albeit at lower levels in comparison to innate immune cells (Figure 29).

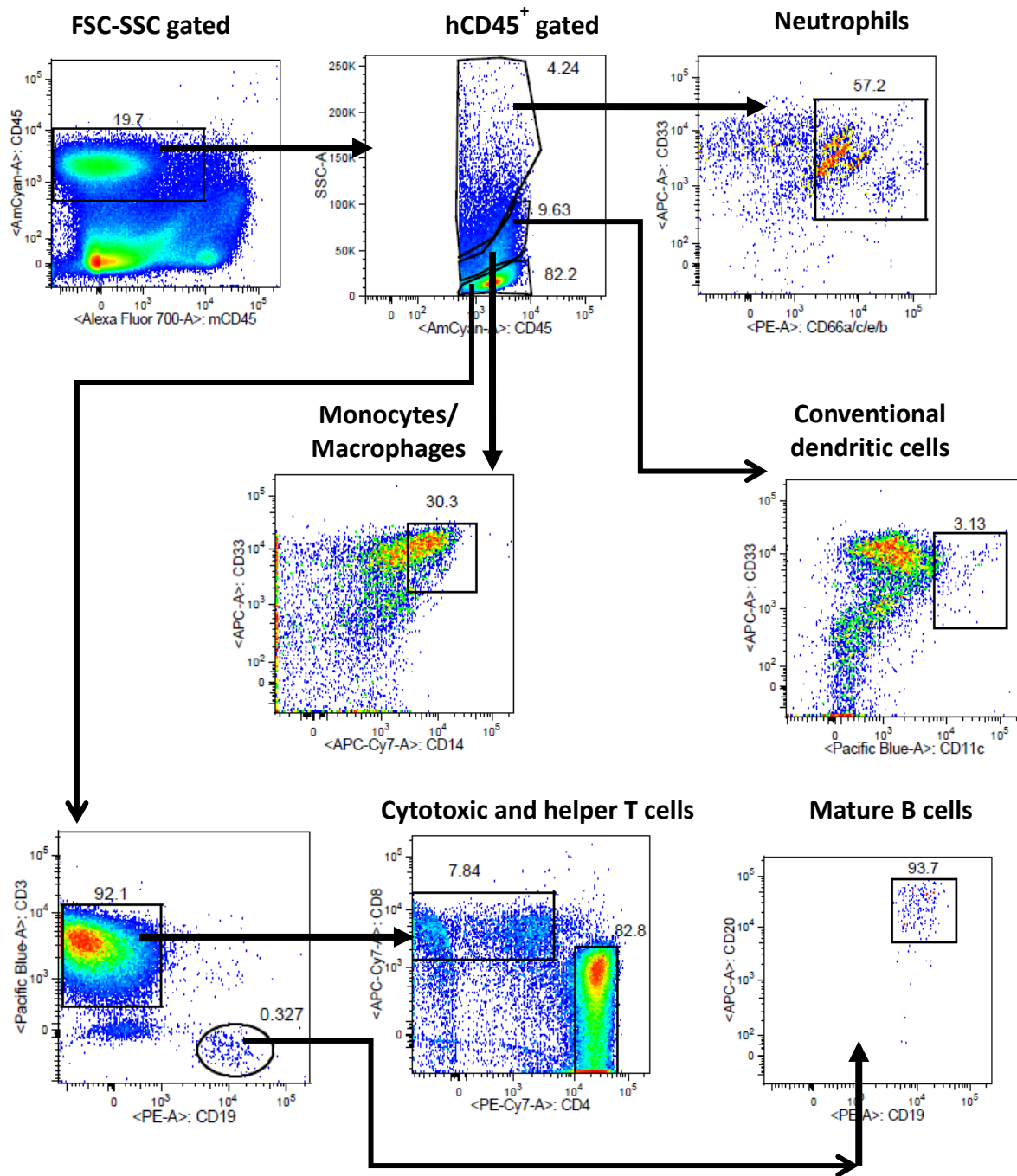


Figure 28. Human immune cells in HIS NSG lung. Representative dot blots show flow cytometric gating strategy applied to identify human innate and adaptive cells (FSC/SSC leukocytes → human CD45⁺ granulocytes → human CD33⁺CD66^{a/c/e/b} neutrophils; FSC/SSC leukocytes → human CD45⁺ monocytes → human CD33⁺CD14⁺ monocytes/macrophages; FSC/SSC leukocytes → human CD45⁺ monocytes → human CD33⁺CD11c⁺ dendritic cells; FSC/SSC leukocytes → human CD45⁺ lymphocytes → human CD3⁺ T cells and CD19⁺ B cells; human CD3⁺ T cells → CD4⁺ T cells and CD8⁺ T cells)

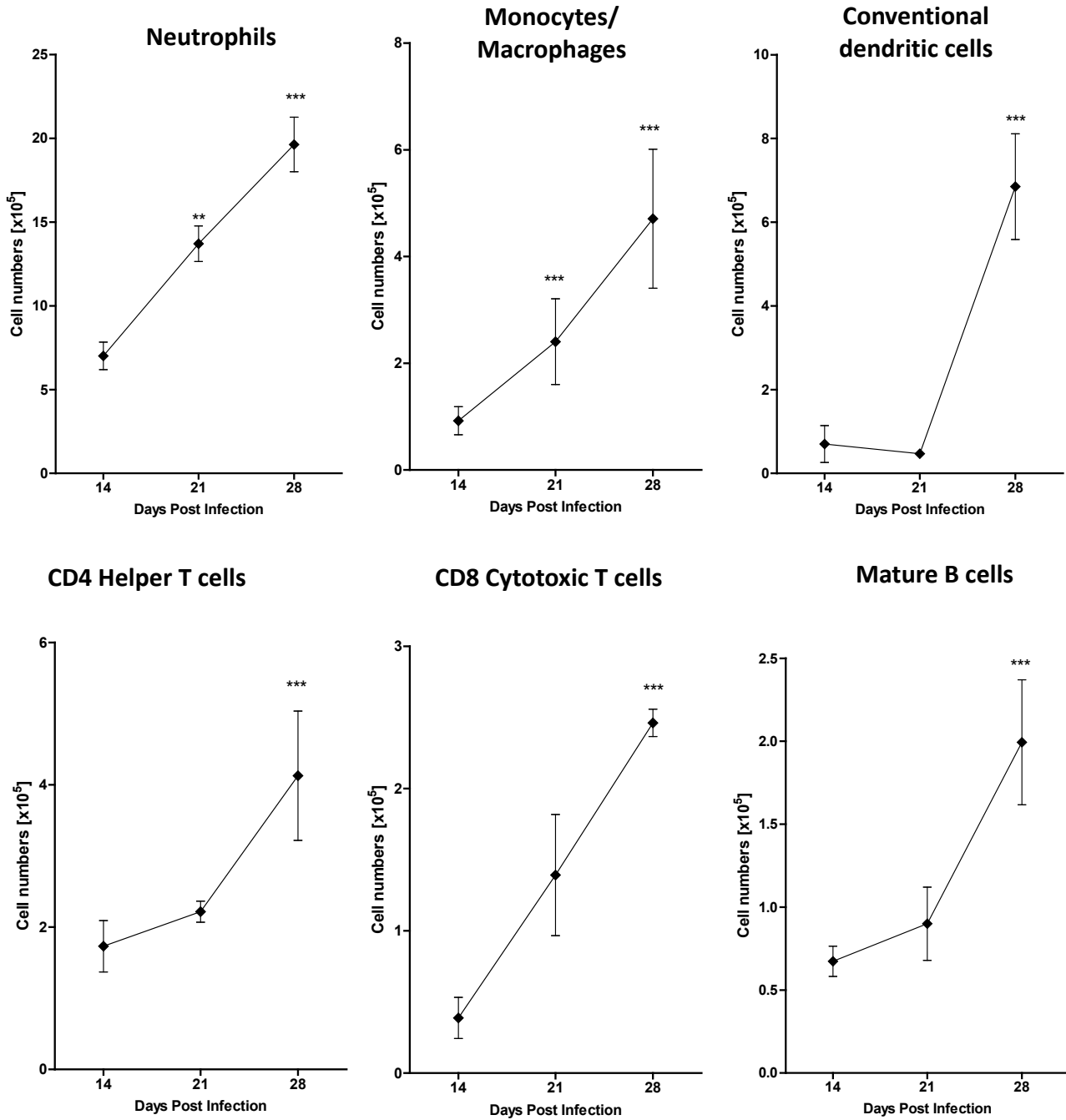
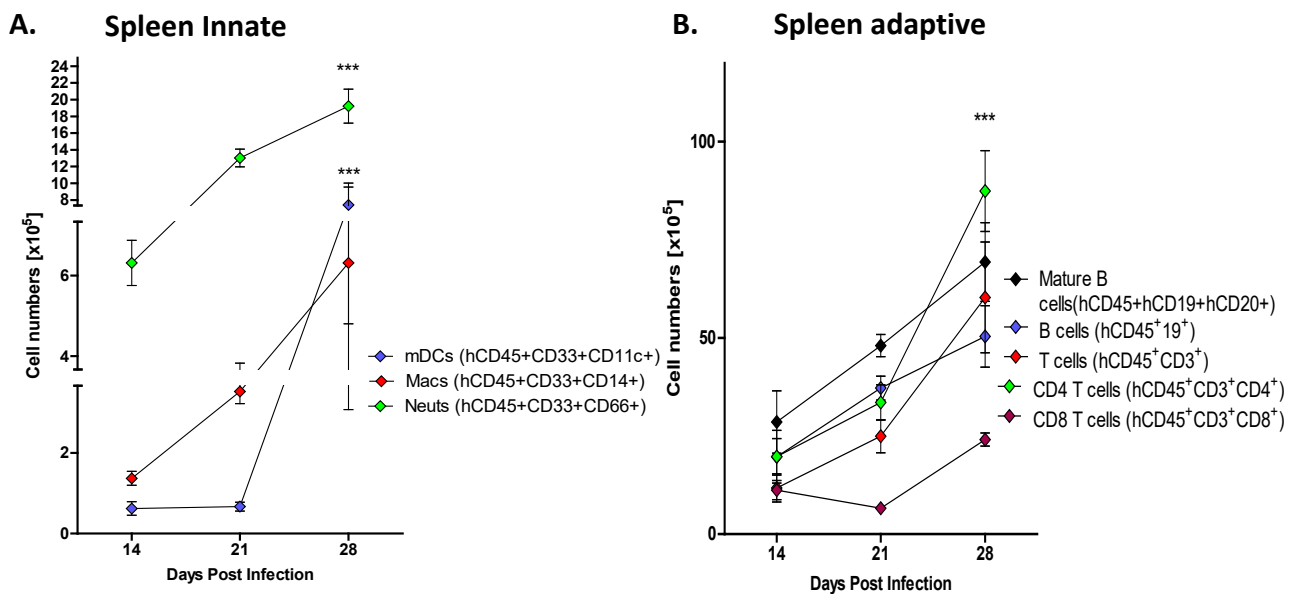


Figure 29. Human immune cells are recruited to the HIS NSG lung upon infection. Line graphs showing the absolute numbers of cells infiltrating the lung at time points 14, 21 and 28 post Mtb infection. Data from one representative experiment out of three independent experiments, n= 6 mice per time point (** p<0.01, *** p<0.001)

Kinetics of the human immune response in non-lung organs post Mtb infection

In order to assess whether Mtb infection also induces an immune response in other organs such as the spleen and bone marrow, flow cytometry analysis was also performed in these organs. Human immune cells of the innate and adaptive branches were also recruited into the spleen from day 14 to day 28 post infection. In contrast to the lung, whence the innate cells were recruited in vast numbers, the greatest number of recruited cells in the spleen consisted of human CD45⁺CD3⁺CD4⁺ T cells and human CD45⁺CD3⁺CD19⁺CD20⁺ B cells (Figure 30B). Human CD45⁺CD33⁺CD66⁺ neutrophils were still the largest population of splenic innate cells by day 28 post infection, followed by human CD45⁺CD33⁺CD11c⁺ dendritic cells and human CD45⁺CD33⁺CD14⁺ macrophages (Figure 30A). Interestingly in the bone marrow, the human CD45⁺CD33⁺CD11c⁺ dendritic cells (Figure 30C) were recruited to the bone marrow while the human CD45⁺CD19⁺ B cells egressed out of the bone marrow (Figure 30D). Thus these human CD45⁺CD33⁺CD11c⁺ dendritic cells may be migratory DCs carrying antigens and whole bacteria into the bone marrow while the human CD45⁺CD19⁺ B cells seem to be immature B cells that are egressing out of the bone marrow to required sites such as the lung and the spleen where they mature to CD45⁺CD19⁺CD20⁺ B cells. This collective data from the lung, spleen and bone marrow shows a dynamic movement of various immune cells between different organs in order to generate a local and systemic immune response to the Mtb infection.



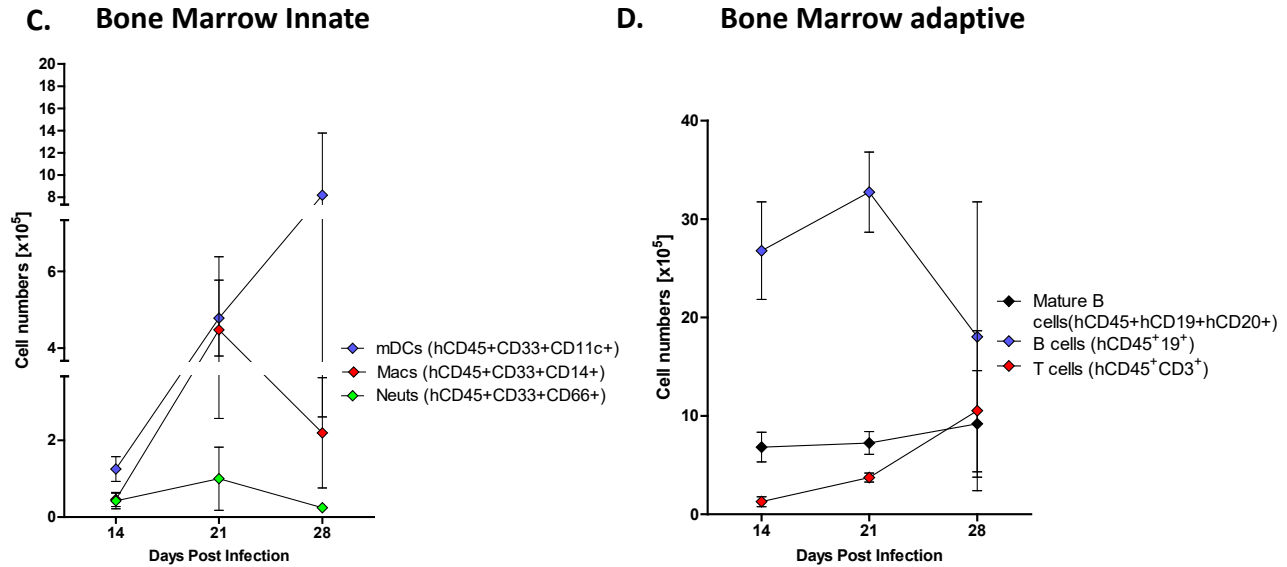


Figure 30. HIS NSG mice have a systemic immune response upon infection. Line graphs showing the absolute numbers of cells infiltrating the spleen and infiltrating/egressing in the bone marrow at time points 14, 21 and 28 post Mtb infection. Data from one representative experiment out of three independent experiments, $n = 6$ mice per time point (** $p < 0.01$, *** $p < 0.001$)

Kinetics of the human pulmonary biomolecules post Mtb infection

Immune/inflammatory biomolecules are involved in the recruitment of the various cells that are crucial in granuloma initiation and development; hence these biomolecules were assessed in lung homogenates. These biomolecules were categorized as pro-inflammatory cytokines, Th17 cytokines, Th2 cytokines, T cell regulation cytokines, T cell activation cytokines, chemokines, growth factors and B cell antibodies (Table 10). There was an increase in pro-inflammatory cytokines such as TNF- α , IL-1 β , IL-6 and IFN- γ and an increase in chemokines such as MCP-1 and IP-10 from day 14 to day 28 postinfection (Figure 31). There was also an increase in the anti-inflammatory IL-10 cytokine and a significant increase in the human specific neutrophil associated pro-inflammatory IL-8 chemokine. Furthermore, mucosal IgA antibody also significantly increased as the disease progressed. This mostly pro-inflammatory response is consistent with previous studies carried out in other animal models and TB human lung samples (ref). Thus the above data suggests that in the HIS NSG lung, a basic functional immune response is generated towards Mtb.

Cytokines and chemokines

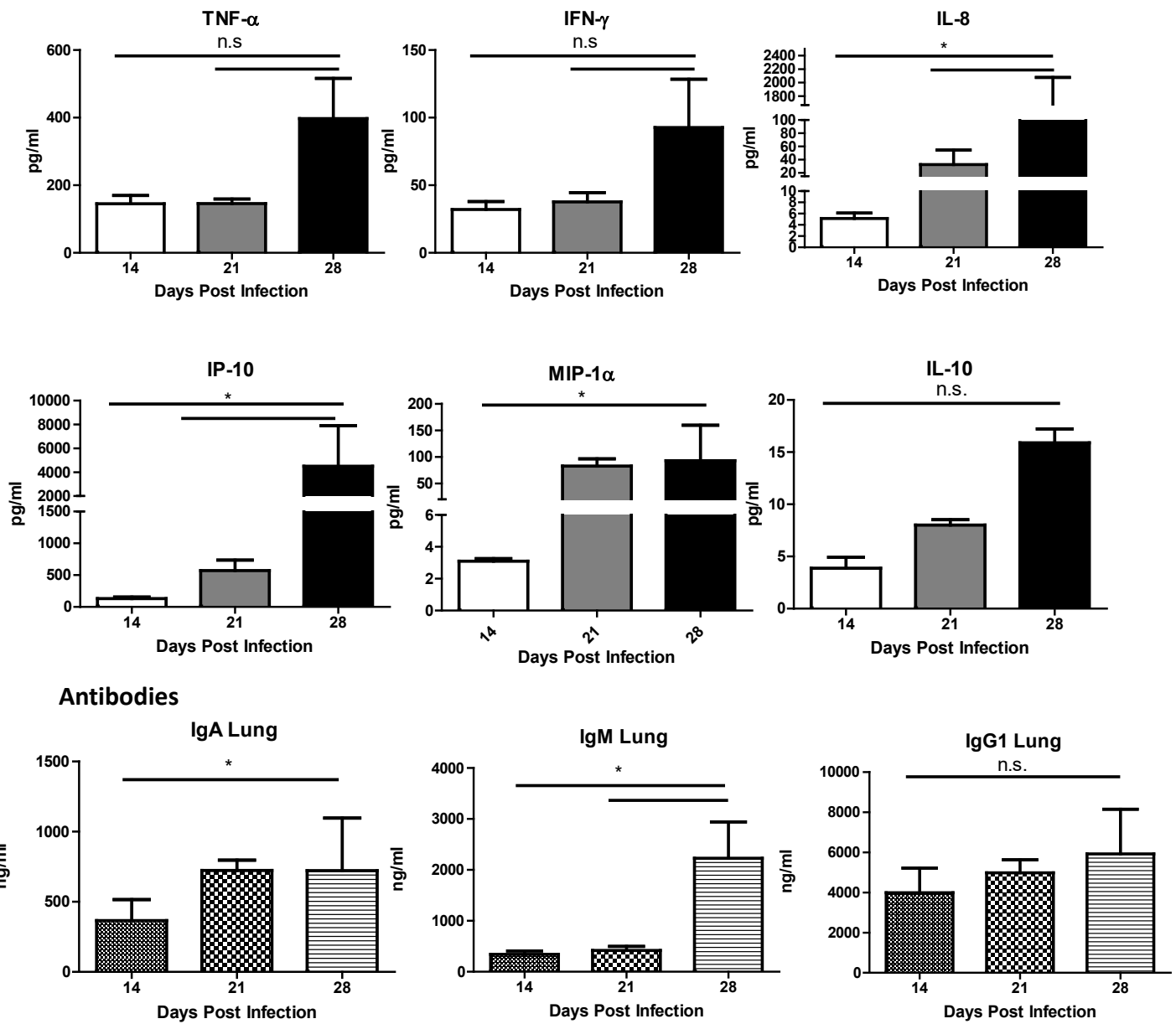


Figure 31. Human biomolecules are secreted in the HIS NSG lung upon infection. Bar graphs showing representative cytokines, chemokines and antibodies produced in the lung at time points 14, 21 and 28 post mtb infection. Data from one representative experiment out of two independent experiments, n= 6 mice per time point (***) p<0.001, ** p<0.01)

Category	Comment
Proinflammatory	Significant increase: IL-8, IL-1 β , IL-6, IL-1ra Increase: IFN-g, TNF- α Not detected: IL-2, IL-15
Th17	Not detected: IL-17
Th2	Increase: IL-9
T cell regulation	Increase: IL-10
T cell activation	No difference: IL-12p70
Chemokine	Increase: MCP-1, Eotaxin, Basic FGF, MIP1- α , MIP1- β , IP-10, RANTES
Growth Factor	Increase: G-CSF, GM-CSF, PDGF-BB, VEGF
Antibody	Significant increase: IgA, IgM Increase: IgG1; IgG2, IgG3, IgG4 No difference: IgE

Table10. Biomolecules characterized in HIS NSG lung

Spatial-organization of the lung human immune cells post Mtb infection

Biomolecules not only influence cell migration, but also influence cellular spatio-organization. In order to assess the reorganised lung architecture, left lung sections were stained and independently graded by a clinical pathologist (Provitro/ Charite Perlin Pathology). At day 14 post infection most HIS NSG lungs consisted of small non-necrotic myeloid aggregates surrounded by lymphocytes and non-involved tissue (Figure 32). At day 21 post infection, the lungs were mostly made up of coalesced parenchyma known as tuberculosis pneumonia while at day 28 post infection, granulomas consisted of a number of large non-necrotizing granulomas and large caseous necrotic granulomas with smaller adjacent caseous necrotic granulomas (Figure 32). Some HIS NSG mice regardless of the initial stem cell donor, had small caseous necrotic granulomas at day 14 and day 21 post infection; giving credence to the speculation that granuloma development is not necessarily linear in progression (ref). Cumulatively, these data demonstrate that the HIS NSG mouse has the ability to model lung granuloma initiation and formation with the associated human pulmonary immune response.

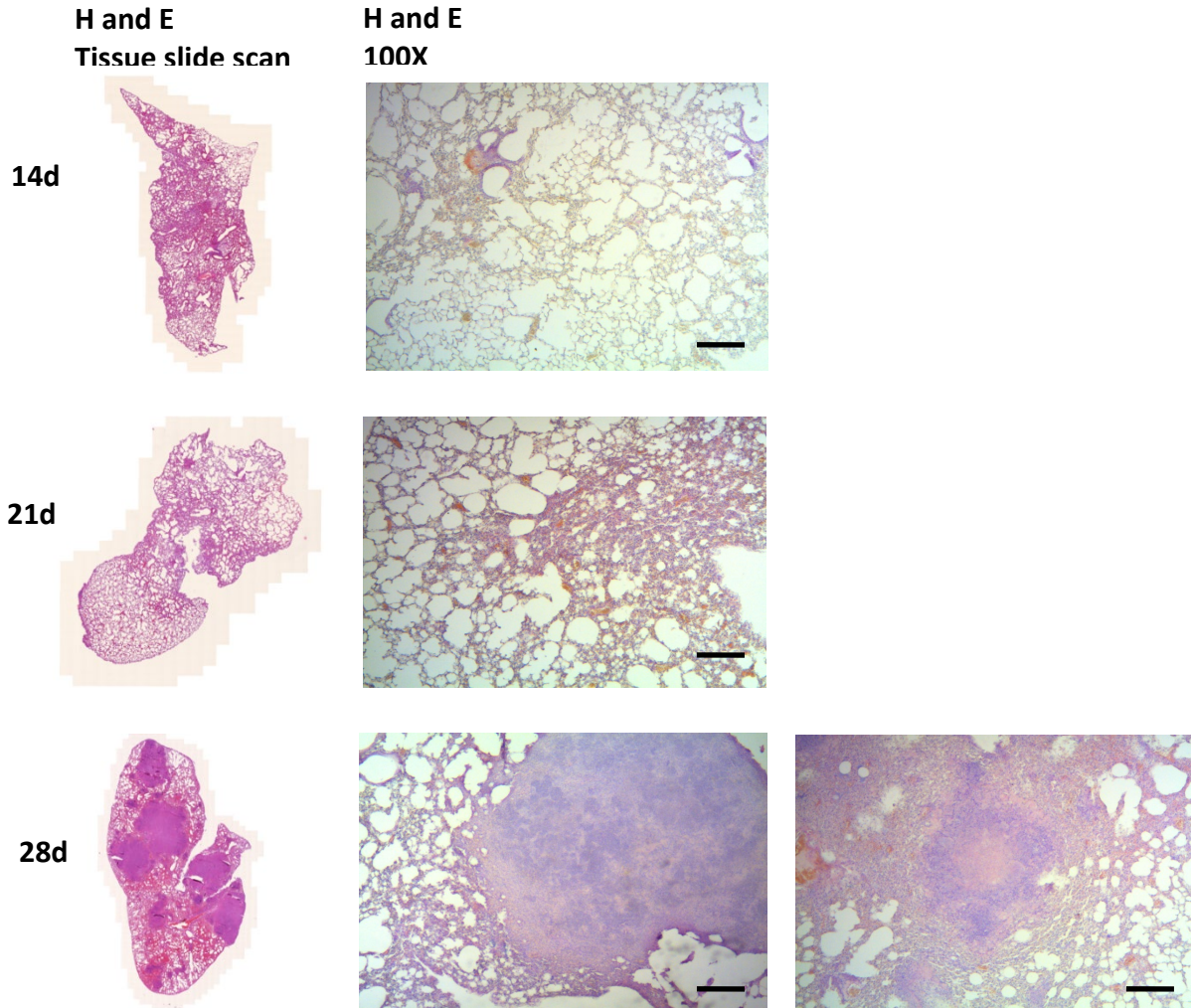


Figure 32. HIS NSG lung architecture changes as the disease progresses. Entire left lung lobes collected from representative HIS NSG mice at time points 14, 21 and 28 post Mtb infection showed increased loss of spongy architecture as the disease progressed. Hematoxylin and Eosin stain Tissue slide scan; Hematoxylin and Eosin stain 100X, scale bar=200um

Sequential lung tissue sections were also stained with CD68 macrophages, CD15 neutrophils, CD4 T cells and CD20 B cells in order to visually confirm the cell infiltration observed via flow cytometry. As the disease progressed, the lung infiltrates got more organized with the macrophages and neutrophils in the center, with more macrophages and neutrophils making an inner rim followed by T cells and B cells making an outer cuff by day 28 (Figure 33). In particular, caseous necrotic granulomas in the HIS NSG day 28 post Mtb infected lung had cell phenotypes that were organized in a pattern similar to that observed in active pulmonary TB patients (Figure 34).

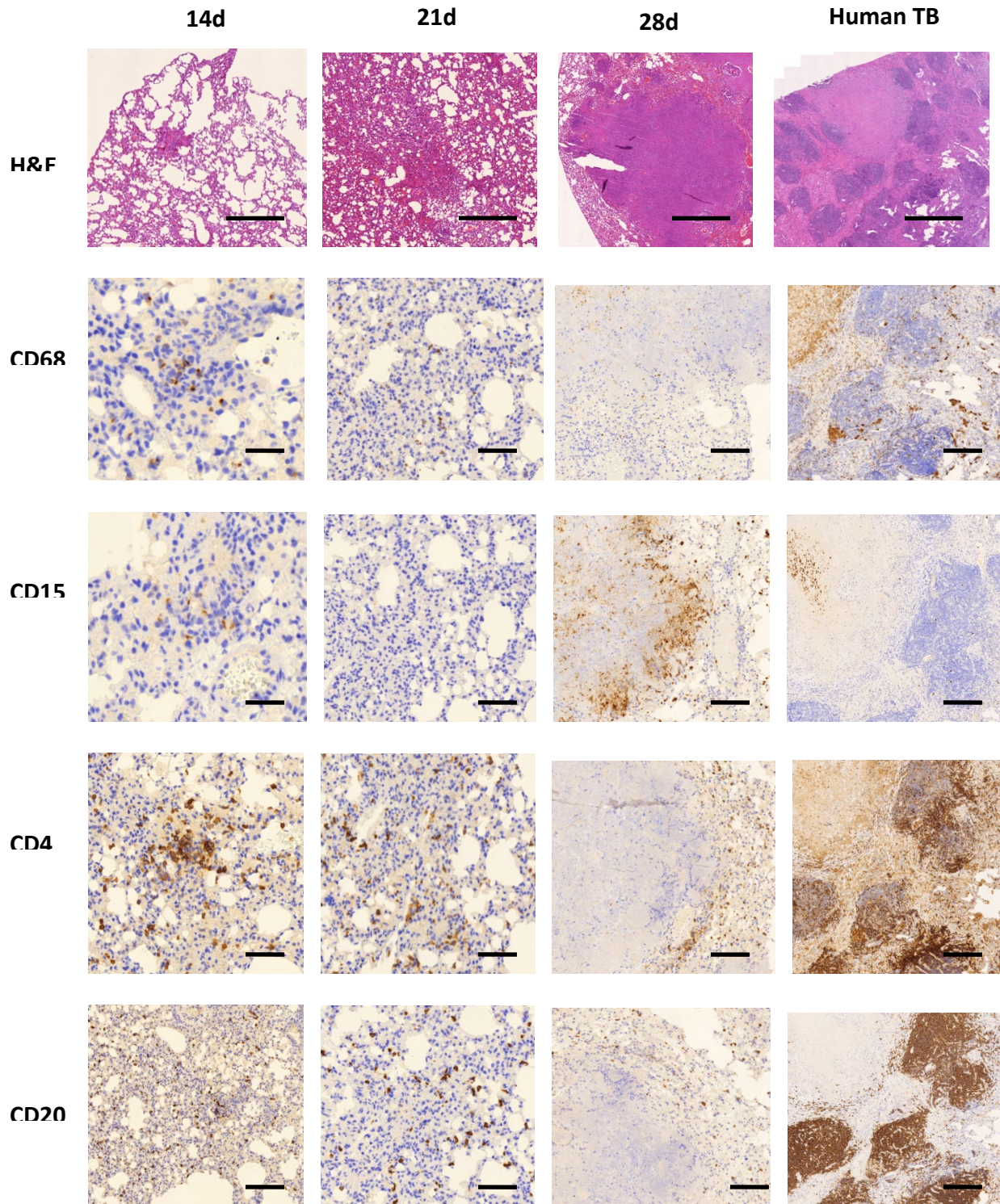


Figure33. Recruited human immune cells develop a human like organization. Microscopic analysis (Hematoxylin and Eosin 20X, scale bar=1000um) in representative HIS NSG lungs at d14, 21 and 28 post infection was carried out. In addition, Human immune-stains of CD68 macrophages, CD15 neutrophils, CD4 T cells and CD20 B cells was also performed (100X, scale bar=200um).

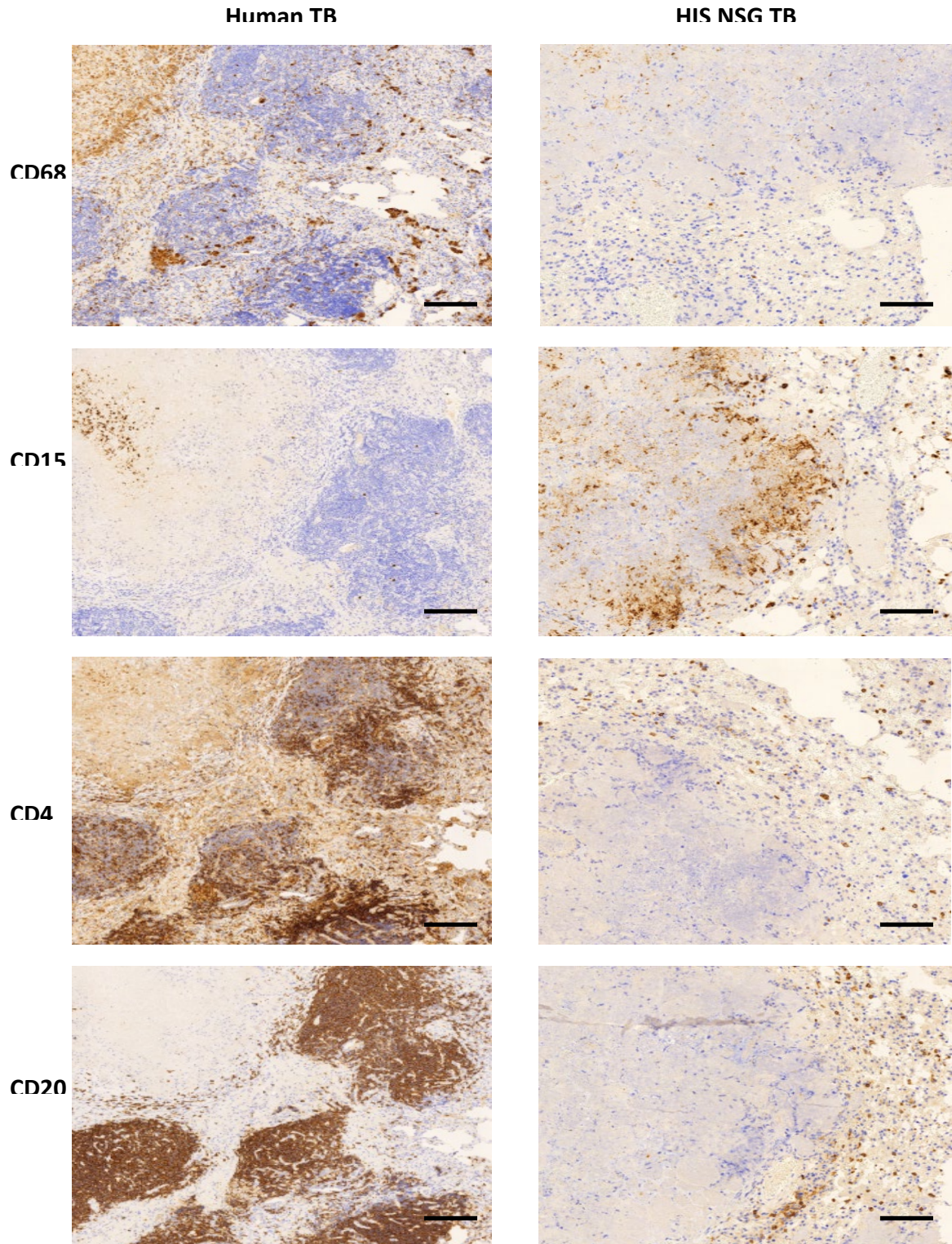


Figure34. Enhanced view of human like organization in HIS NSG lung. An enlarged high power view of human immune-stains of CD68 macrophages, CD15 neutrophils, CD4 T cells and CD20 B cells taken of a representative HIS NSG lung in order to compare to a human TB sample(400X, scale bar=50um)

Discussion

Human Immune System mouse as a model for Pulmonary Tuberculosis infection

As Robert Koch told his students; “Gentlemen, remember mice are not men” hence, even though the observations stated in this thesis add another animal model to the established coterie, caution should be taken in interpreting these results as the HIS mouse is still a chimera. Nevertheless, the purpose of a model is to restrict a system in a manageable format to provide answers despite certain limitations (279). These limitations include the presence of murine innate system, murine endothelium, murine epithelium and murine stroma. Hence, though the generated human mononuclear phagocytic network readily engulfs Mtb, some of the residual murine innate system and murine non-hematopoietic system also phagocytize Mtb. This dual species phagocytosis could influence the immune response that is consequently generated and this could have an influence on the end point pathology that has being described in this thesis.

The first question I posed in this model was the feasibility of using the fetal liver stem cell HIS mouse to investigate the development of pulmonary granulomas subsequent to aerosol Mtb infection. In this thesis I have therefore introduced a new small animal model that does develop human-like caseous necrotic granulomas containing human immune cells as the disease progresses. Furthermore, heterogeneous granuloma pathology in individual HIS mouse lungs samples and across various stem cell donors was also observed. These human-like granulomas had an immunephenotype and spatial organization reminiscent of pathological samples observed in some human patients; in particular to what is observed in pediatric or immunocompromised patients (232, 281). These granulomas ranged from solid non necrotic granulomas, tuberculoid pneumonia and caseous necrotic granulomas. This granuloma heterogeneity exhibited by the various donors is in line to what has been observed in infected NHPs but is lacking in traditional inbred mouse strains.

Nevertheless, there was one particular granuloma type absent in the HIS NSG mouse. These are cavitory granulomas which are observed in the upper lobes of 40-87% pulmonary TB patients. Cavitory granulomas are of great interest in terms of disease transmission, treatment response and the development of antibiotic resistance (282). Cavitory granulomas have been reported to

develop in some NHPs (39) and in rare instances in rabbits (283) and in the Kramnik mouse (284). A hodgepodge of reasons could explain the development of cavitary tuberculosis granulomas in humans and non-human primates but not in the HIS mouse. These include anatomical differences between large and small mammals, one primary infection versus multiple reinfections, sensitization prior to infection and the age at which TB infection occurs (child or adult) (285).

NHPs and humans are upright mammals whose lungs are anatomically designed as 3 right lobes and 2 left lobes while mice have 4 right lobes and 1 left lobe. NHPs and human lungs also have interlobular septae which helps in supporting lung weight (286). This interlobular structure is lacking in mice and rabbits. Due to the effects of gravity and being upright; the upper lobes have a higher alveolar pressure, higher diameter, reduced capillary density and less mobility (285, 287). The upper lobes also have less lymphatic drainage, less connectivity to the regional lymphnodes and less immunosurveillance in comparison to the lower lobes (285, 288). Therefore at the height of the infection all these factors in addition to lower breathing amplitude (289, 290) could allow for an increase in the number of bacilli in the upper lobe. This leads to an increased number of infected macrophages, an increased number of recruited neutrophils and eventually a necrotic cascade that is speculatively believed to lead to granuloma liquefaction and finally caseation. The correlation between being upright and the increased probability of developing cavitary granulomas in the upper lobes was shown in *Mtb* infected rabbits that were kept upright in a harness for 11 hours each day (291). Cavitation in rabbits was also observed upon using a clinical *Mtb* strain suggesting that the virulence of the bacteria could play a role in the development of cavitary TB (283). Further supporting this link are studies done in the Kramnik mouse using clinical strains of *Mtb* (284). Therefore, in order to test the feasibility of the HIS mouse as a possible model of cavitary TB; experiments that take into account upper lobe pressure differences by the use of harnesses and bacteria virulence by the use of clinical strains would be desirable. Further experimental conditions such as reinfection or mixed strain infections (292) instead of the single infection carried out in this thesis could also be employed, as there is speculation that a person who is exposed to greater than 6 hours per day to an active TB patient over a consistent period of time has a greater likelihood of developing cavitary TB (293, 294).

All HIS NSG and PBS NSG infected mice exhibited some clinical features of TB such as weight loss showing susceptibility to infection. The cough clinical feature was not observed since mice do not have the family of airway epithelial nerves that can trigger the cough reflex (296). Hence the HIS NSG mouse in this thesis was not used as a model for transmission. In some murine models for human pneumonia (298), cough was induced by making the mice inhale capsaicin (299). This form of mechanical stimulation could be applied in future HIS NSG studies in order to study Mtb transmission dynamics (303).

All HIS NSG and PBS NSG infected mice showed signs of disseminated TB in organs such as the spleen, liver, kidney and bone marrow which is another feature of susceptibility to infection. The HIS system that develops in these humanized mice has more in common with a human newborn infant or an immunocompromised individual than with an immunocompetent adult individual (296, 297). This is due to the fact that the stem cells were acquired from fetal material that developed in a sterile environment (the womb) with minimal contact with pathogens and foreign antigens. In addition, the mice were kept in specific pathogen free facility; hence, these mice had a naïve phenotype-low functionality immune system in comparison to a free living human adult. In regards to bacterial infection, human newborns and children due to this naïve phenotype-low functionality immune system are more susceptible to infection and exhibit disseminated pathology in comparison to human adults whom display cavitary TB (300, 301). Undeniably, human newborns are one of the greatest groups at risk for mortality and morbidity to infection (WHO Global health observatory data 2015). Indeed, the primary purpose of the BCG vaccine is to prevent disseminated TB and TB meningitis.

By histological analysis, no TB was seen in the meninges, brain or spinal cord. This could be due to the ultra-low dose single infection administered to the HIS mice in comparison to multiple reinfections with clinical strains in a high exposure household. Clinical strains of Mtb have been shown to cross *in vitro* human blood brain cultures (302) and specific Mtb genotypes have been found in patients' cerebrospinal fluid (304). This suggests that virulence plays a role in the degree of cerebral TB exhibited. This was confirmed *in vivo* by infecting BALB/C mice via the intratracheal route with specific Mtb genotypes isolated from patients' cerebrospinal fluid (305). The cerebrospinal isolates caused infection and inflammation in the brain and the

meninges while the H37RV strain hardly infected the brain. This places more emphasis in carrying out studies in the HIS mice using clinical strains of Mtb. Furthermore, incorporating fluorescent bacteria, fluorescent tracers and whole mount immunohistochemistry will aid in deciphering a brain-cerebrospinal-cervical lymphnode-lymphatic connection separate from the traditional blood brain barrier (306), and add knowledge on the dissemination route from the lung to the brain.

Another example of how susceptible the HIS NSG mice used in this thesis were is by the time frame in which they succumbed to disease. B6 mouse or BalbC mice are usually infected with 200CFU and at this dose, their immune system controls the disease for greater than 100 days. Meanwhile, HIS NSG mice used in this thesis succumbed by 5 weeks post infection while Calderon et al engrafted BLT mice succumbed to disease 8-10 weeks post Mtb infection (242). None of the HIS mice in this thesis and in the Calderon BLT study developed any form of latency, thus showing that the HIS NSG mouse model is optimally used for active progressive disease due to its original immune deficient background and stem cell source. Therefore, future experiments using the Cornell model as a template could be performed in order to get a more latent-like disease. The Cornell mouse model is a form of latency model where upon Mtb infection; the mice are given the antibiotics isoniazid and pyrazinimide approximately 20 minutes after infection (307). This forms an environment of no detectable bacilli in the organs and upon immunosuppression the development of reactivated TB (308). As antibiotics are used, this does not reflect the true latency/subclinical form that are observed in NHPs and humans. Nevertheless, an adaptation of the Cornell system to the HIS mouse could provide information on drug related latent TB. Recent genetic manipulation of the NSG mouse embryos by CRISPR/Cas 9 technology (309) could lead to a range of susceptible to resistant mice that could still allow for human engraftment. It is conceivable that upon infection, these range of NSG mice could exhibit severe active progressive TB to latent TB as has been currently done in immune-competent diversity outbred mice (310).

On the cellular level, the characteristic Langhans multinucleated giant cells associated with TB granulomas was not observed in the HIS NSG lung samples. Giant cells arise after some macrophages fuse due to an initial reaction with a foreign biomaterial or infectious agent (311).

Giant cell formation seems to be linked to virulence as studies done in an *in vitro* model of human granuloma with highly virulent Mtb resulted in giant cells with greater than 15 nuclei per cell (312). These giant cells also had a lower phagocytic capacity. Specifically, Mtb lipomannan a proinflammatory glycolipid induces GAMs to fuse via a TLR2, ADAM- and beta1 integrin pathway (313). The Mtb strain used in this thesis was the lab strain H37RV that had undergone prior passaging and freeze-thaw cycle. After thawing, the stock is diluted and sonicated to prepare single cell suspension of the approximate infectious dose requested. This process could strip some essential lipids from the Mtb cell wall which induce certain innate mechanisms (314, 315). It is also possible that giant cells arise when a series of macrophages attempt to phagocytize sputum contents which consists of clumped bacteria, necrotic macrophages and necrotic neutrophils (132, 316). instead of single bacterium as done in this thesis.

In this thesis, most of the Mtb bacterium was detected via acid fast stain in myeloid cells. This shows that the murine and human myeloid cells in the HIS NSG mouse readily phagocytize TB bacteria. This exhibited phagocytic capability is consistent with other HIS mouse bacteria studies (196, 197, 198, 240). In particular, HIS mouse bone marrow derived macrophages have been shown to have phagocytic capabilities comparable to human monocyte derived macrophages (264). Even though bacterial counts in the human and mouse compartments were not separately delineated in this thesis; in other HIS mouse studies using pathogens that are less host-restricted such as *Salmonella typhimurium* (264) and BCG (241, 242) human macrophages had greater bacterial counts in comparison to mouse macrophages. Furthermore in two different *S. aureus* studies (276, 277) HIS NSG mice were more susceptible to infection and had a higher bacterial burden in various organs in comparison to irradiated un-reconstituted NSG mice, BalbC and B6 mice. This suggests that for reasons that are still unclear, the human mononuclear phagocytic system is more permissive to bacteria replication (233, 234). In fact, a study comparing alveolar macrophages from B6 mice and macaques showed that both species had a high induction of immune response genes in Mtb *in vitro* infection, but this immune response was species specific as there was no overlap in the genes (318). Other studies have shown that TLR signaling in murine macrophages depends on IRAK4 and IRAK2 while TLR signaling in humans is contingent on IRAK1 (319). The bacteria itself could have certain factors that have a higher degree of affinity for human receptors in comparison to murine receptors of

the same family as has been observed whence *S. aureus* factors HlgBC and CHIPS preferentially attach to human CD88 (320). Furthermore, microarray analysis of human and murine macrophages hint at different internal environments that could place different stresses on Mtb's DNA and its subsequent DNA repair mechanisms. For example, *recX* a homologous recombination gene for Mtb DNA repair is upregulated in mouse macrophages (321) but down regulated in human (322). Therefore, future experiments in which host-pathogen preferences could be elucidated will be by using HIS NSG EGFP mice with fluorescent reporter Mtb strains or DNA barcoded Mtb strains. The NSG EGFP mouse strain retains the immunodeficiency of the NSG background but has an additional transgenic green fluorescent protein expressed in all murine cells. This will allow for simultaneous quantification of human and mouse TB containing phagocytes. Additionally, applying single cell sorting on these particular phagocytes could also reveal on the transcriptomic level key species specific differences between mouse and human myeloid cells.

In this thesis, not only was the Mtb bacterium detected in various granulomas by acid-fast staining; Mtb was also segregated into extracellular bacteria in the necrotic core and intracellular bacteria in the inner myeloid/lymphoid rim in the HIS NSG mouse. Mtb is primarily classified as an intracellular pathogen; hence a recent study showing that phthiocerol dimycocerosates (PDIM) a lipid in Mtb's cell wall, increases the rate at which Mtb escapes from an intracellular vacuole into the cytosol thus leading to greater necrosis hints at this later extracellular phase observed in a liquefied center as means of facilitating transmission (325, 326). Furthermore, in some of the caseous necrotic granulomas, the central region of the necrotic core was not stained via acid fast hinting at a different micro-environment than that found in other parts of the same granuloma; essentially some of the bacteria lost their acid-fastness. It is speculated that acid-fastness is lost due to cell wall thickening as has been seen in XDR TB samples in Iran via atomic force microscopy (343). Hence in future experiments further identification strategies such as using SYBR Gold in conjunction with Auramine-rhodamine and correlative electron microscopy would be applied in order to detect these bacteria (280). Loss of acid-fastness and different bacterial cell-wall phenotypes not only occurs throughout an entire lung tissue sample, but also within the same granuloma (232) due to factors such as hypoxia, pH, nutrient availability and carbon source. The ways by which these factors have influenced

bacteria in the granuloma have been studied in guinea pigs, rabbits, non-human primates (40), the Kramnik mouse (255) and the iNOS mouse (54, 261). These studies could be replicated in the HIS NSG mice, taking into account the role of the human immune system on these factors by incorporating pimonidazole to detect hypoxia (261, 324) or by carrying out structural and quantitative analysis on bacteria fractioned out from the different regions in the granuloma (323). These types of experiments will gain importance as granuloma heterogeneity (232) seems to be linked to the genetic heterogeneity of the bacteria (327). Granuloma and bacteria heterogeneity (328) are also of great importance in regards to treating Tuberculosis disease as the drug kinetics will have a varied range in the same individual. To thus maximize the value of the experimental model, future experiments could include advanced live imaging techniques such as single photon emission computed tomography (SPECT) with radiolabeled ligands such as FDG or ^{125}I -iodo-DPA-713. FDG SPECT could provide live anatomical guidance further delineating granuloma heterogeneity in the same animal over a certain period of time (30, 23901092). The HIS NSG mouse model is thus positioned not only to facilitate studies concerning host cells but also studies of the Mtb bacterium itself.

Kinetics of the human immune response to Tuberculosis infection in HIS mice

Following the establishment of the HIS mouse model for pulmonary Mtb infection, I extended the investigation to provide a human *in vivo* confirmation of the basic processes involved in granuloma initiation and development in relation to other experimental animal models such as the rabbit (75), guinea pig (329, 330), zebrafish embryos (331) and NHPs (332). This confirmation also took into account granuloma initiation and development studies carried out in the traditional B6 mouse, the BalbC mouse and the Kramnik mouse (255, 333).

The overall kinetics of the human immune response to tuberculosis in the HIS NSG lung described in this thesis is in line with studies carried out in the previously mentioned animal models (334). Upon Mtb infection, monocyte/macrophages, neutrophils and dendritic cells were simultaneously recruited into the lungs with adaptive human immune cells such as T and B cells. As these human immune cells are recruited, an immune response is elicited as exhibited by an increase in various biomolecules such as cytokines, chemokines and antibodies that are secreted in the local lung tissue. This immune response was mostly pro-inflammatory and the

human immune cells were increasingly organized as the disease progressed. Unfortunately, the immune response generated is inadequate as seen by the increasing lung bacteria numbers and bacteria dissemination to other organs such as the bone marrow by day 28 post infection.

Prior to infection, the lung macrophages (alveolar and parenchymal) were observed to be the most abundant innate cell type (335, 336) which was consistent with what has been observed in other studies. However, by day 28 post infection, the human pulmonary CD45⁺CD33⁺CD66⁺ neutrophils were significantly increased and were the largest population of all the human pulmonary immune cells. A likely explanation for these large neutrophilic numbers is that neutrophils are known for their quick infiltration into irritated or infected tissue (337). In fact, depending on the route of infection (intravenous, intradermal or intranasal) and the mycobacteria used (Mtb, *Mycobacterium avium* or BCG); murine neutrophils have been observed to arrive at the injection site between 2 and 24 hours post-infection (339). In effect, murine granulocytes accumulate for up to 21 days in an Mtb infected lung before activated T cells arrive (338). One of the ways by which neutrophils can rapidly arrive to a site of infection while causing minimal injury to the host is by softening their nuclei in order to push aside the blood vessels scaffolding in order to squeeze through (340).

Neutrophils release biomolecules such as IL-10 after the dual activation of TLR2-MyD88 and C-type lectin receptor (CLR) spleen tyrosine kinase (Syk) dependent pathway (339) which aid in the recruitment of other neutrophils, human CD45⁺CD33⁺CD14⁺ monocyte/macrophages, human CD45⁺CD33⁺CD11c⁺ conventional dendritic cells, T cells and B cells (341). Histological examination of the lung tissue sections at various time points post-infection served as visual confirmation of this innate immune cell recruitment via staining of human CD68 macrophages and human CD15 neutrophils. Human CD15 neutrophils were the predominant cell type in the center of HIS NSG lung necrotic granulomas. Furthermore, zones of inflammation and tissue damage were visually observed suggesting that neutrophils are initially beneficial to the host but subsequently detrimental when the infection is not resolved (346). Therefore, it will be quite interesting to study the different waves of neutrophilic recruitment in the HIS NSG mouse after Mtb infection is by high-resolution fluorescent live imaging of a stabilized lung (342).

In this thesis, the macrophages were the primary foci that anchored/interacted with the various immune cells as the disease progressed as was seen by increased organization of other immune cells around the human CD68 macrophages via immuno-stain on HIS NSG lung tissue sections. One possible explanation for this organization is that necrotic macrophages that contained degraded neutrophils and bacteria could have secreted leukotriene B4 to attract more neutrophils (344), while the apoptotic macrophages secreted lactoferrin to attract more mononuclear phagocytes (345). These newly recruited neutrophils, macrophages and dendritic cells act as a secondary layer (myeloid rim) which then interacts with T cells and B cells by day 28 post infection. In comparison to the neutrophils, the conventional dendritic cells arrived in lesser numbers during day 14 and 21 post Mtb infection, but had greatly increased by day 28 post Mtb infection. This lends credence to the fact that at the onset of the infection, the initial parenchymal human dendritic cells which are few in number migrate to the lymphnodes in order to present antigen to the T cells (100) while during the later stages of the infection, the secondary wave of human dendritic cells that arrive in the HIS NSG lung though greater in numbers sub optimally prime the T cells (99), leading to suboptimal bacteria control and dissemination to other organs.

In this thesis, the immune cells were processed from the HIS NSG lung in bulk. However, there are two compartments in the lung; one is the broncho-alveolar space and the other is the parenchyma. Therefore, future studies that distinguish between the alveolar macrophages/dendritic cells in the broncho-alveolar space, the parenchyma macrophages/dendritic cells and newly differentiated macrophages/dendritic cells from recruited monocytes (347) could be carried in the HIS NSG mice as all these different innate cells could have different phenotypes in terms of activation (348) or metabolic status (349) which will affect the quality of the active immune response at different time points. Moreover, additional studies that quantify the parenchyma macrophage turnover rate during Mtb infection (348) could hint at new mechanisms by which parenchyma macrophages and other innate cells (350) could act in wound repair/healing and re-establishment of a certain degree of quiescence in the lung after antibiotic treatment.

Innate immune cell recruitment is not only influenced by cell death (146), but also by biomolecules (71), and these recruited cells secrete cytokines and growth factors (63) that influence the recruited adaptive immune cells. In agreement with cytokine/chemokine studies carried out in active TB patients (351, 352) and other experimental animal models (63, 71), a pro-inflammatory response was exhibited by increased levels of TNF- α , IFN- γ , IL-6 and IL-1 β in the HIS NSG lung homogenates on the protein level as the disease progressed. These cytokines are associated with a Th1 response. Other pulmonary cytokines that increased throughout the disease were the Th2 associated IL-9 and the T-reg associated IL-10 hinting at a subliminal anti-inflammatory response. In addition, pulmonary chemokines that also increased as the disease progressed were IP-10, MIP-1 α and interestingly, the human specific pro-inflammatory IL-8 chemokine.

To my knowledge, this is the first study that has kinetically followed human IL-8 *in vivo* in TB, as studies investigating the role of IL-8 in tuberculosis and other diseases have primarily been done in human cells or guinea pigs (353). Mice do not have a gene that codes for IL-8 hence murine homologues are used as functional equivalents (354). IL-8 is a chemokine that is secreted by cells such as the macrophage and plays a major role in neutrophil recruitment (355). IL-8 is of great interest in the human TB field as there have been studies that link a dominant IL-8 allele to increased susceptibility to Mtb particularly in individuals of African descent (356). From the data gathered in this thesis, some speculations for the role of IL-8 in active progressive disease could be put forth as follows. In the first stage, IL-8 directly binds to Mtb and these binding increases the phagocytic capability of macrophages and neutrophils (357). Secondly, the neutrophils secrete more IL-8 and other chemokines such as MIP-1 α and MCP-1 (358). The initial amount of IL-8 secreted during this first stage is beneficial as IL-8 and the other chemokines attract DCs and monocytes/macrophages to interact with various neutrophils. However, in the later stages of the disease whence the amount of IL-8 is still high, this becomes detrimental as an excessive number of neutrophils will release free radicals, proteases and elastase causing major tissue damage (359). Surprisingly, another cytokine of interest in human TB, the IL-17 cytokine was not detected in the HIS NSG lung homogenates. This was especially surprising as IL-17 has been associated with neutrophil recruitment that causes severe TB (360) as exhibited by the caseous necrotic granulomas. Perhaps, the luminex kit used had low sensitivity for detecting IL-17 or

perhaps by using the lab strain Mtb H37RV, certain virulence factors that would induce high levels of IL-17 as seen in a study that used virulent Mtb HN878 (113) were absent. In order to quantify and visualize IL-17 as the disease progresses, future experiments could incorporate a highly sensitive ELISA and chromogenic analysis on the HIS NSG lung tissue sections for visual confirmation of IL-17 and other biomolecules with their associated cells (362).

In this thesis, there was an influx of B cells in the HIS NSG lungs post Mtb infection and these B cells were located in the outer lymphocyte cuff, interspersed with the T cells. These B cells in HIS NSG lung were not organized into lymphoid follicular like structures as seen in some NHP (139) and human TB granulomas (130). As the NSG strain lacks certain cytokines and growth factors that aid in the development of proper lymphnodes, there is the possibility that the human B cells that are generated in the HIS NSG system, do not have the right scaffold which will permit them to form aggregates with the T cells to ensure optimal antigen presentation and activation. B cell associated biomolecules such as IL-6 and IgA increased from day 14 to day 28 in the HIS NSG lung post Mtb infection. IL-6 production could initially aid in increasing the T cell response (129, 361), but later on be a factor in causing severe pathology as observed in autoimmune diseases such as multiple sclerosis (363). As previously stated, there was an increase in lung bacterial burden in spite of the high IgA levels. The IgA antibody produced in the HIS NSG system could be of low functionality, as two recent studies showed that antibodies from latent TB individuals were better at phagolysosome fusion, had enhanced macrophage killing of Mtb and inflammasome activation in comparison to active TB patients (364, 365).

The T cells in particular the human CD45⁺CD3⁺CD4⁺ T cells were the largest number of adaptive immune cells in the HIS NSG lung post Mtb infection and were intermingled with the B cells and the human CD45⁺CD3⁺CD8⁺ T cells in the outer lymphocyte cuff (130, 139). The CD4 T cells during the initial phase of the infection first surround small aggregates of innate immune cells probably to enhance innate immune cell killing mechanisms via the production of INF- γ and TNF- α (110). The CD8 T cells also enhance innate immune cell killing mechanisms during the initial phase of the infection via the production of cytokines; but it is also probable that the CD8 T cells release cytotoxic molecules such as the granzymes, perforin and granulysin to destroy infected innate immune cells (123). As previously mentioned, there is a high bacterial burden in

the HIS NSG lung, leading to the speculation that even though there are a significant number of T cells recruited to the lung, the response generated is inadequate. Factors that could have contributed to this inadequate response are low T cell activation or T cell anergy as seen by the IL12p70 which is a cytokine linked to T cell activation was unchanged throughout the time course. Other factors that could have caused this inadequate response are an impaired antigenic specific response by the CD4 granuloma associated T cells (167), impairment in CD8 granuloma associated T cells in releasing cytotoxic molecules (125) or due to the lack of human HLA in the HIS NSG system (190). Moreover, the balance of pro and anti-inflammatory cytokines in the bulk HIS NSG lung is skewed towards the pro-inflammatory side with a more pro-signature linked to higher bacterial burden (351). In fact a recent NHP study, showed that individual granulomas that had T cells that secreted both pro and anti-inflammatory cytokines upon a certain Mtb antigen combination had greater bacterial clearance suggesting that a balance between pro and anti-inflammatory cytokines is necessary to control bacterial replication and that future HIS NSG Mtb studies should include NSG strains with enhanced features (366) such as human transgenic cytokine and human HLAs in order to properly assess the functionality and the Mtb specific responses of the various human immune cells.

Not only was an immune response generated in the lung, there was also an immune response generated in other organs such as the spleen and the bone marrow. Concurrent to an immune response generated in these organs, bacteria dissemination occurred in a manner similar to cancer metastasis from the primary site to other organs (371). A possible speculation of how this occurs in the HIS NSG mouse system; is that after the granuloma has been established, dendritic cells and other innate immune cells not only migrate to the lymphnodes for T cell activation (100), but also to other organs such as the spleen and bone marrow via the lymphatics and via newly created blood vessels (372). Indeed, there was an increase in VEGF in the HIS NSG lung post Mtb infection which gives credence to the possible induction of angiogenesis by Mtb in order to maximize the survival rate of the bacteria in the host (373). Hence, not only was there an influx of innate and adaptive cells in organs such as the spleen, but the immune cells were organized in a caseous necrotic granuloma pathology by day 28 post infection as a means to contain the infection. However, due to the systemic bacterial infection occurring throughout the HIS NSG body, it is possible that a form of emergency granulopoiesis

(374) is taking place as seen by the low neutrophil numbers in the bone marrow in relation to the high neutrophil numbers in the lung. Such excessive granulopoiesis occurs in the bone marrow due to factors such as cytokines/chemokines influencing the haematopoietic stem cells (375) or by direct infection of the stem cells (376). Thus, there is an increasing realization in the TB field that the bone marrow has a role in Mtb infection, not only as a site that aids in replenishing immune cells in the lungs, but also as a reservoir for Mtb by the infection of non-haematopoietic mesenchymal stem cells (377). This could also explain the long treatment times and reactivation that is observed in certain TB patients, thus future HIS NSG studies that will compare novel TB drugs would include assays that check for drug penetrance in the lung granuloma (378) and in the bone marrow itself.

Concluding notes

Collectively, my thesis has shown the first human fetal liver derived stem cell humanized mouse for the study of tuberculosis and its associated pathology. Using the figure below as a guide of where my data stands in the present state of the TB field (Figure 35 box), I have confirmed that low dose aerosolized infection occurs, that there are signs of active disease, that various lesions and granulomas do develop, and in particular that caseous necrotic granulomas develop. The data I have presented in this thesis was mainly shows the basic immune cell phenotypes, their basic cellular-spatial organization and certain biomolecules; on the organ scale, tissue scale and the cellular scale.

With new technologies such as inductively coupled plasma mass spectrometry (ICP-MS) commonly known as CYTOF, it is now possible to apply 100 markers simultaneously on the same sample. Therefore, not only can the classically studied immune cells be categorized by activation status and other markers of interest, but; rare combinational cell types such as the innate lymphoid cells and myeloid derived suppressor cells (379) can be easily examined. CYTOFs can also have a laser attached to ablate tissue sections which permits direct local imaging of the immune cells (367).

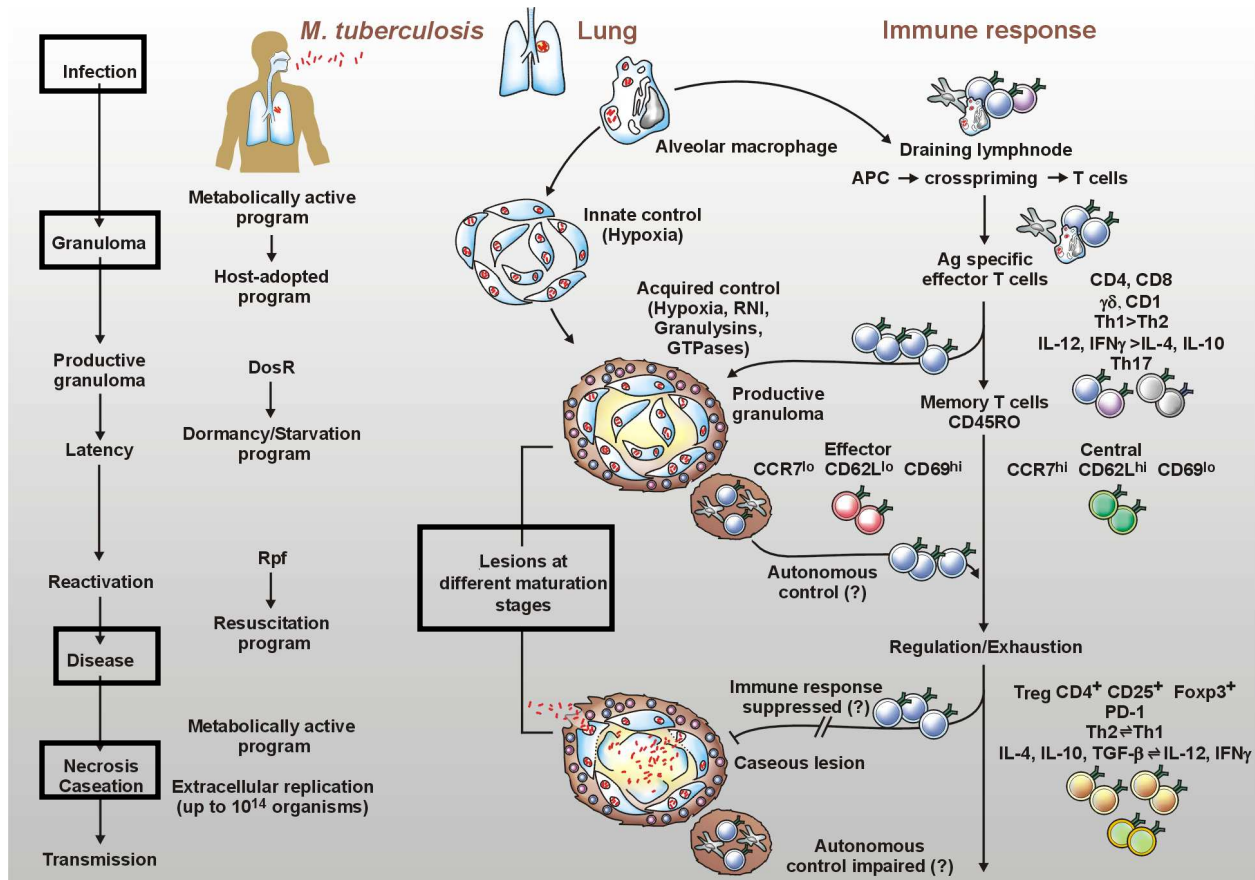


Figure35. Possibility to study cellular and molecular mechanisms of TB in HIS NSG mice (Source: Courtesy of Professor S.H.E. Kaufmann)

As more biomarkers specific for tuberculosis are being accepted (381), future HIS NSG studies could include transcriptomics, proteomics, metabolomics and epigenomics in order to understand tuberculosis on the molecular scale in this system (380). Furthermore, there is now a move in the humanized mouse/infectious disease field to switch to enhanced NSG strains with transgenic human cytokines (IL-3, GM-CSF and CSF1) which have more functional human myeloid cells upon engraftment or NSG strains with transgenic human HLAs that develop more functional human T cells upon engraftment (368). Using these enhanced strains will not only permit the confirmation of key cellular and molecular mechanisms to TB in individual granulomas (369), but also the ways by which these mechanisms are changed due to drugs (253), HDTs (370), therapeutic vaccines (111) and HIV co-infection (162).

References

1. R. Koch Die Ätiologie der Tuberkulose J. Schwalbe (Ed.), Gesammelte Werke von Robert Koch, Verlag von Georg Thieme, Leipzig (1912), pp. 428–445 [(1882) Vol. 1] **Lecture**
2. T. Schlich Ein Symbol medizinischer Fortschrittshoffnung. Robert Koch entdeckt den Erreger der Tuberkulose H. Schott (Ed.), Meilensteine der Medizin, Harenberg, Düsseldorf (1996), pp. 368–374 **Paul Ehrlich reaction to Robert Koch lecture**
3. Gradmann C. Robert Koch and the white death: from tuberculosis to tuberculin. *Microbes and Infection*. 2006; 8(1):294-301.
4. Global tuberculosis report. [Internet]. World Health Organization. 2015 [cited January 15th 2017]. Available from: http://www.who.int/tb/publications/global_report/en/
5. Mansoor N, Scriba TJ, de Kock M, Tameris M, Abel B, Keyser A et al. HIV-1 infection in infants severely impairs the immune response induced by Bacille Calmette-Guerin vaccine. *The Journal of Infectious Diseases*. 2009;199(7):982-90
6. Weiner J 3rd, Kaufmann SH. Recent advances towards tuberculosis control: vaccines and biomarkers. *Journal of Internal Medicine*. 2014;275(5):467-80
7. Grode L, Seiler P, Baumann S, Hess J, Brinkmann V, Nasser Eddine A et al. Increased vaccine efficacy against tuberculosis of recombinant Mycobacterium bovis bacille Calmette-Guérin mutants that secrete listeriolysin. *The Journal of Clinical Investigation*. 2005;115(9):2472-9
8. Desel C, Dorhoi A, Bandermann S, Grode L, Eisele B, Kaufmann SH. Recombinant BCG ΔureC hly+ induces superior protection over parental BCG by stimulating a balanced combination of type 1 and type 17 cytokine responses *The Journal of Infectious Diseases*. 2011;14:1573–1584.
9. Farinacci M, Weber S, Kaufmann SH. The recombinant tuberculosis vaccine rBCG ΔureC::hly(+) induces apoptotic vesicles for improved priming of CD4(+) and CD8(+) T cells. *Vaccine*. 2012;14:7608–7614
10. Study to Evaluate Safety and Immunogenicity of VPM1002 in Comparison With BCG in Newborn Infants in South Africa. Available from: <http://clinicaltrials.gov/ct2/show/NCT01479972?term=vpm1002&rank=2>
11. Study to Evaluate the Safety and Immunogenicity of VPM1002 in Comparison With BCG in HIV-exposed/-Unexposed Newborn Infants in South Africa. Available from: <https://clinicaltrials.gov/ct2/show/NCT02391415>
12. Andersen P, Munk ME, Pollock JM, Doherty TM. Specific immune-based diagnosis of tuberculosis. *Lancet*. 2000;356:1099–104
13. Burdash NM, Manos JP, Ross D, Bannister ER. Evaluation of the Acid-Fast Smear. *Journal of Clinical Microbiology* 1976;4(2):190-191

14. Lalvani A, Pathan AA, McShane H, Wilkinson RJ, Latif M, Conlon CP et al. Rapid detection of Mycobacterium tuberculosis infection by enumeration of antigen-specific T cells. *American Journal of Respiratory and Critical Care Medicine*. 2001;163(4):824-8
15. Ruhwald M, Petersen J, Kofoed K, Nakaoka H, Cuevas LE, Lawson L et al. Improving T-cell assays for the diagnosis of latent TB infection: potential of a diagnostic test based on IP-10. *PloS one*. 2008;3(8):e2858
16. Maertzdorf J, Weiner J 3rd, Kaufmann SH. Enabling biomarkers for tuberculosis control. *The International Journal of Tuberculosis and Lung Disease*. 2012;16(9):1140-8
17. Tientcheu LD, Maertzdorf J, Weiner J, Adetifa M, Mollenkopf HJ, Sutherland JS et al. Differential transcriptomic and metabolic profiles of M. africanum- and M. tuberculosis-infected patients after, but not before, drug treatment. *Genes and Immunity* 2015;16(5)347-55
18. Weiner J 3rd, Parida SK, Maertzdorf J, Black GF, Replibier D, Telaar A et al. Biomarkers of inflammation, immunosuppression and stress with active disease are revealed by metabolomic profiling of tuberculosis patients. *PloS one*. 2012;7(7):e40021
19. Esterhuysen MM, Linhart HG, Kaufmann SH. Can the battle against tuberculosis gain from epigenetic research? *Trends in Microbiology*. 2012;20(5)220-6
20. Berry MP, Garham CM, McNab FW, Xu Z, Bloch SA, Oni T et al. An interferon-inducible neutrophil-driven blood transcriptional signature in human tuberculosis. *Nature*. 2010;466(7309):973-7
21. Maertzdorf J, Weiner J 3rd, Mollenkopf HJ, TBornotTB Network, Bauer T et al. Common patterns and disease-related signatures in tuberculosis and sarcoidosis. *Proceedings of the National Academy of Sciences of the United States of America*. 2012.15;109(20):7853-8
22. Treatment of Tuberculosis Guidelines. [Internet]. World Health Organization. 2010 [cited July 30 2016]. Available from: <http://www.who.int/tb/publications/2010/9789241547833/en/>
23. Lawn SD, Nicol MP. Xpert® MTB/RIF assay: development, evaluation and implementation of a new rapid molecular diagnostic for tuberculosis and rifampicin resistance. *Future Microbiology*. 2011; 6:1067–1082
24. Kang MW, Kim HK, Choi YS, Kim K, Shim YM, Koh WJ et al. Surgical treatment for multidrug-resistant and extensive drug-resistant tuberculosis. *The Annals of Thoracic Surgery*. 2010;89(5):1597-602
25. Udawadia ZF, Amale RA, Ajbani KK, Rodrigues C. Totally drug-resistant tuberculosis in India. *Clinical Infectious Diseases*. 2012;54(4):579-81

26. Merle CS, Fielding K, Sow OB, Ginafon M, Lo MB, Mthiyane T et al. A four-month gatifloxacin-containing regimen for treating tuberculosis. *The New England Journal of Medicine*. 2014;371(17):1588-98
27. Gillespie SH, Crook AM, McHugh TD, Mendel CM, Meredith SK, Murray SR et al. Four-month moxifloxacin-based regimens for drug-sensitive tuberculosis. *The New England Journal of Medicine*. 2014;371(17):1577-87
28. Jindani A, Harrison TS, Nunn AJ, Phillips PP, Churchyard GJ, Charalambous S et al. High-dose rifapentine with moxifloxacin for pulmonary tuberculosis. *The New England Journal of Medicine*. 2014;371(17):1599-608
29. Lee M, Lee J, Carroll MW, Choi H, Min S, Song T et al. Linezolid for treatment of chronic extensively drug-resistant Tuberculosis. *The New England Journal of Medicine*. 2012;367(16):1508-18
30. Coleman MT, Chen RY, Lee M, Lin PL, Dodd LE, Maiello P et al. PET/CT imaging reveals a therapeutic response to oxazolidinones in macaques and humans with tuberculosis. *Science Translational Medicine*. 2014;6(265):265ra167
31. Kaufmann SH, Lange C, Rao M, Balaji KN, Lotze M, Schito M et al. Progress in tuberculosis vaccine development and host-directed therapies--a state of the art review. *The Lancet Respiratory Medicine*. 2014;2(4):301-20
32. Wallstedt H, Maeurer M. The history of tuberculosis management in Sweden. *International Journal of Infectious Diseases*. 2015;32:179-82
33. Fabri M, Stenger S, Shin DM, Yuk JM, Liu PT, Realegeno S et al. Vitamin D is required for IFN-gamma-mediated antimicrobial activity of human macrophages. *Science Translational Medicine*. 2011;3(104):104ra107
34. Montoya D, Inkeles MS, Liu PT, Realegeno S, Teles RM, Vadiya P et al. IL-32 is a molecular marker of a host defense network in human tuberculosis. *Science Translational Medicine*. 2014;6(250):250ra114
35. Gupta UD, Katoch VM. Animal models of tuberculosis. *Tuberculosis*. 2005;85(5-6):277-93
36. Kaufmann SH. Immune response to tuberculosis: experimental animal models. *Tuberculosis*. 2003; 83(1-3):107-11
37. Russell DG, Barry CE 3rd, Flynn JL. Tuberculosis: what we don't know can, and does, hurt us. *Science Magazine*. 2010;328(5980):852-6
38. Gengenbacher M, Kaufmann SH. Mycobacterium tuberculosis: success through dormancy. *Federation of European Microbiological Society Reviews*. 2012;36(3):514-32
39. Flynn JL, Capuano SV, Croix D, Pawar S, Myers A, Zinovik A et al. Non-human primates: a model for tuberculosis research. *Tuberculosis*. 2003;83(1-3):116-8
40. Via LE, Lin PL, Ray SM, Carrillo J, Allen SS, Eum SY et al. Tuberculous granulomas are hypoxic in guinea pigs, rabbits, and nonhuman primates. *Infection and Immunity*. 2008;76(6):2333-40
41. Mehra S, Golden NA, Dutta NK, Midkiff CC, Alvarez X, Doyle LA et al. Reactivation of latent tuberculosis in rhesus macaques by coinfection with simian immunodeficiency virus. *Journal of Medical Primatology*. 2011;40(4):233-43

42. Via LE, Weiner DM, Schimel D, Lin PL, Dayao E, Tankersley SL et al. Differential virulence and disease progression following Mycobacterium tuberculosis complex infection of the common marmoset (*Callithrix jacchus*). *Infection and Immunity*. 2013;81(8):2909-19
43. Lurie MB. THE FATE OF HUMAN AND BOVINE TUBERCLE BACILLI IN VARIOUS ORGANS OF THE RABBIT. *The Journal of Experimental Medicine*. 1928;48(2):155-82
44. Lurie MB. EXPERIMENTAL EPIDEMIOLOGY OF TUBERCULOSIS: THE ROUTE OF INFECTION IN NATURALLY ACQUIRED TUBERCULOSIS OF THE GUINEA PIG. *The Journal of Experimental Medicine*. 1930;51(5):769-76
45. Ramakrishnan L. Revisiting the role of the granuloma in tuberculosis. *Nature Reviews Immunology*. 2012;12(5):352-66
46. Manabe YC, Dannenberg AM Jr, Tyagi SK, Hatem CL, Yoder M, Woolwine SC et al. Different strains of Mycobacterium tuberculosis cause various spectrums of disease in the reabbit model of tuberculosis. *Infection and Immunity*. 2003;71(10):6004-11
47. Palanisamy GS, DuTeau N, Eisenach KD, Cave DM, Theus DA, Kreiswirth BN et al. Clinical strains of Mycobacterium tuberculosis display a wide range of virulence in guinea pigs. *Tuberculosis*. 2009;89(3):203-9
48. Kassa GM, Abebe F, Worku Y, Legesse M, Medhin G, Bjune G, Ameni G. Tuberculosis in Goats and Sheep in Afar Pastoral Region of Ethiopia and Isolation of Mycobacterium tuberculosis from Goat. *Veterinary Medicine International*. 2012;2012:869146
49. Menin A, Fleith R, Reck C, Marlow M, Fernandes P, Pilati C, Bafica A. Asymptomatic cattle naturally infected with Mycobacterium bovis present exacerbated tissue pathology and bacterial dissemination. *PLoS One*. 2013;8(1):e53884
50. Davis JM, Clay H, Lewis JL, Ghori N, Herbomel P, Ramakrishnan L. Real-time visualization of mycobacterium-macrophage interactions leading to initiation of granuloma formation in zebrafish embryos. *Immunity*. 2002;17(6):693-702
51. Tsai MC, Chakravarty S, Zhu G, Xu J, Tanaka K, Koch C et al. Characterization of the tuberculous granuloma in murine and human lungs: cellular composition and relative tissue oxygen tension. *Cellular Microbiology*. 2006;8(2):218-32
52. Kramnik I, Dietrich WF, Demant P, Bloom BR. Genetic control of resistance to experimental infection with virulent Mycobacterium tuberculosis. *Proceedings of the National Academy of Sciences of the United States of America*. 2000;97(15):8560-5
53. Pan H, Yan BS, Rojas M, Shebzukhov YV, Zhou H, Kobzik L et al. Ipr1 gene mediates innate immunity to tuberculosis. *Nature*. 2005;434(7034):767-72
54. Reece ST, Loddenkemper C, Askew DJ, Zedler U, Schommer-Leitner S, Stein M et al. Serine protease activity contributes to control of Mycobacterium tuberculosis in hypoxic lung granulomas in mice. *The Journal of Clinical Investigation*. 2010;120(9):3365-76
55. Ernst JD. The immunological life cycle of tuberculosis. *Nature Reviews Immunology*. 2012;12(8):581-91
56. Abel L, El-Baghdadi J, Bousfiha AA, Casanova JL, Schurr E. Human genetics of tuberculosis: a long and winding road. *Philosophical Transactions of the Royal Society of London. Series B, Biological Sciences*. 2014;369(1645):20130428

57. Sabin FR, Doan CA. The effect of tubercle bacilli and the chemical fractions obtained from analysis on the cells of the connective tissues in rabbits. *Proceedings of the National Academy of Sciences of the United States of America*. 1927;13(7):8560-4
58. Dey B, Bishai WR. Crosstalk between *Mycobacterium tuberculosis* and the host cell. *Seminars in Immunology*. 2014;26(6):486-96
59. Jin MS, Kim SE, Heo JY, Lee ME, Kim HM, Paik SG et al. Crystal structure of the TLR1-TLR2 heterodimer induced by binding of a tri-acylated lipopeptide. *Cell*. 2007;130(6):1071-82
60. Gatfield J, Pieters J. Essential role for cholesterol in entry of mycobacteria into macrophages. *Science*. 2000;288(5471):1647-50
61. Drennan MB, Nicolle D, Quesniaux VJ, Jacobs M, Allie N, Mpagi J et al. Toll-like receptor 2-deficient mice succumb to *Mycobacterium tuberculosis* infection. *The American Journal of Pathology*. 2004;164(1):49-57
62. Thuong NT, Hawn TR, Thwaites GE, Chau TT, Lan NT, Quy HT et al. A polymorphism in human TLR2 is associated with increased susceptibility to tuberculous meningitis. *Genes and Immunity*. 2007;8(5):422-8
63. Etna MP, Giacomini E, Severa M, Coccio EM. Pro- and anti-inflammatory cytokines in tuberculosis: a two-edged sword in TB pathogenesis. *Seminars in Immunology*. 2014;26(6):543-51
64. Keane J, Gershon S, Wise RP, Mirabelle-Levens E, Kasznica J, Schwiertman WD et al. Tuberculosis associated with infliximab, a tumor necrosis factor alpha-neutralizing agent. *The New England Journal of Medicine*. 2011;345(15):1098-104
65. Flesch IE, Kaufmann SH. Activation of tuberculostatic macrophage functions by gamma interferon, interleukin-4, and tumor necrosis factor. *Infection and Immunity*. 1990;58(8):2675-7
66. Newport MJ, Huxley CM, Huston S, Hawrylowicz CM, Oostra BA, Williamson R, Levin M. A mutation in the interferon-gamma-receptor gene and susceptibility to mycobacterial infection. *The New England Journal of Medicine*. 1996;335(26):1941-9
67. Scanga CA, Mohan VP, Tanaka K, Alland D, Flynn JL, Chan J. The inducible nitric oxide synthase locus confers protection against aerogenic challenge of both clinical and laboratory strains of *Mycobacterium tuberculosis* in mice. *Infection and Immunity*. 2001;69(12):7711-7
68. Yang CS, Yuk JM, Jo EK. The role of nitric oxide in mycobacterial infections. *Immune Network*. 2009;9(2):46-52
69. Jagannath C, Actor JK, Hunter RL Jr. Induction of nitric oxide in human monocytes and monocyte cell lines by *Mycobacterium tuberculosis*. *Nitric Oxide*. 1998;2(3):174-86
70. Choi HS, Rai PR, Chu HW, Cool C, Chan ED. Analysis of nitric oxide synthase and nitrotyrosine expression in human pulmonary tuberculosis. *American Journal of Respiratory and Critical Care Medicine*. 2002;166(2):178-86
71. Monin L, Khader SA. Chemokines in tuberculosis: the good, the bad and the ugly. *Seminars in Immunology*. 2014;26(6):552-8

72. Nouailles G, Dorhoi A, Koch M, Zerrahn J, Weiner J 3rd, Fae KC, Arrey F. et al CXCL5-secreting pulmonary epithelial cells drive destructive neutrophilic inflammation in tuberculosis. *The Journal of Clinical Investigation*. 2014;124(3):1268-82
73. Sanchez-Castanon M, Baquero IC, Sanchez-Velasco P, Farinas MC, Ausin F, Leyva-Cobian F. et al. Polymorphisms in CCL5 promoter are associated with pulmonary tuberculosis in northern Spain. *The International Journal of Tuberculosis and Lung Disease*. 2009;13(4):480-5
74. Russell DG, Dant J, Struggill-Koszycki S. Mycobacterium avium-and Mycobacterium tuberculosis-containing vacuoles are dynamic, fusion-competent vesicles that are accessible to glycosphingolipids from the host cell plasmalemma. *Journal of Immunology*.1996;156(12):4764-73
75. Subbian S, Bandyopadhyay N, Tsenova L, O'Brien P, Khetani V, Kushner NL et al. Early innate immunity determines outcome of Mycobacterium tuberculosis pulmonary infection in rabbits. *Cell communication and Signalling*. 2013;11:60
76. Davis JM, Ramakrishnan L. The role of the granuloma in expansion and dissemination of early tuberculous infection. *Cell*. 2009;136(1):37-49
77. Cambier CJ, Takaki KK, Larson RP, Hernandez RE, Tobin DM, Urdahl KB et al. Mycobacteria manipulate macrophage recruitment through coordinated use of membrane lipids. *Nature*.2014;505(7482):218-22
78. Clay H, Volkman HE, Ramakrishnan L. Tumor necrosis factor signaling mediates resistance to mycobacteria by inhibiting bacterial growth and macrophage death. *Immunity*. 2008;29(2):283-94
79. Shafiani S, Tucker-Heard G, Kariyone A, Takatsu K, Urdahl KB. Pathogen-specific regulatory T cells delay the arrival of effector T cells in the lung during early tuberculosis. *The Journal of Experimental Medicine*. 2010;207(7):1409-20
80. WALGREN A. The time-table of tuberculosis. *Tubercle*. 1948;29(11):245-51
81. Mirsky HP, Miller MJ, Lindermann JJ, Kirschner DE. Systems biology approaches for understanding cellular mechanisms of immunity in lymph nodes during infection. *Journal of Theoretical Biology*. 2011;287:160-70
82. Griffiths G, Nystrom B, Sable SB, Khuller GK. Nanobead-based interventions for the treatment and prevention of tuberculosis. *Nature Reviews Microbiology*. 2010;8(11):827-34
83. Tostmann A, Kik SV, Kalisvaart NA, Sebek MM, Verver S, Boeree MJ, van Soolingen D. Tuberculosis transmission by patients with smear-negative pulmonary tuberculosis in a large cohort in the Netherlands. *Clinical Infectious Diseases*. 2008;47(9):1135–1142
84. Hernandez-Pando R, Jeyanathan M, Mengistu G, Aguilar D, Orozco H, Harboe M et al. Persistence of DNA from Mycobacterium tuberculosis in superficially normal lung tissue during latent infection. *Lancet*. 2000; 356(9248):2133–2138
85. Srivastava S, Ernst JD. Cell-to-cell transfer of M. tuberculosis antigens optimizes CD4 T cell priming. *Cell Host and Microbe*.2014;15(6):741-52
86. Turner OC, Basaraba RJ, Orme IM. Immunopathogenesis of pulmonary granulomas in the guinea pig after infection with Mycobacterium tuberculosis. *Infection and Immunity*. 2003;71(2):864–871

87. Steinman RM. The dendritic cell system and its role in immunogenicity. *Annual Review of Immunology*. 1991;9:271-96
88. Wolf AJ, Linas B, Trevejo-Nuñez GJ, Kincaid E, Tamura T, Takatsu K, Ernst JD. *Mycobacterium tuberculosis* infects dendritic cells with high frequency and impairs their function in vivo. *Journal of Immunology*. 2007;179(4):2509–2519
89. Basaraba RJ, Dailey DD, McFarland CT, Shanley CA, Smith EE, McMurray DN, Orme IM. Lymphadenitis as a major element of disease in the guinea pig model of tuberculosis. *Tuberculosis*. 2006;86(5):386-94
90. Lin PL, Pawar S, Myers A, Pegu A, Fuhrman C, Reinhart TA et al. Early events in *Mycobacterium tuberculosis* infection in cynomolgus macaques. *Infection and Immunity*. 2006;74(7):3790-803
91. AR Rich. *The pathogenesis of tuberculosis*. 1944 (1st edn.) Charles C. Thomas, Springfield, IL
92. Lin PL, Ford CB, Coleman MT, Myers AJ, Gawande R, Ioerger T et al. Sterilization of granulomas is common in active and latent tuberculosis despite within-host variability in bacterial killing. *Nature Medicine*. 2014;20(1):75-9
93. Ghesani N, Patrawalla A, Lardizabal A, Saigame P, Fennelly KP. Increased cellular activity in thoracic lymph nodes in early human latent tuberculosis infection. *American Journal of Respiratory and Critical Care Medicine*. 2014;189(6):748-50
94. Harbitz F. Tuberculosis of Lymph Nodes Frequency, Origin, and Relation to Other Tuberculous Lesions, Especially Pulmonary Tuberculosis. *The Journal of Infectious Diseases*. 1917;21(2):196-218
95. Riol-Blanco L, Sanchez N, Torres A, Tejedor A, Narumiya S, Corbi A, Mateos P, Rodriguez-Fernandez J. The chemokine receptor CCR7 activates in dendritic cells two signaling molecules that independently regulate chemotaxis and migratory speed. *Journal of Immunology*. 2005;174(7):4070–80.
96. Ghosh S, Chackerian AA, Parker CM, Ballantyne CM, Behar SM. The LFA-1 adhesion molecule is required for protective immunity during pulmonary *Mycobacterium tuberculosis* infection. *Journal of Immunology*. 2006;176(8):4914–22.
97. Haniffa M, Shin A, Bigley V, McGovern N, Teo P, See P et al. Human tissues contain CD141hi cross-presenting dendritic cells with functional homology to mouse CD103+ nonlymphoid dendritic cells. *Immunity*. 2012;37(1):60-73
98. Schulz O, Jaensson E, Persson EK, Liu X, Worbs T, Agace WW, Pabst O. Intestinal CD103+, but not CX3CR1+, antigen sampling cells migrate in lymph and serve classical dendritic cell functions. *The Journal of Experimental Medicine*. 2009;206(13):3101-14
99. Leepiyasakulchai C, Taher C, Chuguimia OD, Mazurek J, Soderberg-Naucler C, Fernandez C, Skold M. Infection rate and tissue localization of murine IL-12p40-producing monocyte-derived CD103(+) lung dendritic cells during pulmonary tuberculosis. *PloS one*. 2013;8(7):e69287

100. Lozza L, Farinacci M, Bechtle M, Staber M, Zedler U, Baiocchini A, Del Nonno F, Kaufmann SH. Communication between Human Dendritic Cell Subsets in Tuberculosis: Requirements for Naïve CD4(+) T cell Stimulation. *Frontiers in Immunology*. 2014;5:324
101. Tian T, Woodworth J, Sköld M, Behar SM. In vivo depletion of CD11c+ cells delays the CD4+ T cell response to Mycobacterium tuberculosis and exacerbates the outcome of infection. *Journal of Immunology*. 2005; 175 (5) :3268 – 72
102. Hambleton S, Salem S, Bustamante J, Bigley V, Boisson-Dupuis S, Azevedo J, . IRF8 mutations and human dendritic-cell immunodeficiency. *New England Journal of Medicine*. 2011; 365(2):127 – 38
103. Behr MA, Waters WR. Is tuberculosis a lymphatic disease with a pulmonary portal? *The Lancet Infectious Disease*. 2014;14(3):250-5
104. Bhalla K, Chugh M, Mehrotra S, Rathore S, Tousif S, Prakash Dwivedi V et al. Host ICAMs play a role in cell invasion by Mycobacterium tuberculosis and Plasmodium falciparum. *Nature Communications*. 2015.14;6:6049
105. Zhu, J., Yamane, H. & Paul, W.E. Differentiation of effector CD4 T cell populations. *Annual Review of Immunology*. 2010;28:445–489
106. Khader SA, Rangel-Moreno J, Fountain JJ, Martino CA, Reiley WW, Pearl JE et al. In a murine tuberculosis model, the absence of homeostatic chemokines delays granuloma formation and protective immunity. *Journal of Immunology*. 2009;183(12):8004-14
107. Slight SR, Rangel-Moreno J, Gopal R, Lin Y, Fallert Junecko BA, Mehra S et al. CXCR5+ T helper cells mediate protective immunity against tuberculosis. *The Journal of Clinical Investigation*. 2013;123(2):712-26
108. Sakai S, Kauffman KD, Schenkel JM, McBerry CC, Mayer-Barber KD, Masopust D, Barber DL et al. Cutting edge: control of Mycobacterium tuberculosis infection by a subset of lung parenchyma-homing CD4 T cells. *Journal of Immunology*. 2014;192(7):2965-9
109. Filipe-Santos O, Bustamante J, Chapgier A, Vogt G, de Beaucoudrey L, Feinberg J et al. Inborn errors of IL-12/23- and IFN-gamma-mediated immunity: molecular, cellular and clinical features. *Seminars in Immunology*. 2006;18(6):347-61
110. Blomgran R, Desvignes L, Briken V, Ernst JD. Mycobacterium tuberculosis inhibits neutrophil apoptosis, leading to delayed activation of naive CD4 T cells. *Cell Host and Microbe* 2012;11(1):81–90.
111. Reece ST, Kaufmann SH. Floating between the poles of pathology and protection: can we pin down the granuloma in tuberculosis? *Current Opinion in Microbiology*. 2012;15(1):63-70

112. Lockhart E, Green AM, Flynn JL. IL-17 production is dominated by gammadelta T cells rather than CD4 T cells during *Mycobacterium tuberculosis* infection. *Journal of Immunology* 2006;177(7):4662–4669.
113. Gopal R, Monin L, Slight S, Uche U, Blanchard E, Fallert Junecko BA et al. Unexpected role for IL-17 in protective immunity against hypervirulent *Mycobacterium tuberculosis* HN878 infection. *PLoS Pathogen*. 2014;10(5):e1004099.
114. Cowan J, Pandey S, Filion LG, Angel JB, Kumar A, Cameron DW. Comparison of interferon-gamma-, interleukin (IL)-17- and IL-22-expressing CD4 T cells, IL-22-expressing granulocytes and proinflammatory cytokines during latent and active tuberculosis infection. *Clinical and Experimental Immunology*. 2012; 167(2):317–329.
115. Huang D, Chen CY, Zhang M, Qiu L, Shen Y, Du G, Zhou K et al. Clonal immune responses of *Mycobacterium*-specific gDT cells in tuberculous and non-tuberculous tissues during *M. tuberculosis* infection. *PLoS Pathogen*. 2012;7(2):e30631.
116. Venuprasad K, Kong YC, Farrar MA. Control of Th2-mediated inflammation by regulatory T cells. *The American Journal of Pathology*. 2010;177(2):525-31
117. de Waal Malefyt R, Haanen J, Spits H, Roncarolo MG, te Velde A, Figdor C et al. IL-10 and v-IL-10 strongly reduce antigen specific human T cell responses by diminishing the antigen presenting capacity of monocytes via down-regulation of class II MHC expression. *The Journal of Experimental Medicine*. 1991;174(4):915-24
118. Kursar M, Koch M, Mittrucker HW, Nouailles G, Bonhagen K, Kamradt T, Kaufmann SH. Cutting Edge: Regulatory T cells prevent efficient clearance of *Mycobacterium tuberculosis*. *Journal of Immunology* 2007;178(5):2661–5.
119. Guyot-Revol V., Innes J. A., Hackforth S., Hinks T., Lalvani A. Regulatory T cells are expanded in blood and disease sites in patients with tuberculosis. *The American Journal of Respiratory and Critical Care Medicine*. 2006;173(7):803–810.
120. Chiacchio T., Casetti R., Butera O., et al. Characterization of regulatory T cells identified as CD4⁺CD25^{high}CD39⁺ in patients with active tuberculosis. *Clinical and Experimental Immunology*. 2009;156(3):463–470.
121. Green AM, Mattila JT, Bigbee CL, Bongers KS, Lin PL, Flynn JL. CD(4+) regulatory T cells in a cynomolgous macaque model of *Mycobacterium tuberculosis* infection. *The Journal of Infectious Disease*. 2010;202(4):533-41
122. Muller I, Cobbold SP, Waldmann H, Kaufmann SH (1987) Impaired resistance to *Mycobacterium tuberculosis* infection after selective in vivo depletion of L3T4+ and Lyt-2+ T cells. *Infection and Immunity*. 1987; 55(9): 2037–2041.
123. Chen CY, Huang D, Wang RC, Shen L, Zeng G, Yao S et al. A critical role for CD8 T cells in a nonhuman primate model of tuberculosis. *PLoS Pathogen*. 2009;5(4):e1000392.

124. Prezzemolo T, Guggino G, La Manna MP, Di Liberto D, Dieli F, Caccamo N. Functional Signatures of Human CD4 and CD8 T cell Responses to *Mycobacterium tuberculosis*. *Frontiers in Immunology*. 2014;5:180.
125. Andersson J, Samarina A, Fink J, Rahman S, Grundstrom S. Impaired expression of perforin and granulysin in CD8+ T cells at the site of infection in human chronic pulmonary tuberculosis. *Infection and Immunity*. 2007;75(11):5210-22
126. Van Rhijin, Moody DB. CD1 and mycobacterial lipids activate human T cells. *Immunological reviews*. 2015;264(1):138-53
127. Allan LL, Stax AM, Zheng DJ, Chung BK, Kozak FK, Tan R, van den Elzen P. CD1d and CD1c expression in human B cells is regulated by activation and retinoic acid receptor signaling. *Journal of Immunology*. 2011;186(9):5261-72
128. Gitlin AD, Nussenzweig MC. Immunology: Fifty years of B lymphocytes. *Nature*. 2015;517(7533):139-41
129. Achkar JM, Chan J, Casadevall A. B cells and antibodies in the defense against *Mycobacterium tuberculosis* infection. *Immunological reviews*. 2015;264(1):167-81
130. Ulrichs T., Kosmiadi G.A., Trusov V., Jörg S., Pradl L., Titukhina M., Mishenko V., Gushina N., Kaufmann S.H. Human tuberculous granulomas induce peripheral lymphoid follicle-like structures to orchestrate local host defence in the lung. *Journal of Pathology*. 2004;204:217–228.
131. Maglione P.J., Xu J., Chan J. B cells moderate inflammatory progression and enhance bacterial containment upon pulmonary challenge with *Mycobacterium tuberculosis*. *Journal of Immunology*. 2007;178:7222–7234.
132. Eum, S.Y., Kong, J.H., Hong, M.S., Lee, Y.J., Kim, J.H., Hwang, S.H., et al, Neutrophils are the predominant infected phagocytic cells in the airways of patients with active pulmonary TB. *Chest*. 2010; 137(1): 122–128.
133. Verrall, A.J., Netea, M.G., Alisjahbana, B., Hill, P.C., van Crevel, R. Early clearance of *Mycobacterium tuberculosis*: a new frontier in prevention. *Immunology*. 2014; 141(4): 506–513.
134. Elkington P., Shiomi T., Breen R., Nuttall R. K., Ugarte-Gil C. A., Walker N. F., et al. MMP-1 drives immunopathology in human tuberculosis and transgenic mice. *The Journal of Clinical Investigation*. 2011; 121(5): 1827–1833.
135. Shafiani S., Tucker-Head G., Kariyone A., Takatsu K., Urdahl KB. Pathogen-specific regulatory T cells delay the arrival of effector T cells in the lung during early tuberculosis. *The Journal of Experimental Medicine*. 2010;207(7):1409-20
136. Rao M., Valentini D., Poiret T., Dodoo E., Parida S., Zulma A., et al. B in TB: B Cells as Mediators of Clinically Relevanz Immune Responses in Tuberculosis. *Clinical Infectious Diseases*. 2015;15:S225-34
137. Torrado E, Fountain JJ, Robinson RT, Martino CA, Pearl JE, Rangel-Moreno J., et al. Differential and site specific impact of B cells in the protective immune response to *Mycobacterium tuberculosis* in the mouse. *PLoS One*. 2013;8(4):e61681

138. Kozakiewicz L, Chen Y, Xu J, Wang Y, Dunussi-Joannopoulos K, Ou Q, et al. B cells regulate neutrophilia during *Mycobacterium tuberculosis* infection and BCG vaccination by modulating the interleukin-17 response. *PLoS Pathogens*.2013;9(7):e1003472
139. Phuah JY, Mattila JT, Lin PL, Flynn JL. Activated B cells in the granulomas of nonhuman primates infected with *Mycobacterium tuberculosis*. *The American Journal of Pathology*.2012;181(2):508-14
140. Ulrichs T, Kosmiadi GA, Jörg S, Pradl L, Titukhina M, Mishenko V, et al. Differential organization of the local immune response in patients with active cavitary tuberculosis or with nonprogressive tuberculoma. *The Journal of Infectious Diseases*.2005;192(1):89-97
141. Sia IG, Wieland ML., Current concepts in the management of tuberculosis. *Mayo Clinic Proceedings*. 2011;86(4):348-61
142. Lerner TR, Borel S, Guitierrez MG. The innate immune response in human tuberculosis. *Cellular Microbiology*. 2015;17(9):1277-85
143. Bylund, J., Brown, K.L., Movitz, C., Dahlgren, C., Karlsson, A. Intracellular generation of superoxide by the phagocyte NADPH oxidase: how, where, and what for? *Free Radical Biology and Medicine*. 2010; 49(12):1834–1845.
144. Braian, C., Hogeia, V, Stendahl, O. *Mycobacterium tuberculosis*- induced neutrophil extracellular traps activate human macrophages. *Journal of Innate Immunity*.2013;5(6):91-602.
145. Rivas-Santago B, Hernandez-Pando R, Carranza C, Juarez E, Contreras JL, Aguilar-Leon D, et al. Expression of cathelicidin LL-37 during *Mycobacterium tuberculosis* infection in human alveolar macrophages, monocytes, neutrophils and epithelial cells. *Infection and Immunity*. 2008;76(3):935-41
146. Tan, B.H., Meinken, C., Bastian, M., Bruns, H., Legaspi, A., Ochoa, M.T., et al. Macrophages acquire neutrophil granules for antimicrobial activity against intracellular pathogens. *Journal of Immunology*.2006;177(3):1864-71
147. Botella, H., Peyron, P., Levillain, F., Poincloux, R., Poquet, Y., Brandli, I., et al. *Mycobacterial* p(1)-type ATPases mediate resistance to zinc poisoning in human macrophages. *Cell Host and Microbe*.2011;10(3): 248–259.
148. Miller, J.L., Velmurugan, K., Cowan, M.J., Briken, V. The type I NADH dehydrogenase of *Mycobacterium tuberculosis* counters phagosomal NOX2 activity to inhibit TNF- α -mediated host cell apoptosis. *PLoS Pathogens*.2010; 6(4): e1000864.
149. Shin, D.-M., Jeon, B.-Y., Lee, H.-M., Jin, H.S., Yuk, J.-M., Song, C.-H., et al. *Mycobacterium tuberculosis* eis regulates autophagy, inflammation, and cell death through redox-dependent signaling. *PLoS Pathogens* 2010. 6(12): e1001230.
150. Jayakumar, D., Jacobs, W.R., and Narayanan, S. Protein kinase E of *Mycobacterium tuberculosis* has a role in the nitric oxide stress response and apoptosis in a human macrophage model of infection. *Cell Microbiology* 2008. 10: 365–374.
151. Danelishvili, L., Everman, J.L., McNamara, M.J., and Bermudez, L.E. Inhibition of the plasma-membrane-associated serine protease cathepsin G by *Mycobacterium tuberculosis*

- Rv3364c suppresses caspase-1 and pyroptosis in macrophages. *Frontiers in Microbiology* 2011. 2: 281.
152. Chen M, Divangahi M, Gan H, Shin DS, Hong S, Lee DM, et al. Lipid mediators in innate immunity against tuberculosis: opposing roles of PGE2 and LXA4 in the induction of macrophage death. *The Journal of Experimental Medicine*. 2008;205(12): 2791-801
 153. Mothe BR, Lindestam Arlehamn CS, Dow C, Dillon MB, Wiseman RW, Bohn P, et al. The TB-specific CD4+ T cell immune repertoire in both cynomolgus and rhesus macaques largely overlap with humans. *Tuberculosis*. 2015;S1472-9792(15)30061-5
 154. Du G, Chen CY, Shen Y, Qiu L, Huang D, Wang R, Chen ZW. TCR repertoire, clonal dominance, and pulmonary trafficking of +mycobacterium-specific CD4+ and CD8+ T effector cells in immunity against tuberculosis. *Journal of Immunology*. 2010;185(7):3490-7
 155. Axelsson- Robertson R, Ju JH, Kim HY, Zumla A, Maeurer M. Frequency of Mycobacterium tuberculosis-specific CD8+ T-cells in the course of anti-tuberculosis treatment. *International Journal of Infectious Diseases*. 2015;32:13-22
 156. Tully G, Kortsik C, Höhn H, Zehbe I, Hitzler WE, Neukirch C. et al. Highly focused T cell responses in latent human pulmonary Mycobacterium tuberculosis infection. *Journal of Immunology*. 2005;174(4):2174-84
 157. Schubert OT, Ludwig C, Kogadeeva M, Zimmermann M, Rosenberger G, Gengenbacher M et al. Absolute Proteome Composition and Dynamics during Dormancy and Resuscitation of Mycobacterium tuberculosis. *Cell Host and Microbe*. 2015;18(1):96-108
 158. Comas I, Chakravarti J, Small PM, Galagan J, Niemann S, Kremer K. et al, Human T cell epitopes of Mycobacterium tuberculosis are evolutionarily hyperconserved. *Nature Genetics*. 2010;42(6):498-503
 159. Srivastavas S, Ernst JD. Cutting edge: Direct recognition of infected cells by CD4 T cells is required for control of intracellular Mycobacterium tuberculosis in vivo. *Journal of Immunology*. 2013;191(3):1016-20
 160. Yao S, Huang D, Chen CY, Halliday L, Wang RC, Chen ZW. CD4+ T cells contain early extrapulmonary tuberculosis dissemination and rapid TB progression and sustain multi-effector functions of CD8+T and CD3- lymphocytes: mechanisms of CD4+ T cell immunity. *Journal of Immunology*. 2014;192(5):2120-32
 161. Lin PL, Rutledge T, Green AM, Bigbee M, Fuhrman C, Klein E, Flynn JL. CD4 T cell depletion exacerbates acute Mycobacterium tuberculosis while reactivation of latent infection is dependent on severity of tissue depletion in cynomolgus macaques. *AIDS research and Human Retroviruses*. 2012;28(12):1690-702
 162. Diedrich CR, Mattila JT, Klein E, Janssen C, Phuah J, Sturgeon TJ et al. Reactivation of latent tuberculosis in cynomolgus macaques infected with SIV is associated with early peripheral T cell depletion and not virus load. *PLoS One*. 2010;5(3):e9611
 163. Silva AA, Mauad T, Saldiva PHN, Pires-Neto RC, Coletta RD, Graner E, et al. Immunophenotype of lung granulomas in HIV and non-HIV associated tuberculosis. *MEDICALEXPRESS*. 2014;1(4):174-179
 164. Dorhoi A, Kaufmann SH. Perspectives on host adaptation in response to Mycobacterium tuberculosis: modulation of inflammation. *Seminars in immunology*. 2014;26(6):533-42

165. Orme IM, Robinson RT, Cooper AM. The balance between protective and pathogenic immune responses in the TB-infected lung. *Nature Immunology*. 2015;16(1):57-63
166. Barry S, Breen R, Lipman M, Johnson M, Janossy G. Impaired antigen-specific CD4(+) T lymphocyte responses in cavitary tuberculosis. *Tuberculosis*. 2009;89(1):48-53
167. Fan L, Xiao H, Mai G, Su B, Ernst J, Hu Z. Impaired M. tuberculosis Antigen-Specific IFN- γ response without IL-17 Enhancement in Patients with Severe Cavitary Pulmonary Tuberculosis. *PLoS One*. 2015;10(5):e0127087
168. Kim MJ, Wainwright HC, Locketz M, Bekker LG, Walther GB, Dittrich C, et al. Caseation of human tuberculosis granulomas correlates with elevated host lipid metabolism. *EMBO Molecular Medicine*. 2010;2(7):258-74
169. Einarsdottir T, Lockhart E, Flynn JL. Cytotoxicity and secretion of gamma interferon are carried out by distinct CD8 T cells during Mycobacterium tuberculosis infection. *Infection and Immunity*. 2009;77(10):4621-30
170. Macdonald LE, Karow M, Stevens S, Auerbach W, Poueymirous WT, Yasenchak J, et al. Proceedings of the Natural Academy of Sciences of the United States of America. 2014;111(14):5147-52
171. Shultz LD, Ishikawa F, Greiner DL. Humanized mice in translational biomedical research. 2007; 7(2):118-30
172. Bosma, G. C., Custer, R. P. & Bosma, M. J. A severe combined immunodeficiency mutation in the mouse. *Nature*. 1983; 301(5900):527-530
173. Mosier, D. E., Gulizia, R. J., Baird, S. M. & Wilson, D. B. Transfer of a functional human immune system to mice with severe combined immunodeficiency. *Nature*. 1988; 335(3187):256-259
174. McCune JM, Namikawa R, Kaneshima H, Shultz LD, Liberman M, Weissman IL. The SCID-hu mouse: murine model for the analysis of human hematolymphoid differentiation and function. *Science*. 1988;241(4873):1632-9
175. Shultz LD; Schweitzer PA, Christianson SW, Gott B, Schweitzer IB, Tennent B. et al. Multiple defects in innate and adaptive immunologic function in NOD/LtSZ-scid mice. *Journal of Immunology*. 1995;154(1):180-91
176. Mombaerts P, Iacomini J, Johnson RS, Herrup K, Tonegawa S, Paipaionnou VE. RAG-1-deficient mice have no mature B and T lymphocytes. *Cell*. 1992;68(5):869-77
177. Shinkai Y, Rathbun G, Lam KP, Oltz EM, Stewart V, Mendelsohn M et al. RAG-2-deficient mice lack mature lymphocytes owing to inability to initiate V(D)J rearrangement. 1992;68(5):855-67
178. Traggiai E, Chicha L, Mazzucchelli L, Bronz L, Piffaretti JC, Lanzavecchia A, Manz MG. Development of a human adaptive immune system in cor blood cell-transplanted mice. *Science*. 2004;304(5667):104-7
179. Shultz LD, Lyons BL, Burzenski LM, Gott B, Chen X, Chaleff S et al. Human lymphoid and myeloid cell development in NOD/LtSZ-scid IL2R gamma null mice engrafted with mobilized human hemopoietic stem cells. *Journal of Immunology*. 2005;174(10):6477-89

180. Cao, X, Shores EW, Hu-Li J, Anver MR, Kelsall BL, Russell SM et al. Defective lymphoid development in mice lacking expression of the common cytokine receptor γ -chain. *Immunity*. 1995; 2(3): 223–238
181. DiSanto, J. P., Muller, W., Guy-Grand, D., Fischer, A. & Rajewsky, K. Lymphoid development in mice with a targeted deletion of the interleukin 2 receptor γ -chain. *Proceedings of the National Academy of Sciences of the United States of America*. 1995;92(2):377-81
182. Rochman Y, Spolski R, Leonard WJ. New insights into the regulation of T cells by gamma (c) family cytokines. *Nature reviews. Immunology*. 2009;9(7):480-90
183. Marsden MD, Zack JA. Studies of retroviral infection in humanized mice. *Virology*. 2015;479-480:297-309
184. Brehm MA, Cuthbert A, Yang C, Miller DM, Dilorio P, Laning J et al. Parameters for establishing humanized mouse models to study human immunity: analysis of human hematopoietic stem cell engraftment in three immunodeficient strains of mice bearing the IL2rgamma (null) mutation. *Clinical Immunology*. 2010;135(1):84-98
185. Takenaka K, Prasolava TK, Wang JC, Mortin-Toth SM, Khalouei S, Gan OI et al. Polymorphism in Sirpa modulates engraftment of human hematopoietic stem cells. *Nature Immunology*. 2007; 8(12):1313-23
186. Ponomaryov T, Peled A, Petit I, Taichman RS, Habler L, Sandbank J et al. Induction of the chemokine stromal-derived factor-1 following DNA damage improves human stem cell function. *The Journal of Clinical Investigation*. 2000;106(11):1331-9
187. Lepus CM, Gibson TF, Gerber SA, Kawikova I, Szczepanik M, Hossain J et al. Comparison of human fetal liver, umbilical cord blood, and adult blood hematopoietic stem cell engraftment in NOD-scid/gammac^{-/-}, Balb/c-Rag1^{-/-}gammac^{-/-}, and C.B-17-scid/bg immunodeficient mice. *Human Immunology*. 2009;70(10):790-802
188. Yuan J, Nguyen CK, Liu X, Kanellopoulou C, Muljoo SA. Lin28b reprograms adult bone marrow hematopoietic progenitors to mediate fetal-like lymphopoiesis. *Science*. 2012;335(6073):1195-200
189. Doulatov S, Notta F, Laurenti E, Dick JE. Hematopoiesis: a human perspective. *Cell Stem Cell*. 2012;10(2):120-36
190. Brehm MA, Shultz LD, Luban J, Greiner DL. Overcoming current limitations in humanized mouse research. *The Journal of Infectious diseases*. 2013;Suppl2:S125-30
191. Rongvaux A, Takizawa H, Strowig T, Willinger T, Eynon EE, Flavell RA, Manz MG. Human hemato-lymphoid system mice: current use and future potential for medicine. *Annual review of Immunology*. 2013;31:635-74
192. Leung C, Chijioke O, Cujer C, Chatterjee B, Antsiferova O, Landtwing V et al. Infectious diseases in humanized mice. *European Journal of Immunology*. 2013;43(9):2246-54
193. Lüdtke A, Oestereich L, Ruibal P, Wurr S, Pallasch E, Bockholt S et al. Ebola virus disease in mice with transplanted human hematopoietic stem cells. *Journal of Virology*. 2015;89(8):4700-4
194. Arnold L, Tyagi RK, Meija P, Swetman C, Gleeson J, Perignon JL, Druilhe P. Further improvements of the *P. falciparum* humanized mouse model. *PLoS One*. 2011;6(3):e18045

195. Wege AK, Florian C, Ernst W, Zimara N, Schleicher U, Hanses F et al. Leishmania major infection in humanized mice induces systemic infection and provokes a nonprotective human immune response. *PLoS Neglected Tropical Diseases*. 2012;6(7):e1741
196. Libby SJ, Brehm MA, Greiner DL, Shultz LD, McClelland M, Smith KD et al. Humanized nonobese diabetic-scid IL2 gammanull mice are susceptible to lethal Salmonella Typhi infection. *Proceedings of the National Academy of Sciences of the United States of America*. 2010;107(35):15589-94
197. Ernst W, Zimara N, Hanses F, Männel DN, Seelbach-Göbel B, Wege AK. Humanized mice, a new, model to study the influence of drug treatment on neonatal sepsis. *Infection and Immunity*. 2013;81(5):1520-31
198. Unsinger J, McDonough JS, Shultz LD, Ferguson TA, Hotchkiss RS. Sepsis-induced human lymphocyte apoptosis and cytokine production in “humanized” mice. *Journal of Leukocyte Biology*. 2009;86(2):219-27
199. Skirecki T, Kawiak J, Machaj E, Pojda Z, Wasilewska D, Czubak J, Hoser G. Early severe impairment of hematopoietic stem and progenitor cells from the bone marrow caused by CLP sepsis and endotoxemia in a humanized mice model. *Stem Cell Research and Therapy*. 2015;6:142
200. Mota J, Rico-Hesse R. Humanized mice show clinical signs of dengue fever according to infecting virus genotype. *Journal of Virology*. 2009;83(17):8638-45
201. Mota J, Rico-Hesse R. Dengue virus tropism in humanized mice recapitulates human dengue fever. *PLoS One*. 2011;6(6):e20762
202. Sridharan A, Chen Q, Tang KF, Ooi EE, Hibberd ML, Chen J. Inhibition of megakaryocyte development in the bone marrow underlies dengue virus-induced thrombocytopenia in humanized mice. *Journal of Virology*. 2013;87(21):11648-58
203. Billerbeck E, Horwitz JA, Labitt RN, Donovan BM, Vega K, Budell WC et al. Characterization of human antiviral adaptive immune responses during hepatotropic virus infection in HLA-transgenic human immune system mice. *Journal of Immunology*. 2013;191(14):1753-64
204. Strowig T, Gurer C, Ploss A, Liu YF, Arrey F, Sashihara JJ et al. Priming of protective T cell responses against virus-induced tumors in mice with human immune system components. *The Journal of Experimental Medicine*. 2009;206(6):1423-34
205. Heuts F, Rottenberg ME, Salamon D, Rasul E, Adori M, Klein G et al. T cells modulate Epstein-Barr virus latency phenotypes during infection of humanized mice. *Journal of Virology*. 2014;88(6):3235-45
206. Lee EK, Joo EH, Song KA, Choi B, Kim M, Kim SH et al. Effects of lymphocyte profile on development of EBV-induced lymphoma subtypes in humanized mice. *Proceedings of the National Academy of Sciences of the United States of America*. 2015;112(42):13081-6
207. Stoddart CA, Maidji E, Galkina SA, Kosikova G, Rivera JM, Moreno ME et al. Superior human leukocyte reconstitution and susceptibility to vaginal transmission in humanized NOD-scid IL-2Rg(-/-) (NSG) BLT mice. *Virology*. 2011;17(1):154-60

208. Gorantla S, Makarov E, Finke-Dwyer J, Castanedo A, Holguin A, Gebhart CL et al. Links between progressive HIV-1 infection of humanized mice and viral neuropathogenesis. *The American Journal of Pathology*. 2010;177(6):2938-49
209. Balazs AB, Chen J, Hong CM, Rao DS, Yang L, Baltimore D. Antibody-based protection against HIV infection by vectored immunoprophylaxis. *Nature*. 2011;481(7379):81-4
210. Mestas J, Hughes CC. Of mice and not men: differences between mouse and human immunology. *Journal of Immunology*. 2004;172(5):2731-8
211. Seok J, Warren HS, Cuenca AG, Mindrinos MN, Baker HV, Xu W et al. Genomic responses in mouse models poorly mimic human inflammatory diseases. *Proceedings of the National Academy of Sciences of the United States of America*. 2013;110(9):3507-12
212. Takao K, Miyakawa T. Genomic responses in mouse models greatly mimic human inflammatory diseases. *Proceedings of the National Academy of Sciences of the United States of America*. 2015;112(4):1167-72
213. Kimmelman J, Mogil JS, Dirnagl U. Distinguishing between exploratory and confirmatory preclinical research will improve translation. *PLoS Biology*. 2014;12(5):e1001863
214. Drake AC. Of mice and men: what rodent models don't tell us. *Cellular and Molecular Immunology*. 2013;10(4):284-5
215. McKenzie R, Fried MW, Sallie R, Conjeevaram H, Bisceglie AM, Park Y et al. Hepatic failure and lactic acidosis due to fialuridine (FIAU9, an investigational nucleoside analogue for chronic hepatitis B. *The New England Journal of Medicine*. 1995;333(17):1099-105
216. Cynamon MH, Klemens SP, Sharpe CA, Chase S. *Antimicrobial Agents and Chemotherapy*. 1999;43(5):1189-91
217. Williams KN, Stover CK, Zhu T, Tasneen R, Tyagi S, Grosset JH, Nuermberger E. Promising antituberculous activity of the oxazolidinone PNU-100480 relative to that of linezolid in a murine model. *Antimicrobial Agents and Chemotherapy*. 2009;53(4):1314-9
218. Xu D, Nishimura T, Nishimura S, Zhang H, Zheng M, Guo YY et al. Fialuridine induces acute liver failure in chimeric TK-NOG mice: a model for detecting hepatic drug toxicity prior to human testing. *PLoS Medicine*. 2014;11(4):e1001628
219. Harriff MJ, Cansler ME, Toren KG, Canfield ET, Kwak S, Gold MC, Lewinsohn DM. Human lung epithelial cells contain Mycobacterium tuberculosis in a late endosomal vacuole and are efficiently recognized by CD8⁺ T cells. *PLoS One*. 2014;9(5):e97515
220. Parasa VR, Rahman MJ, Nguyen Hoang AT, Svensson M, Brighenti S, Lerm M. Modeling Mycobacterium tuberculosis early granuloma formation in experimental human lung tissue. *Disease Models and Mechanisms*. 2014;7(2):281-8
221. Jäger J, Marwitz S, Tiefenau J, Rasch J, Shevchuk O, Kugler C et al. Human lung tissue explants reveal novel interactions during Legionella pneumophila infections. *Infection and Immunity*. 2014;82(1):275-85
222. Huh D, Matthews BD, Mammoto A, Montoya-Zavala M, Hsin Y, Ingber DE. Reconstituting organ-level functions on a chip. *Science*. 2010;328(5986):1662-8

223. Cunningham-Bussel A, Zhang T, Nathan CF. Nitrite produced by *Mycobacterium tuberculosis* in human macrophages in physiologic oxygen impacts bacterial ATP consumption and gene expression. *Proceedings of the National Academy of Sciences of the United States of America*. 2013;110(45):E4256-65
224. Vogt G, Nathan C. In vitro differentiation of human macrophages with enhanced antimycobacterial activity. *The Journal of Clinical Investigation*. 2011;121(10):3889-901
225. Merchant RK, Schwartz DA, Helmers RA, Dayton CS, Hunninghake GW. Bronchoalveolar lavage cellularity. The distribution in normal volunteers. *The American Review of Respiratory Disease*. 1992;146(2):448-53
226. Herrera MT, Torres M, Nevels D, Perez-Redondo CN, Ellner JJ, Sada E, Schwander SK. Compartmentalized bronchoalveolar IFN- γ and IL-12 response in human pulmonary tuberculosis. *Tuberculosis*. 2009;89:38-47
227. Schwander S, Dheda K. Human lung immunity against *Mycobacterium tuberculosis*: insights into pathogenesis and protection. *American Journal of Respiratory and Critical Care Medicine*. 2011;183(6):696-707
228. Maji A, Misra R, Kumar Mondal A, Kumar D, Bajaj D, Singhal A et al. Expression profiling of lymph nodes in tuberculosis patients reveal inflammatory milieu at site of infection. *Scientific Reports*. 2015;5:15214
229. Brighenti S, Andersson J. Local immune responses in human tuberculosis: learning from the site of infection. *The Journal of Infectious Disease*. 2012;205 Suppl2:S316-24
230. Lee M, Cho SN, Barry CE 3rd, Song T, Kim Y, Jeong I. *The New England Journal of Medicine*. 2015;373(3):290-1
231. Prideaux B, Via LE, Zimmerman MD, Eum S, Satathy J, O'Brien P et al. The association between sterilizing activity and drug distribution into tuberculosis lesions. *Nature Medicine*. 2015;21(10):1223-7
232. Lenaerts A, Barry CE 3rd, Dartois V. Heterogeneity in tuberculosis pathology, microenvironments and therapeutic responses. *Immunological Reviews*. 2015;264(1):288-307
233. Pan X, Yang Y, Zhang JR. Molecular basis of host specificity in human pathogenic bacteria. *Emerging Microbes and Infections*. 2014;3(3):e23
234. Douam F, Gaska JM, Winer BY, Ding Q, von Schaewen M, Ploss A. Genetic Dissection of the Host Tropism of Human-Tropic Pathogens. *Annual Review of Genetics*. 2015; Vol 49
235. Bitzegeio J, Bankwitz D, Hueging K, Haid S, Brohm C, Ziesel MB et al- Adaptation of hepatitis C virus to mouse CD81 permits infection of mouse cells in the absence of human entry factors. *PLoS Pathogens*. 2010;6:e1000978
236. Tsai YH, Disson O, Bierne H, Lecuit M. Murinization of internalin extends its receptor repertoire, altering *Listeria monocytogenes* cell tropism and host responses. *PLoS Pathogen*. 2013;9(5):e1003381
237. Comas I, Coscolla M, Luo T, Borrell S, Holt KE, Kato-Maeda M et al. Out-of-Africa migration and Neolithic coexpansion of *Mycobacterium tuberculosis* with modern humans. *Nature Genetics*. 2013;45(10):1176-82

238. Tu W, Zheng J, Liu Y, Sia SF, Liu M, Qin G et al. The aminophosphonate pamidonate controls influenza pathogenesis by expanding a gammadelta T cell population in humanized mice. *The Journal of Experimental Medicine*. 2011;208(7):1511-22
239. Zheng J, Wu WL, Liu Y, Xiang Z, Liu M, Chan KH et al. The Therapeutic Effect of Pamidronate on Lethal Avian Influenza A H7N9 Virus Infected Humanized mice. *PLoS One*. 2015;10(8):e0135999
240. Song J, Willinger T, Rongvaux A, Eynon EE, Stevens S, Manz MG et al. A mouse model for the human pathogen *Salmonella typhi*. *Cell Host and Microbe*. 2010;8(4):369-76
241. Heuts F, Gavier-Widen D, Carow B, Juarez J, Wigzell H, Rottenberg ME. CD4+ cell-dependent granuloma formation in humanized mice with mycobacteria. *Proceedings of the National Academy of Sciences of the United States of America*. 2013;110(16):E4256-65
242. Calderon VE, Valbuena G, Goetz Y, Judy BM, Huante MB, Sutjita P et al. A humanized mouse model of tuberculosis. *PLoS One*. 2013;8(5):e63331
243. Lee J, Brehm MA, Greiner D, Shultz LD, Kornfeld H. Engrafted human cells generate adaptive immune responses to *Mycobacterium bovis* BCG infection in humanized mice. *Bmc Immunology*. 2013;14:53
244. Laskin DL, Weinberger B, Laskin JD. Functional heterogeneity in liver and lung macrophages. *Journal of Leukocyte Biology*. 2001;70(2):163-70
245. Gordon S, Plüddermann A, Martinez Estrada F. Macrophage heterogeneity in tissues: phenotypic diversity and functions. *Immunological Reviews*. 2014;262(1):36-55
246. Fennelly KP, Jones-Lopez EC. Quantity and Quality of Inhaled Dose Predicts Immunopathology in Tuberculosis. *Frontiers in Immunology*. 2015;6:313
247. Volkman HE, Clay H, Beery D, Chang JC, Sherman DR, Ramakrishnan L. Tuberculous granuloma formation is enhanced by a mycobacterium virulence determinant. *PLoS One*. 2004;2(11):e367
248. Maertzdorf J, McEwen G, Weiner J 3rd, Tian S, Lader E, Schriek U et al. Concise gene signature for point-of-care classification of tuberculosis. *EMBO molecular medicine* 2015;8(2):86-95
249. Calvori C, Frontali L, Leoni L, Tecce G. Effect of rifamycin on protein synthesis. *Nature*.1965;207(995):417-8
250. Mallolas J, Sarasa M, Nomdedeu M, Soriano A, Lopez-Pua, Blancho JL et al. Pharmacokinetic interaction between rifampicin and ritonavir-boosted atazanavir in HIV-infected patients. *HIV Medicine*. 2007; 8(2):131-4
251. Cohen KA, Abeel T, Manson McGuire, Desjardins CA, Munsamy V, Shea TP et al. Evolution of Extensively Drug-Resistant Tuberculosis over Four Decades: Whole Genome Sequencing and Dating Analysis of *Mycobacterium tuberculosis* Isolates from KwaTulu-Natal. *PLoS One*. 2015;12(9):e1001880
252. Shortening Treatment by Advancing Novel Drugs (STAND). Available from: <https://clinicaltrials.gov/ct2/show/results/NCT02342886>
253. Dawson R, Diacon AH, Everitt D, van NieKerk, Donald PR, Burger DA et al. Efficiency and safety of the combination of moxifloxacin, pretomanid (PA-824), and pyrazinamide during the first 8 weeks of antituberculosis treatment: a phase 2b, open-label, partly

- randomised trial in patients with drug-susceptible or drug-resistant pulmonary tuberculosis. *Lancet*.2015;385(9979):1738-47
254. Hunter RL, Actor JK, Hwang SA, Karev V, Jagannath C. Pathogenesis of post primary tuberculosis: immunity and hypersensitivity in the development of cavities. *Annals of clinical and laboratory sciences*. 2014;44(4):365-87
255. Irwin SM, Driver E, Lyon E, Schrupp C, Ryan G, Gonzalez-Juarrero M et al. Presence of multiple lesion types with vastly different microenvironments in C3HeB/FeJ mice following aerosol infection with *Mycobacterium tuberculosis*. *Disease models and mechanisms*. 2015;8(6):591-602
256. Guirado E, Schlesinger LS. Modeling the *Mycobacterium tuberculosis* Granuloma-the Critical Battlefield in Host Immunity and Disease. 2013;4:98
257. Heitmann L, Abad Dar M, Schreiber T, Erdmann H, Behrends J, McKenzie AN et al. The IL-13/IL-4Ra axis is involved in tuberculosis-associated pathology. *The Journal of Pathology*.2014;234(3):338-50
258. Major S, Turner J, Beamer G. Tuberculosis in CBA/J mice. *Veterinary pathology*. 2013;50(6):1016-21
259. Hoff DR, Ryan GJ, Driver ER, Ssemakulu CC, De Groote MA, Basaraba RJ, Lenaerts AJ. Location of intra- and extracellular *M. tuberculosis* populations in lungs of mice and guinea pigs during disease progression after drug treatment. *PLoS One*. 2014;6(3):e17550
260. Nikonenko BV, Averbakh MM Jr, Lavebratt C, Schurr E, Apt AS. Comparative analysis of mycobacterial infections in susceptible I/St and resistant A/Sn inbred mice. *Tubercle and lung disease: the official journal of the International Union against Tuberculosis and Lung disease*.2000;80(1):15-25
261. Duque-Correa MA, Kühl AA, Rodriguez PC, Zedler U, Schommer-Leitner S, Rao M et al. Macrophage arginase-1 controls bacterial growth and pathology in hypoxic tuberculosis granulomas. *Proceedings of the National Academy of Sciences of the United States of America*. 2014;111(38):E4024-32
262. Cheung AM, Nguyen LV, Carles A, Beer P, Miller PH, Knapp DJ et al. Analysis of the clonal growth and differentiation dynamics of primitive barcoded human cord blood cells in NSG mice. *Blood*. 2013;122(18):3129-37
263. Cosgun KN, Rahmig S, Mende N, Reinke S, Hauber I, Schäfer C et al. Kit regulates HSC engraftment across the human-mouse species barrier. *Cell Stem Cell*. 2014;15(2):227-38
264. Tanaka S, Saito Y, Kunisawa J, Kurashima Y, Wake T, Suzuki LD et al. Development of mature and functional human myeloid subsets in hematopoietic stem cell-engrafted NOD/SCID/IL2rgKO mice. *Journal of immunology*. 2012;188(12):6145-55
265. Rongvaux A, Willinger T, Martinek J, Strowig T, Gearty SV, Teichmann LL et al. Development and function of human innate immune cells in a humanized mouse model. *Nature Biotechnology*. 2014;32(4):364-72
266. Gille C, Orlikowsky TW, Spring B, Hartwig UF, Wilhelm A, Wirth A et al. Monocytes derived from humanized neonatal NOD/SCID/IL2Rg(null) mice are phenotypically immature and exhibit functional impairments. *Human immunology*. 2012;73(4):346-54

267. Levy O. Innate immunity of the newborn: basic mechanisms and clinical correlates. *Nature Review Immunology*. 2007;7(5):379-90
268. Basha S, Surendran N, Pichichero M. Immune responses in neonates. *Expert review of Clinical Immunology*. 2014;10(9):1171-84
269. Halkias J, Yen B, Tayloe KT, Reinhartz O, Winoto A, Robey EA, Melichar AJ. Conserved and divergent aspects of human T-cell development and migration in humanized mice. *Immunology and cell biology*. 2015; 93(8):716-26
270. Brugman MH, Wiekmeijer AS, van Eggermond M, Wolvers-Terrero I, Langerak AW, de Haas EF et al. Development of a diverse human T-cell repertoire despite stringent restriction of hematopoietic clonality in the thymus. *Proceedings of the Natural Academy of Sciences of the United States of America*. 2015;112(44):E6020-7
271. Watanabe Y, Takahashi T, Okajima A, Shiokawa M, Ishii N, Katano I et al. The analysis of the functions of human B and T cells in humanized NOD/shi-scid/gammac (null) (NOG) mice (hu-HSC NOG mice). *International immunology*. 2009;21(7):843-58
272. Choi B, Chun E, Kim M, Kim ST, Yoon K, Lee KY, Kim SJ. Human B cell development and antibody production in humanized NOD/SCID/IL-2Rg (null) (NSG) mice conditioned by busulfan. *Journal of Clinical Immunology*. 2011;31(2):253-64
273. Chang H, Biswas S, Tallarico AS, Sarkis PT, Geng S, Panditrao MM, Zhu Q, Marasco WA. Human B-cell ontogeny in humanized NOD/SCID gc (null) mice generates a diverse yet auto/poly- and HIV-1- reactive antibody repertoire. *Genes and Immunity*. 2012;13(5):399-410
274. Ippolito GC, Hoi KH, Reddy ST, Carroll SM, Ge X, Rogosch T et al. Antibody repertoires in humanized NOD-scid-IL2Rg (null) mice and human B cells reveals human-like diversification and tolerance checkpoints in the mouse. *PLoS One*. 2012;7(4):e35497
275. Akkina R, Allam A, Balazs AB, Blankson JN, Burnett JC, Casasres S et al. Improvements and Limitations of Humanized Mouse Models for HIV research: NIH/NIAID “Meet the Experts” 2015 Workshop Summary. *AIDS research and human retroviruses*. 2016;32(2):109-19
276. Knop J, Hanses F, Leist T, Atchin NM, Buchholz S, Gläsner J, Gessner A, Wege AK. *Staphylococcus aureus* Infection in Humanized mice: A New Model to Study Pathogenicity Associated with Human Immune Response. *The Journal of Infectious diseases*. 2015;212(3):435-44
277. Tseng CW, Biancotti JC, Berg BL, Gate D, Kolar SL, Müller S et al. Increased Susceptibility of Humanized NSG mice to Panton-Valentine Leukocidin and *Staphylococcus aureus* Skin Infection. *PLoS Pathogen*. 2015;11(11):e1005292
278. Vuyyuru R, Liu H, Manser T, Alugupalli KR. Characteristics of *Borellia hermsii* infection in human hematopoietic stem cell-engrafted mice mirror those of human relapsing fever. *Proceedings of the Natural Academy of Sciences of the United States of America*. 2011;108(51):20707-12
279. Young D. Animal models of tuberculosis. *European journal of Immunology*. 2009;39(8):2011-4

280. Ryan GJ, Shapiro HM, Lenaerts AJ. Improving acid-fast fluorescent staining for the detection of mycobacteria using a new nucleic acid staining approach. *Tuberculosis*. 2014;94(5):511-8
281. Hunter RL. Pathology of post primary tuberculosis of the lung: an illustrated critical review. *Tuberculosis*. 2011;91(6):497-509
282. Saeed W. Cavitating pulmonary tuberculosis: a global challenge. *Clinical Medicine*. 2012;12(1):40-1
283. Subbian S, Tsenova L, Yang G, O'Brien P, Parsons S, Peixoto B et al. Chronic pulmonary cavitory tuberculosis in rabbits: a failed host immune response. *Open Biology*. 2011;1(4):110016
284. Lanoix JP, Lenaerts AJ, Nuermberger EL. Heterogeneous disease progression and treatment response in a C3HeB/FeJ mouse model of tuberculosis. *Disease models and mechanisms*. 2015;8(6):603-10
285. Cardona PJ. The key role of exudative lesions and their encapsulation: lessons learned from the pathology of human pulmonary tuberculosis. *Frontiers in microbiology*. 2015;6:612
286. Osborne DR, Effmann EL, Hedlund LW. Postnatal growth and size of the pulmonary acinus and secondary lobule in man. *AJR. American journal of roentgenology*. 1983;140(3):449-54
287. Glenn RW, Robertson HT. Spatial distribution of ventilation and perfusion: mechanisms and regulation. *Comprehensive Physiology*. 2011;1(1):375-95
288. DOCK W. Effect of posture in alveolar gas tension in tuberculosis: explanation for favored sites of chronic pulmonary lesions. *A.M.A. archives of internal medicine*. 1954;94(5):700-8
289. Gurney JW, Schroeder BA. Upper lobe lung disease: physiologic correlates. Review. *Radiology*. 1988;167(2):359-66
290. Suki B, Sato S, Parameswaran H, Szabari MV, Takahashi A, Bartolak-Suki E. Emphysema and mechanical stress-induced lung remodeling. *Physiology*. 2013;28(6):404-13
291. Medlar EM, Sasano KT. The Interplay of the Cells of the Hematopoietic Tissues in Rabbits Infected Experimentally with the Tubercle Bacillus: The Origin of the Monocyte Considered. *The American journal of pathology*. 1936;12(6):825-854
292. Cohen T, van Helden PD, Wilson D, Colijin C, McLaughlin MM, Abubakar I, Warren RM. Mixed-strain mycobacterium tuberculosis infections and the implications for tuberculosis treatment and control. *Clinical microbiology reviews*. 2012;25(4):708-19
293. Pottenger FM. PULMONARY TUBERCULOSIS. THE IMPORTANCE OF THE CLINICAL HISTORY IN ITS DIAGNOSIS. *California and western medicine*. 1930;32(1):9-13
294. Fox GJ, Barry SE, Britton WJ, Marks GB. Contact investigation for tuberculosis: a systematic review and meta-analysis. *The European respiratory journal*. 2013;41(1):140-56
295. Scott GD, Fryer AD, Jacoby DB. Quantifying nerve architecture in murine and human airways using three-dimensional computational mapping. *American journal of respiratory and molecular biology*. 2012;48(1):10-6

296. Basha S, Surendran N, Pichichero M. Immune response in neonates. Expert review of clinical immunology. 2014;10(9):1171-84
297. Zasada M, Kwinta P, Durlak W, Bik-Multanowski M, Madetko-Talowska A, Pietrzyk JJ. Development and maturation of the immune system in preterm neonates: results from a whole genome expression study. Biomed research international. 2014;498318
298. Mizgerd JP, Skerrett SJ. Animal models of human pneumonia. American journal of physiology. Lung cellular and molecular physiology. 2008;294(3):L387-98
299. Iwata T, Ito I, Niimi A, Ikegami K, Marumo S, Tanabe N et al. Mechanical Stimulation by Postnasal Drip Evokes Cough. PLoS One. 2015;10(11):e0141823
300. Newton SM, Brent AJ, Anderson S, Whittaker E, Kampmann B. Paediatric tuberculosis. The Lancet. Infectious diseases. 2008;8(8):498-510
301. Fox GJ, Orlova M, Schurr E. Tuberculosis in Newborns: The Lessons of the “ Lübeck Disaster”(1929-1933). PLoS Pathogens. 2016;12(1):e1005271
302. Jain SK, Paul-Satyaseela M, Lamichhane G, Kim KS, Bishai WR. Mycobacterium tuberculosis invasion and traversal across an in vitro human blood-brain barrier as a pathogenic mechanism for central nervous system tuberculosis. The Journal of infectious diseases. 2006;193(9):1287-95
303. Jones-Lopez EC, Fregona G, Marques-Rodrigues P, Hadad DJ, Molina LP, Vinhas S et al. Importance of cough and M. tuberculosis strain type as risks for increased transmission within households. PLoS One. 2014;9(7):e100984
304. Arvanitakis Z, Long RL, Hershfield ES, Manfreda J, Kabani A, Kunimoto D, Power C. M. tuberculosis molecular variation in CNS infection: evidence for strain-dependent neurovirulence. Neurology. 1998;50(6):1827-32
305. Hernandez Pando R, Aguilar D, Cohen I, Guerrero M, Ribon W, Acosta P, Orozco H et al. Specific bacterial genotypes of Mycobacterium tuberculosis cause extensive dissemination and brain infection in an experimental model. Tuberculosis. 2010;90(4):268-77
306. Louveau A, Smirnov I, Keyes TJ, Eccles JD, Rouhani SJ, Peske JD et al. Structural and functional features of central nervous system lymphatic vessels. Nature. 2015;523(7560):337-41
307. MCCUNE R, Jr, MCDERMOTT W, TOMPSETT R. The fate of Mycobacterium tuberculosis in mouse tissues as determined by the microbial enumeration technique.II. The conversion of tuberculosis infection to the latent state by the administration of pyrazinamide and a companion drug. The Journal of Experimental Medicine. 1956;104(5):763-802
308. Scanga CA, Mohan VP, Joseph H, Yu K, Chan J, Flynn JL. Reactivation of latent tuberculosis: variations on the Cornell murine model. Infection and Immunity. 1999;67(9):4531-8
309. Li F, Cowley DO, Banner D, Holle E, Zhang L, Su L. Efficient genetic manipulation of the NOD-RAG1-/-IL2RgammaC-null mouse by combining in vitro fertilization and CRISPR/CasO technology. Scientific Reports. 2014;4:5290
310. Niazi MK, Dhulekar N, Schmidt D, Major S, Cooper R, Abeijon C et al. Lung necrosis and neutrophils reflect common pathways of susceptibility to Mycobacterium tuberculosis

- in genetically diverse, immune-competent mice. *Disease Models and Mechanisms*. 2015;8(9):1141-53
311. Brodbeck WG, Anderson JM. Giant cell formation and function. *Current opinion in hematology*. 2009;16(1):53-7
312. Lay G, Poquet Y, Salek-Peyron P, Puissegur MP, Botanch C, Levillain F et al. Langhans giant cells from M. tuberculosis-induced human granulomas cannot mediate mycobacterial uptake. *The Journal of Pathology*. 2007;211(1):76-85
313. Puissegur MP, Lay G, Gilleron M, Botella L, Nigou J, Marrakchi H et al. Mycobacterial lipomannan induces granuloma macrophage fusion via a TLR2-dependent, ADAM9- and beta1 integrin-mediated pathway. *Journal of Immunology*. 2007;178(5):316-9
314. Converse PJ, Eisenach KD, Theus SA, Nuermberger EL, Tyagi S, Ly LH et al. The impact of mouse passaging of Mycobacterium tuberculosis strains prior to virulence testing in the mouse and guinea pig aerosol models. *PLoS One*. 2010;5(4):e010289
315. Domenech P, Reed MB. Rapid and spontaneous loss of phthiocerol dimycocerosate (PDIM) from Mycobacterium tuberculosis grown in vitro: implications for virulence studies. *Microbiology*. 2009;155(Pt 11):3532-43
316. Orme IM. A new unifying theory of the pathogenesis of tuberculosis. *Tuberculosis*. 2014;94(1):8-14
317. Velayati AA, Farnia P, Masjedi MR. The totally drug resistant tuberculosis (TDR-TB). *International journal of clinical and experimental medicine*. 2013;6(4):307-9
318. Zinman G, Brower-Sinning R, Emeche CH, Ernst J, Huang G, Mahony S et al. Large scale comparison of innate responses to viral and bacterial pathogens in mouse and macaque. *PLoS One*. 2011;6(7):e22401
319. Sun J, Li N, Oh KS, Dutta B, Vayttaden SJ, Lin B et al. Comprehensive RNAi-based screening of human and mouse TLR pathways identifies species-specific preferences in signaling protein use. *Science signaling*. 2016;9(409):ra3
320. Spaan AN, Vrieling M, Wallet P, Badiou C, Reyes-Robles T, Ohneck EA et al. The staphylococcal toxins γ -haemolysin AB and CB differentially target phagocytes by employing specific chemokine receptors. *Nature Communications*. 2014;5:5438
321. Schnappinger D, Ehrt S, Voskuil MI, Mangan JA, Monahan IM, Dolganov G et al. Transcriptional Adaptation of Mycobacterium tuberculosis within Macrophages: Insights into the Phagosomal Environment. *The Journal of Experimental Medicine*. 2003;198(5):693-704
322. Fontan P, Aris V, Ghanny S, Soteropoulos P, Smith I. Global transcriptional profile of Mycobacterium tuberculosis during THP-1 human macrophage infection. *Infection and immunity*. 2008;76(2):717-25
323. Bhamidi S, Scherman MS, Jones V, Crick DC, Belisle JT, Brennan PJ, McNeil MR. Detailed structural and quantitative analysis reveals the spatial organization of the cell walls of in vivo grown Mycobacterium leprae and in vitro grown Mycobacterium tuberculosis. *The journal of Biological Chemistry*. 2011;286(26):23168-77

324. Prosser G, Bradenburg J, Reiling N, Barry CE 3rd, Wilkinson RJ, Wilkinson KA. The bacillary and macrophage response to hypoxia in tuberculosis and the consequences for T cell antigen recognition. *Microbes and Infection*. 2017;19(3):177-192
325. Silva MT, Pestana NT. The in vivo extracellular life of facultative intracellular bacterial parasites: role in pathogenesis. *Immunobiology*. 2013;218(8):325-37
326. Quigley J, Hughitt VK, Velikovskiy CA, Mariuzza RA, El-Sayed NM, Briken V. The Cell Wall Lipid PDIM Contributes to Phagosomal Escape and Host Cell Exit of *Mycobacterium tuberculosis*. *MBio*. 2017;8(2).pii:e00148-17
327. Martin CJ, Carey AF, Fortune SM. A bug's life in the granuloma. *Seminars in Immunopathology*. 2016;38(2):213-20
328. Liu Q, Via LE, Luo T, Liang L, Liu X, Wu S et al. Within patient microevolution of *Mycobacterium tuberculosis* correlates with heterogeneous responses to treatment. *Scientific reports*. 2015;5:17507
329. Basaraba RJ, Smith EE, Shanley CA, Orme IM. Pulmonary lymphatics are primary sites of *Mycobacterium tuberculosis* infection in guinea pigs infected by aerosol. *Infection and Immunity*. 2006;74(9):5397-401
330. Turner OC, Basaraba RJ, Orme IM. Immunopathogenesis of pulmonary granulomas in the guinea pig after infection with *Mycobacterium tuberculosis*. *Infection and Immunity*. 2003;71(2):864-71
331. Tobin DM, Roca FJ, Oh SF, McFarland R, Vickery TW, Ray JP et al. Host genotype-specific therapies can optimize the inflammatory response to mycobacterial infections. *Cell*. 2012;148(3):434-46
332. Mehra S, Pahar B, Dutta NK, Conerly CN, Philippi-Falkenstein K, Alvarez X, Kaushal D. Transcriptional reprogramming in nonhuman primate (rhesus macaque) tuberculosis granuloma. *PLoS One*. 2010;5(8):e12266
333. Chackerian AA, Alt JM, Perera TV, Dascher CC, Behar SM. Dissemination of *Mycobacterium tuberculosis* is influenced by host factors and precedes the initiation of T-cell immunity. *Infection and Immunity*. 2002;70(8):4501-9
334. O'Garra A, Redford D, McNamee D, Bloom CI, Wilkinson RJ, Berry MP. The immune response in tuberculosis. *Annual review of immunology*. 2013;31:475-527
335. Ganbat D, Seehase S, Richter EE, Vollmer E, Reiling N, Fellenberg K et al. Mycobacteria infect different cell types in the human lung and cause species dependent cellular changes in infected cells. *BMC Pulmonary Medicine*. 2016;16:19
336. Olsen HH, Grunewald J, Tornling G, Sköld CM, Eklund A. Bronchoalveolar lavage results are independent of season, age, gender and collection site. *PLoS One*. 2012;7(8):e43644
337. Bardoel BW, Kenny EF, Sollberger G, Zychlinsky A. The balancing act of neutrophils. *Cell Host and Microbes*. 2014;15(5):526-36
338. Kim WS, Kim JS, Cha SB, Han SJ, Kim H, Kwon KW et al. Virulence-Dependent Alterations in the Kinetics of Immune Cells during Pulmonary Infection by *Mycobacterium tuberculosis*. *PLoS One*. 2015;10(12):e0145234

339. Zhang X, Majlesso L, Deriaud E, Leclerc C, Lo-Man R. Coactivation of Syk Kinase and MyD88 adaptor protein pathways by bacteria promotes regulatory properties of neutrophils. *Immunity*. 2009;31(5):761-71
340. Barzilai S, Yadav SK, Morrell S, Roncata F, Klein E, Stoler-Barak L et al. Leukocytes Breach Endothelial Barriers by Insertion of Nuclear lobes and Disassembly of Endothelial Actin Filaments. *Cell Reports*. 2017;18(3):685-699
341. Scapini P, Cassatella MA. Social networking of human neutrophils within the immune system. *Blood*. 2014;124(5):710-9
342. de Oliveira S, Rosowski EE, Huttenlocher A. Neutrophil migration in infection and wound repair: going forward in reverse. *Nature Reviews. Immunology*. 2016;16(6):378-91
343. Velayati AA, Farnia P, Merza MA, Zhavnerko GK, Tabarsi P, Titov LP et al. New insight into extremely drug-resistant tuberculosis: using atomic force microscopy. *The European Respiratory Journal*. 2010;36(6):1490-3
344. Repasy T, Martinez N, Lee J, West K, Li W, Kornfeld H. Bacillary replication and macrophage necrosis are determinants of neutrophil recruitment in tuberculosis. *Microbes and Infection*. 2015;17(8):564-74
345. Bournazou I, Pound JD, Duffin R, Bournazos S, Melville LA, Brow SB et al, Apoptotic human cells inhibit migration of granulocytes via release of lactoferrin. *The Journal of Clinical Investigation*. 2009;119(1):20-32
346. Lowe DM, Redford PS, Wilkinson RJ, O'Garra A, Martineau AR. Neutrophils in tuberculosis: friend or foe? *Trends in Immunology*. 2012;33(1):14-25
347. Mihret A. The role of dendritic cells in Mycobacterium tuberculosis infection. *Virulence*. 2012;3(7):654-9
348. Guirado E, Schlesinger LS, Kaplan G. Macrophages in tuberculosis: friend or foe. *Seminars in Immunopathology*. 2013;35(5):568-83
349. O'Neill LA, Pearce EJ. Immunometabolism governs dendritic cell and macrophage function. *The Journal of Experimental Medicine*. 2016;213(1):15-23
350. Dorhoi A, Kaufmann SH. Versatile myeloid cell subsets contribute to tuberculosis-associated inflammation. *European Journal of Immunology*. 2015;45(8):2191-202
351. Nemeth J, Winkler HM, Boeck L, Adegnika AA, Clement E, Mve TM et al. Specific cytokine patterns of pulmonary tuberculosis in Central Africa. *Clinical Immunology*. 2011;138(1):50-9
352. Torraso E, Cooper AM. Cytokines in the balance of protection and pathology during mycobacterial infections. *Advances in Experimental Medicine and Biology*. 2013;783:121-40
353. Lyons MJ, Yoshimura T, McMurray DN. Mycobacterium bovis BCG vaccination augments interleukin-8 mRNA expression and protein production in guinea pig alveolar macrophages infected with Mycobacterium tuberculosis. *Infection and Immunity*. 2002;70(10):5471-8
354. Hol J, Wihelmsen L, Haraldsen G. The murine IL-8 homologue KC, MIP-2 and LIX are found in endothelial cytoplasmic granules but not in Weibel-Palade bodies. *Journal of Leukocyte Biology*. 2010;87(3):501-8

355. Singer M, Sansonetti PJ. Il-8 is a key chemokine regulating neutrophil recruitment in a new mouse model of Shigella-induced colitis. *Journal of Immunology*. 2004;173(6):4197-206
356. Ma X, Reich RA, Wright JA, Tooker HR, Teeter LD, Musser JM, Graviss EA. Association between interleukin-8 gene alleles and human susceptibility to tuberculosis disease. *The Journal of Infectious Disease*. 2003;188(3):349-55
357. Krupa A, Fol M, Dyiadek BR, Kepka E, Wojciechowska D, Brzostek A et al. Binding of CXCL8/IL-8 to Mycobacterium tuberculosis Modulates the Innate Immune Response. *Mediators of Inflammation*. 2015;2015:124762
358. Hilda JN, Narasimhan M, Das SD. Neutrophils from pulmonary tuberculosis patients show augmented levels of chemokines MIP-1 α , IL-8 and MCP-1 which further increase upon in vitro infection with mycobacterial strains. *Human Immunology*. 2014;75(8):914-22
359. Ong CW, Elkington PT, Brihla S, Ugarte-Gil C, Tome-Esteban MT, Tezera LB et al. Neutrophil-Derived MMP-8 Drives AMPK-Dependent Matrix Destruction in Human Pulmonary Tuberculosis. *PLoS Pathogen*. 2015;11(5):e1004917
360. Lyadova IV, Panteleev AV. Th1 and Th17 Cells in Tuberculosis: Protection, Pathology and Biomarkers. *Mediators of Inflammation*. 2015;15:854507
361. Kozakiewicz L, Phuah J, Flynn J, Chan J. The role of B cells and humoral immunity in Mycobacterium tuberculosis infection. *Advances in Experimental Medicine and Biology*. 2013;783:225-50
362. Palmer MV, Thacker TC, Waters WR. Analysis of Cytokine Gene Expression using a Novel Chromogenic In-situ Hybridization Method in Pulmonary Granulomas of Cattle Infected Experimentally by Aerosolized Mycobacterium bovis. *Journal of Comparative Pathology*. 2015;153(2-3):150-9
363. Barr TA, Shen P, Brown S, Lampropoulou V, Roch T, Lawrie S et al. B cell depletion therapy ameliorates autoimmune disease through ablation of IL-6-producing B cells. *The Journal of Experimental Medicine*. 2012;209(5):1001-10
364. Lu LL, Chung AW, Rosebrock TR, Ghebremichael M, Yu WH, Grace PS et al. A Functional Role for Antibodies in Tuberculosis. *Cell*. 2016;167(2):433-443
365. Zimmermann N, Thormann V, Hu B, Köhler AB, Imai-Matsushima A, Lochr C et al. Human isotype-dependent inhibitory antibody responses against Mycobacterium tuberculosis. *EMBO Molecular Medicine*. 2016;8(11):1325-1339
366. Gideom HP, Phuah J, Myers AJ, Bryson BD, Rodgers MA, Coleman MT et al. Variability in tuberculosis granuloma T cell responses exists, but a balance of pro- and anti-inflammatory cytokines associated with sterilization. *PLoS Pathogen*. 2015;11(5):e1004603
367. Giesen C, Wang HA, Scapiro D, Zivanovic N, Jacobs A, Harrendorf B et al. Highly multiplexed imaging of tumor tissues with subcellular resolution by mass cytometry. *Nature methods*. 2014;11(4):417-22
368. Theocharides AP, Rongvaux A, Fritsch K, Flavell RA, Manz Mg, Humanized hematolymphoid system mice. *Haematologica*. 2016;101(1):5-19

369. Subbian S, Tsenova L, Kim MJ, Wainwright HC, Visser A, Bandyopadhyay N et al. Lesion-Specific Immune Response in Granulomas of Patients with Pulmonary Tuberculosis: A Pilot Study. *PLoS One*. 2015;10(5):e0132249
370. Iannaccone M, Dorhoi A, Kaufmann SH. Host-directed therapy of tuberculosis: what is in it for microRNA? *Expert Opinion on Therapeutic Targets*. 2014;18(5):491-4
371. Popper HH. Progression and metastasis of lung cancer. *Cancer Metastasis Reviews*. 2016;35(1):75-91
372. Polena H, Boudou F, Tilleul S, Dubois-Colas N, Lecointe C, Rakotasamimanana N et al. *Mycobacterium tuberculosis* exploits the formation of new blood vessels for its dissemination. *Scientific Reports*. 2016;6:33162
373. Osherov N, Ben-Ami R. Modulation of Host Angiogenesis as a Microbial Survival Strategy and Therapeutic Target. *PLoS Pathogens*. 2016;12(4):e1005479
374. Manz MG, Boettcher S. Emergency granulopoiesis. *Nature Reviews. Immunology*. 2014;14(5):302-14
375. Nombela-Arrieta C, Isringhausen S. The Role of the Bone Marrow Stromal Compartment in the Hematopoietic Response to Microbial Infections. *Frontiers in Immunology*. 2017;7:689
376. Tornack J, Reece ST, Bauer WM, Vogelzang A, Bandermann S, Zedler U et al- Human and Mouse Hematopoietic Stem Cells Are a Depot for Dormant *Mycobacterium tuberculosis*. *PLoS One*. 2017;12(1):e0169119
377. Das B, Kashino SS, Pulu I, Kalita D, Swami V, Yeger H et al. CD271(+) bone marrow mesenchymal stem cells may provide a niche for dormant *Mycobacterium tuberculosis*. *Science Translational Medicine*. 2013;5(170):170ra13
378. Prideaux B, Via LE, Zimmerman MD, Eum S, Sarathy J, O'Brien P et al. The association between sterilizing activity and drug distribution into tuberculosis lesions. *Nature Medicine*. 2015;21(10):1223-7
379. Knaut JK, Jörg S, Oberbeck-Mueller D, Heinemann E, Scheuermann L, Brinkmann V et al. Lung-residing myeloid-derived suppressors display dual functionality in murine pulmonary tuberculosis. *American Journal of Respiratory and Critical Care Medicine*. 2014;190(9):1053-66
380. Linderman JJ, Clifone NA, Piennar E, Gong C, Kirschner DE. A multi-scale approach to designing therapeutics for tuberculosis. *Integrative Biology*. 2015;7(5):591-609
381. Weiner J, Kaufmann SH. High-throughput and computational approaches for diagnostic and prognostic host tuberculosis biomarkers. *International Journal of Infectious Diseases*. 2017;56:258-262

Abbreviations

Mtb	<i>Mycobacterium tuberculosis</i>
TB	Tuberculosis
HIV	Human Immunodeficiency Virus
BCG	Bacille Calmette- Guérin
Hly	listeriolysin gene
PPD	purified protein derivative
IGRAs	Interferon-Gamma Release Assays
ESAT-6	6 kDa early secretory antigenic target
CFP-10	10 kDa culture filtrate antigen
RD1	region of difference 1
SLE	systemic lupus erythematosus
MDR-TB	multi-drug resistant tuberculosis
XDR-TB	extensively drug resistant tuberculosis strains
(TDR-TB)	totally drug resistant tuberculosis
IFN- γ	interferon gamma
IL	interleukin
PET	positron emission tomography
CT	computerized tomography
SPECT	single photon emission computed tomography
Pa	pretomanid
M	moxifloxacin
Z	pyrazinamide
HDTs	host directed therapies
GAMs	granuloma associated macrophages

NHPs	Non-human primates
SIV	Simian Immune deficiency virus
FDG	2-deoxy-2-(18F)-fluoro-D-glucose
CFU	colony forming unit
M. bovis	<i>Mycobacterium bovis</i>
<i>M. marinium</i>	<i>Mycobacterium marinium</i>
Ipr-1	intracellular pathogen resistance 1
sst-1	super susceptibility to tuberculosis 1
iNOS	inducible nitric oxide
TNF- α	tumor necrosis factor alpha
PAMPs	pathogen- associated molecular patterns
LM	lipomannan
ManLam	mannose-capped Lipoarabinomannan
PIMs	phosphatidyl-myo-inositol mannosides
PRRs	pattern recognition receptors
TLRs	Toll like receptors
CRs	complement receptors
MRs	mannose receptors
SRs	scavenger receptors
DC-SIGN	Dendritic cell-specific intracellular adhesion molecule-3-Grabbing non-integrin
AECs	Airway epithelial cells
DCs	dendritic cells
CCL	Chemokine motif ligand
CXCL	C-X-C motif chemokine ligand
ROI	reactive oxygen intermediates

RNI	reactive nitrogen intermediates
NO	nitrogen oxide
ESX	early secreted antigen 6 kilodaltons (ESAT-6) secretion system
MMP-9	matrix metalloproteinase 9
APCs	antigen presenting cells
MHC	major histocompatibility class
LFA-1	lymphocyte function-associated antigen 1
ICAM-1	intercellular adhesion molecule 1
MSMD	Mendelian susceptibility to mycobacterial disease
IFNGR1	IFN γ receptor 1
STAT1	Signal Transducers and Activators of Transcription 1
IL12RB1	IL-12 receptor β 1
NEMO	nuclear factor- κ B (NF- κ B) essential modulator
CYBB	cytochrome b-245
IRF8	interferon regulatory factor 8
HMBPP	(E)-4-hydroxy-3-methyl-but-2-enyl pyrophosphate phosphoantigen
NKs	natural killer cells
Th	T-helper
T regs	regulatory T cells
TGF- β 1	transforming growth factor-beta 1
gdTs	gamma delta T cells
CTLs	cytolytic T cells
MAITs	mucosal associated invariant T cells
ROS	reactive oxygen species
NETS	neutrophil extracellular traps

Eis	enhanced intracellular survival gene
nuoG	NADH-quinone oxidoreductase subunit G
LXA4	lipoxin A4
PGE2	prostaglandin E2
PBMCs	peripheral blood mononuclear cells
BAL	bronchoalveolar lavage
SCID	severe combined immunodeficiency mutation
NOD	non-obese diabetic
Rag1	recombination-activation gene 1
IL-2Rg	interleukin 2 receptor gamma chain
BRG	BalbC Rag2 null IL-2R gamma null
NSG	NOD SCID IL-2 receptor gamma null
NRG	NOD Rag1 null IL-2 receptor gamma null
SIRPa	signal regulatory protein alpha
HSCs	hematopoietic stem cell
HPCs	hematopoietic stem and progenitor cells
HLA	human leukocyte antigen
Hu-HSC	Human hematopoietic stem cell
HIS	Human Immune System
PBL	peripheral blood leukocytes
BLT	bone marrow-liver-thymus
SDF-1	stromal derivative factor 1
Hu-Hep	Hu-hepatocyte
CD	cluster of differentiation
CaCl ₂	Calcium chloride

MgCl ₂	Magnesium chloride
RT	room temperature
BD	Beckton Dickson
BSA	bovine serum albumin
MNC	mono-nuclear cell layer
FACs	fluorescence-activated cell sorting
FMO	fluorescent minus one
ADC	albumin dextrose catalase
WHO	World Health Organization
MPIIB	Max Planck Institute of Infection Biology, Berlin

Frida T. Arrey

Work address: Max Planck Institute for Infection Biology
Chariteplatz 1; Campus Charité Mitte D-10117 Berlin, Germany
(00 49) 30 28 460 573 (lab phone)

Educational History

Oct 2010-Present date

Doctoral Thesis

Human Immune System Mouse model for Pulmonary Tuberculosis

Professor Dr. Stefan H.E. Kaufmann
Max Planck Institute for Infection Biology, Berlin, Germany

Aug 2004-May 2005

Masters Thesis

The analyses of *Schistosoma mansoni* mobile genetic elements
via luciferase/expression vector based detection of promoter activity

Professor Paul Brindley
Tulane University, School of Public health and Tropical Medicine, New Orleans; LA, USA
Degree awarded: Masters in Science in Public Health May 2005

Aug 2001-May 2004

Bachelors Thesis

The effects of pollution on Lichens in Swope Park, Kansas city, MO

Professor Mary Haskins
Rockhurst University, Kansas City; MO, USA
Degree awarded: Bachelors in Science May 2004, Biology Major and Physics Minor

Lab-based Research Experience

- Oct 2010-Present date** **PhD Student, Max Plank Institute for Infection Biology, Berlin, Germany**
Bio level safety 3 expertise for *in vivo* and *in vitro* handling, processing and analyzing of murine and human samples.
On adult mice: intra-nasal administration, intra-tracheal injections, oral gavage administration, tail bleeds and sub-cutaneous injections.
- Oct 2005-Oct 2010** **Research Assistant, Rockefeller University, NYC; NY, USA**
Professor Ralph Steinman and Professor Christian Münz
Bio level safety 2 expertise for *in vivo* and *in vitro* handling, processing and analyzing of murine and human samples
On newborn mice: intra-hepatic injections and retro-orbital injections
On adult mice: intra-peritoneal injections, intra-muscular injections and retro-orbital injections
- Aug 2004-2005** **Masters Student, Tulane University, New Orleans; LA, USA**
Basic cell culture and genetic cloning
- May 2003-Mar 2004** **Bachelors Student, Rockhurst University**
Sample collection using grid survey

Peer-reviewed Publications

Brilot F, Strowig T, Roberst SM, **Arrey F** and Münz C. NK cell survival mediated through the regulatory synapse with human DCs requires IL-15 α . J Clin Invest. 2007 Nov; 117(11):3316-29.

Heller KN, **Arrey E**, Steinherz P, Portlock C, Chadburn A, Kelly K and Münz C. Patients with Epstein Barr virus-positive lymphomas have decreased CD4 (+) T-cell responses to the viral nuclear antigen 1. Int J Cancer. 2008 Dec 15;123(12):2824-31

Strowig T, Brilot F, **Arrey E**, Bougras G, Thomas D, Muller WA and Münz C. Tonsillar NK cells restrict B cell transformation by the Epstein-Barr virus via IFN- γ . PLoS Pathog. 2008 Feb 8;4(2):e27

Gurer C, Strowig T, Brilot F, Pack M, Trumpfheller C, **Arrey F**, Park CG, Steinman RM, Münz C. Targeting the nuclear antigen 1 of Epstein-Barr virus to the human endocytic receptor DEC-205 stimulates protective T-cell responses. *Blood*. 2008 Aug 15; 112(4):1231-9.

Strowig T, Gurer C, Ploss A, Liu YF, **Arrey F**, Sashihara J, Koo G, Rice CM, Young JW, Chadburn A, Cohen JI and Münz C. Priming of protective T cell responses against virus-induced tumors in mice with human immune system components. *J Exp Med*. 2009 Jun 8;206(6):1423-3

Gannagé M, Dormann D, Albrecht R, Dengjel J, Torossi T, Rämer PC, Lee M, Strowig T, **Arrey F**, Conenello G, Pypaert M, Andersen J, García-Sastre A and Münz C. Matrix protein 2 of influenza A virus blocks autophagosome fusion with lysosomes. *Cell host Microbe* 2009 Oct 22;6(4):367-80.

Strowig T, Chijioke O, Carrega P, **Arrey F**, Meixlsperger S, Rämer PC, Ferlazzo G and Münz C. Human NK cells of mice with reconstituted human immune system components require preactivation to acquire functional competence. *Blood*. 2010 Nov 18;116(20):4158-67

Maamary J, **Arrey F**, Gao Q, García-Sastre A, Steinman RM, Palese P and Nchinda G. Newcastle disease virus expressing a dendritic cell-targeted HIV gag protein induces a potent gag-specific immune response in mice. *J Virol*. 2011 Mar;85(5):2235-46.

Nouailles G, Dorhoi A, Koch M, Zerrahn J, Weiner J 3rd, Faé KC, **Arrey F**, Kuhlmann S, Bandermann S, Loewe D, Mollenkopf HJ, Vogelzang A, Meyer-Schwesinger C, Mittrücker HW, McEwen G, Kaufmann SH. CXCL5-secreting pulmonary epithelial cells drive destructive neutrophilic inflammation in tuberculosis. *J Clin Invest*. 2014 Mar;124(3):1268-82.

Conference presentations

A Human Immune System mouse model for Mycobacterium tuberculosis infection, September 8th 2012; Humanise d mice workshop European Congress of Immunology Glasgow 2012

Poster presentations

Humanized mouse model for Tuberculosis, May 16th 2011; 6th European Network of Immunology Institutes Immunology Summer School